UNIVERSIDADE FEDERAL DE VIÇOSA

Development of a phage cocktail against *Klebsiella pneumoniae* with potential use in animal production

Jose Junior Ferreira Soares
Magister Scientiae

VIÇOSA - MINAS GERAIS
2025

JOSE JUNIOR FERREIRA SOARES

Development of a phage cocktail against *Klebsiella pneumoniae* with potential use in animal production

Dissertation submitted to the Agricultural Microbiology Graduate Program of the Universidade Federal de Viçosa in partial fulfillment of the requirements for the degree of *Magister Scientiae*.

Adviser: Sergio Oliveira de Paula

Co-adviser: Denise M. Soares Bazzolli

VIÇOSA - MINAS GERAIS
2025

Ficha catalográfica elaborada pela Biblioteca Central da Universidade Federal de Viçosa - Campus Viçosa

T
S676d
2025

Soares, José Junior Ferreira, 2000-
Development of a phage cocktail against *Klebsiella pneumoniae* with potential use in animal production / José Junior Ferreira Soares. – Viçosa, MG, 2025.
1 dissertação eletrônica (92 f.): il. (algumas color.).

Texto em inglês.
Inclui apêndice.
Orientador: Sérgio Oliveira de Paula.
Dissertação (mestrado) - Universidade Federal de Viçosa, Departamento de Biologia Geral, 2025.
Referências bibliográficas: f. 56-63.
DOI: https://doi.org/10.47328/ufvbbt.2025.639
Modo de acesso: World Wide Web.

1. Suíno - Doenças - Controle biológico. 2. *Klebsiella pneumoniae* - Controle biológico. 3. Bacteriófagos. I. Paula, Sérgio Oliveira de, 1976-. II. Universidade Federal de Viçosa. Departamento de Biologia Geral. Programa de Pós-Graduação em Microbiologia Agrícola. III. Título.

CDD 22. ed. 636.4089691014

Bibliotecário(a) responsável: Euzébio Luiz Pinto CRB-6/3317

JOSE JUNIOR FERREIRA SOARES

Development of a phage cocktail against *Klebsiella pneumoniae* with potential use in animal production

Dissertation submitted to the Agricultural Microbiology Graduate Program of the Universidade Federal de Viçosa in partial fulfillment of the requirements for the degree of *Magister Scientiae*.

APPROVED: August 4, 2025.

Assent:

Jose Junior Ferreira Soares
Author

Sergio Oliveira de Paula
Adviser

ACKNOWLEDGMENTS

I dedicate the end of this cycle, marked by this work, to my family and friends, who were a safe harbor through so many moments along this journey.

I thank the Federal University of Viçosa (UFV), where I completed both my undergraduate and master's degrees, for all the knowledge, infrastructure, and opportunities provided to me. To the Graduate Program in Microbiology and the Department of Microbiology at UFV, my deepest gratitude for the constant support, education, and welcoming environment.

To my advisor, Professor Sérgio Oliveira, thank you for believing in me since my undergraduate years, when I was just an intern full of doubts and dreams. Your steady and patient guidance was essential for my growth as a scientist and as a person. To my co-advisor, Denise, I am immensely grateful for your dedication, your partnership, and your invaluable help with the experiments involving larvae, which greatly contributed to the development of this work.

I am also thankful to the professors and staff at UFV, who directly or indirectly contributed to my academic journey. To my evaluation committee, thank you very much for your time, careful reading, and valuable feedback.

Special thanks to Flávia, the postdoc in our lab and a member of my committee, for her generosity and for always lending a hand when I needed it — your support was indispensable at many points. I also extend my thanks to Jéssica, Luciana and Paloma, postdocs who also helped me with wisdom, patience, and camaraderie.

To the lab friends who were by my side — Diana, Fabi, Laís, and Ana — I leave my affection and gratitude for all the exchanges, conversations, and moments of mutual support. Each of you made this path lighter and more meaningful.

To Adriele, my friend, mentor, and role model. If this dissertation exists today, it is because you stood by me from the very beginning. You guided me when everything was still confusing, taught me with patience, and believed in me even when I couldn't. No words will ever be enough to express how grateful I am for everything you've done for me. Your presence was decisive at every stage of this work — none of this would have been possible without you.

Thalya, my companion on this road, in dreams and in struggles. We entered the master’s program together and walked this path side by side. You were comfort, motivation, and a companion in both joy and pain. Sharing this phase of life with you was a gift, and knowing we had each other throughout gave me strength to keep going, even on the hardest days.

To my closest friends, Thiago and Charles, I leave a heartfelt thank-you full of affection and gratitude. Thiago, my senior from both undergrad and the master's program, was a key presence from the beginning. With you, I learned so much — through serious talks, academic doubts, and the laughs that saved our days. Even though you moved away earlier this year, your friendship remains alive in me. Thank you for being such a valuable support. Charles, you came from Manaus and quickly became home. When Thiago left, you stayed — and more than that, you looked after me. Your friendship was shelter, laughter, and care. I can’t imagine this journey without your generous and constant presence. Thank you for being by my side.

To my housemates at TocaGado, Gustavo, Nikolas, Marlon and Gabriel, thank you for the warmth, the laughs, and the brotherhood we built. It was at home that I found strength on the hardest days and joy in the simplest ones.

I could not fail to express my deepest gratitude to my grandparents, who with so much effort, love, and sacrifice helped me get to this point. They are the ones who, even without having the same opportunities, fought to ensure I could study, graduate, and dream bigger. They are the people who cheer the loudest for every one of my achievements, and it is for them that I keep moving forward. To my sister Brunna, who has always supported me with love and stood by me even when things felt too hard, my eternal affection. And to my aunt Floripes, for all the support, care, and encouragement throughout my education and life, my most sincere gratitude.

To every person who, in some way, was part of this journey: my sincerest thanks. This work carries a little piece of each one of you.

This work has been sponsored by the following Brazilian research agencies: Coordination for the Improvement of Higher Education Personnel (CAPES; Financing code 001), Minas Gerais State Foundation for Research Aid (FAPEMIG) and National Council of Scientific and Technological Development (CNPq).

ABSTRACT

SOARES, Jose Junior Ferreira, M.Sc., Universidade Federal de Viçosa, August, 2025. **Development of a phage cocktail against *Klebsiella pneumoniae* with potential use in animal production**. Adviser: Sergio Oliveira de Paula. Co-adviser: Denise Mara Soares Bazzolli.

In this study, a cocktail composed of four bacteriophages with therapeutic potential was developed and evaluated for the control of *Klebsiella pneumoniae*, an opportunistic bacterium of great clinical and veterinary importance, frequently associated with multidrug resistance and outbreaks in intensive livestock production systems, especially in swine farming. The research focused on isolating phages active against the *Klebsiella* genus, with emphasis on *K. pneumoniae* strains isolated from pigs. Seven distinct phages were obtained from environmental samples, five of which showed lytic activity against different *K. pneumoniae* strains. Four phages with the most promising results in inhibiting bacterial growth and preventing biofilm formation were selected for biological characterization, including host range, plaque morphology, adsorption time, burst size, and thermal stability. The combination of these four phages resulted in a cocktail capable of suppressing *K. pneumoniae* growth in bacterial growth curves and preventing biofilm formation — both essential aspects for combating persistent infections in livestock environments. The efficacy of the cocktail was confirmed using an in vivo *Galleria mellonella* larvae model, showing survival rates above 90% under both prophylactic and coinfection conditions. Moreover, the treatment proved to be safe, with no signs of toxicity observed in the control larvae. The results highlight the potential of bacteriophages as viable and safe therapeutic alternatives in the face of the growing threat of antimicrobial resistance in animal production. This study provides a solid foundation for the development of phage-based products applicable in the field and paves the way for future validations in higher animal models, contributing to the advancement of more sustainable and effective strategies for controlling infections in pigs.

Keywords: bacteriophages; *Klebsiella pneumoniae*; phage cocktail; pig farming; antimicrobial resistance

RESUMO

SOARES, Jose Junior Ferreira, M.Sc., Universidade Federal de Viçosa, agosto de 2025. **Desenvolvimento de um coquetel de fagos contra *Klebsiella pneumoniae* com potencial uso na produção animal**. Orientador: Sergio Oliveira de Paula. Coorientadora: Denise Mara Soares Bazzolli.

Neste trabalho, foi desenvolvido e avaliado um coquetel composto por quatro bacteriófagos com potencial terapêutico voltado ao controle de *Klebsiella pneumoniae*, uma bactéria oportunista de grande importância clínica e veterinária, frequentemente associada à resistência a múltiplos antibióticos e a surtos em sistemas intensivos de produção animal, especialmente na suinocultura. A pesquisa concentrou-se no isolamento de fagos ativos contra o gênero *Klebsiella*, com ênfase em cepas de *K. pneumoniae* isoladas de suínos. Foram obtidos sete isolados distintos a partir de amostras ambientais, dos quais cinco demonstraram atividade lítica contra cepas distintas de *K. pneumoniae*. Quatro desses fagos, com os melhores resultados na inibição do crescimento bacteriano e na prevenção da formação de biofilme, foram selecionados para caracterização biológica, incluindo espectro de ação, morfologia das placas de lise, tempo de adsorção, *burst size* e estabilidade térmica. A combinação desses quatro isolados resultou na formulação de um coquetel fágico capaz de suprimir o crescimento de *K. pneumoniae* em curvas de crescimento e de impedir a formação de biofilmes — aspectos essenciais no combate a infecções persistentes em ambientes pecuários. A eficácia do coquetel foi confirmada em modelo in vivo com larvas de *Galleria mellonella*, alcançando taxas de sobrevivência superiores a 90% tanto em regime profilático quanto em coinfecção. Além disso, o tratamento demonstrou segurança, sem sinais de toxicidade nas larvas controle. Os resultados obtidos evidenciam o potencial dos bacteriófagos como alternativas terapêuticas viáveis e seguras frente à crescente ameaça da resistência antimicrobiana no contexto da produção animal. Este estudo estabelece uma base sólida para o desenvolvimento de produtos fágicos aplicáveis em campo e abre caminho para validações futuras em modelos animais superiores, contribuindo para o avanço de estratégias mais sustentáveis e eficazes no controle de infecções em suínos.

Palavras-chave: bacteriófagos ; *Klebsiella pneumoniae*; coquetel fágico; suinocultura; resistência antimicrobiana

SUMMARY

1. INTRODUCTION

Antimicrobial resistance (AMR) is one of the greatest threats to global public health, undermining the effectiveness of treatments and complicating infection control in both humans and animals (Dhingra *et al*., 2020; Ajulo *et al*., 2024). The excessive and often indiscriminate use of antibiotics in veterinary medicine—and particularly in intensive livestock systems—has favored the emergence and spread of multidrug-resistant strains of various pathogens, including *Klebsiella pneumoniae* (Yang *et al.*, 2019; Wareth *et al*., 2020).

Although widely recognized for its clinical impact on human health, *K. pneumoniae* has gained increasing attention in veterinary medicine and animal production, being associated with diseases such as pneumonia, septicemia, and urinary tract infections in different animal species. In swine farming, the bacterium has been frequently isolated from respiratory and intestinal samples, both in diseased and apparently healthy animals, indicating not only its role in infections but also its potential as a silent reservoir of resistance genes (Wareth *et al*., 2020; Ribeiro *et al*., 2022).

The detection of extended-spectrum β-lactamase (ESBL)-producing strains and the genetic similarity between animal- and human-derived isolates further raise concerns about interspecies transmission and highlight the urgency for integrated actions based on the One Health concept (Dong *et al*., 2022). Additionally, practices such as the use of swine waste as fertilizer contribute to environmental contamination, reinforcing the cycle of resistance gene dissemination across animal, human, and environmental health (Zhu *et al*., 2021).

Given the growing limitations in developing new antibiotics, alternative strategies have gained relevance, including the use of bacteriophages. These viruses exhibit high specificity, self-replication at the site of infection, and effective action against biofilms and multidrug-resistant strains, making them a promising approach for bacterial infection control (Kasman *et al*., 2022).

This dissertation aims to investigate the therapeutic potential of bacteriophage cocktails against multidrug-resistant *Klebsiella pneumoniae* strains, with a focus on the context of animal production, contributing to the advancement of effective and sustainable alternatives in the fight against AMR.

2. LITERATURE REVIEW

2.1 Antimicrobial Resistance

Antimicrobial resistance (AMR) is a global challenge that threatens modern medicine, compromising the effectiveness of essential treatments and complicating infection control in hospital and community settings (Kumar *et al*., 2018). The excessive and inappropriate use of antibiotics has accelerated the emergence of resistant microorganisms, making the prevention and treatment of various infectious diseases increasingly complex. Recognizing the severity of the issue, the World Health Organization (WHO) published, in 2017, a list of priority antimicrobial-resistant pathogens, highlighting those resistant to beta-lactams and fluoroquinolones, which are widely used in clinical practice (Dhingra *et al*., 2020). The scale of the problem is alarming.

In 2019, antimicrobial resistance was responsible for approximately 1.3 million deaths worldwide, and estimates suggest that if effective measures are not adopted, this number could reach up to 10 million deaths annually by 2050. The economic impacts are also significant. In the United States, annual costs related to treating resistant infections exceeded 4.6 billion dollars. Globally, the World Bank projects economic losses surpassing 1 trillion dollars per year by 2030, potentially doubling by 2050 even under optimistic scenarios (Ajulo *et al*., 2024).

Historically, before the discovery of antibiotics, infections such as pneumonia, tuberculosis, and syphilis were common causes of death. The discovery of penicillin by Alexander Fleming in 1928 and the introduction of streptomycin in 1944 revolutionized medicine, ushering in the so-called “golden era” of antimicrobials (1930–1960), during which approximately 20 new classes of antibiotics were developed. Among these classes are sulfonamides, which inhibit folic acid synthesis; beta-lactams, which prevent bacterial cell wall formation; and aminoglycosides, such as streptomycin, which inhibit protein synthesis. Other important classes include tetracyclines, macrolides, polymyxins, rifamycins, glycopeptides, and chloramphenicol, each with specific mechanisms targeting different bacterial components. However, since then, few new classes have been introduced, and many bacteria have developed efficient mechanisms to evade these drugs’ actions (Dhingra *et al*., 2020).

Microbial resistance is a natural process but has been amplified by the misuse of antibiotics in humans and animals. Resistance is established and disseminated mainly through

two mechanisms: spontaneous mutations and horizontal gene transfer. Mutations may alter the molecular targets of drugs or increase the production of degrading enzymes. Horizontal gene transfer allows bacteria to acquire resistance genes from other bacteria via three primary routes: conjugation (direct DNA transfer through cell-to-cell contact), transformation (uptake of free DNA from the environment), and transduction (transfer mediated by bacteriophages). These mechanisms enable rapid and efficient dissemination of resistance even among different bacterial species (Figure 1) (Chis *et al*., 2022).

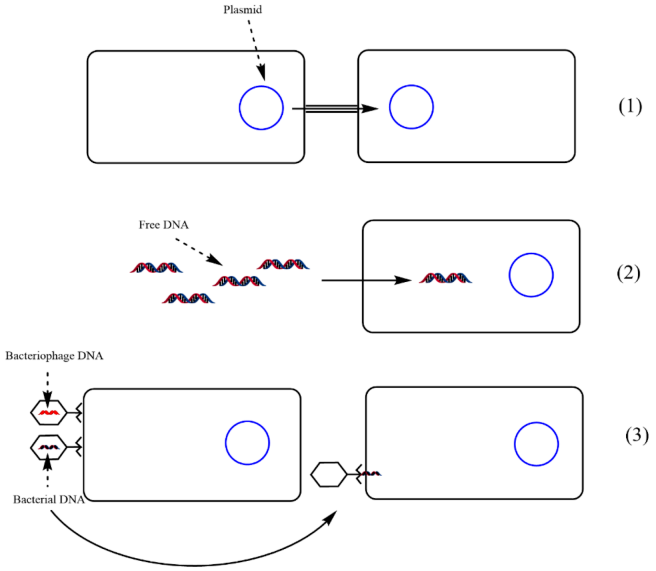

Figure 1. Genetic transfer in AMR — (1) conjugation, (2) transformation, (3) transduction. (Chis *et al*., 2022).

Moreover, Mobile Genetic Elements (MGEs) play a central role in this process. Plasmids, integrons, transposons, and insertion sequences act as vectors for resistance genes, promoting their mobilization among bacteria. Plasmids, for example, replicate independently from the main genome and carry genes conferring resistance to various antibiotics, such as beta-lactams and colistin. Integrons capture DNA fragments and insert them into specific genomic sites, often associated with other MGEs, increasing the spread of resistance. Transposons and insertion sequences promote the movement of these genes within and between genetic molecules (Chis *et al*., 2022).

The severity of antimicrobial resistance is also understood through clinical classifications of resistant pathogens, which are essential for guiding diagnosis and treatment. Multidrug-resistant (MDR) bacteria exhibit resistance to at least three different classes of antimicrobials, significantly limiting therapeutic options. Extensively drug-resistant (XDR)

strains show even broader resistance, remaining susceptible to only one or two drug classes, making clinical treatment more complex and risky. Finally, pan-drug resistant (PDR) bacteria are resistant to all available antimicrobials, representing a critical situation as infections become virtually untreatable with current resources (Dhingra *et al*., 2020).

Despite the urgency, the development of new antibiotics has been limited by various factors. High costs (estimated between 1.2 and 2.6 billion dollars per drug), long development timelines (10 to 20 years), and stringent regulatory processes make this field unattractive to the pharmaceutical industry. Since these drugs are typically used for short durations and their rational use is encouraged, financial returns are limited. Therefore, many companies prioritize the development of medications for chronic diseases and alternative therapies, which are more profitable and have higher demand (Kumar *et al*., 2018).

As alternatives to traditional antibiotic use, several approaches have been explored to combat antimicrobial resistance. Phage therapy, which uses specific bacteriophages to eliminate pathogenic bacteria, has gained attention due to its specificity and ability to overcome resistance. Additionally, antimicrobial peptides, natural molecules active against microorganisms, show promising therapeutic potential. The use of nanoparticles also emerges as an innovative strategy, facilitating targeted delivery of antimicrobial agents and enhancing their effectiveness. Vaccines specific to resistant pathogens represent another important preventive tool, reducing infection incidence. Lastly, microbiome modulators are being studied to restore bacterial balance and inhibit the growth of resistant strains, contributing to a more integrated approach to fighting resistance (Kumar *et al*., 2018; *Chis et al*., 2022).

Finally, the lack of educational campaigns, the absence of accurate data on antibiotic consumption, and poor sanitation conditions in many regions hinder the control of AMR. Public engagement is impaired by misinformation about the proper use of antimicrobials and the risks associated with self-medication. Combating AMR requires coordinated actions among governments, healthcare professionals, industry, and civil society to promote rational antibiotic use, foster research into new alternatives, and ensure adequate hygiene and treatment conditions (Chis *et al*., 2022).

2.2 Genus *Klebsiella*

The *Klebsiella* genus comprises encapsulated, non-motile, rod-shaped, oxidase-negative and Gram-negative bacteria that are widely distributed in the environment, in animals, and in humans (Figure 2). These bacteria belong to the Enterobacteriaceae family,

which includes several genera relevant to both the normal microbiota and clinical infections, such as *Escherichia*, *Salmonella*, *Enterobacter*, among others. The clinical relevance of the *Klebsiella* genus lies in its ability to cause opportunistic infections, particularly in hospitalized patients, and in its potential to develop resistance to multiple classes of antimicrobial agents (Dong *et al*., 2022).

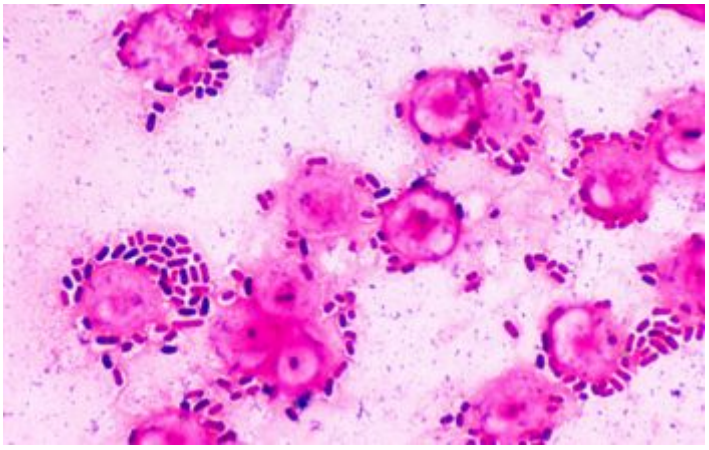

Figure 2. Erasmus MC. Klebsiella pneumoniae – Gram staining and characteristics. Available at: https://www.erasmusmc.nl/en/research/clinical-microbiology. Accessed on: Jun 26, 2025.

The most important species is *Klebsiella pneumoniae*, but other species such as *K. oxytoca*, *K. variicola*, *K. aerogenes*, and newly described species like *K. michiganensis* and *K. huaxiensis* have also gained prominence due to their involvement in human infections. Many of these species share similar phenotypic and genetic characteristics, making their differentiation by traditional methods difficult and requiring molecular and genomic approaches for accurate identification (Dong *et al*., 2022).

One of the main clinical challenges related to the *Klebsiella* genus is the increasing antimicrobial resistance observed among its isolates. The ability of these bacteria to acquire exogenous genetic material through mobile elements such as plasmids, transposons, and integrons facilitates the rapid spread of genes conferring resistance to various classes of antibiotics. This genetic plasticity has enabled the emergence of resistant strains that frequently exhibit resistance to critical antibiotics such as β-lactams (including carbapenems), aminoglycosides, quinolones, and polymyxins, thus limiting available therapeutic options (Zhu *et al*., 2021).

In the clinical context, multidrug-resistant clones from various *Klebsiella* species have been associated with hospital outbreaks and severe infections, especially in intensive care units. Some clonal complexes, such as CC258 and related groups, are widely distributed globally and are often responsible for the dissemination of resistance genes, including those encoding carbapenemases and other β-lactamase enzymes. This scenario represents a serious public health problem, as it complicates clinical management, increases mortality, and raises hospital costs (Russo *et al*., 2019).

Another concerning aspect is the emergence of strains that combine multidrug resistance with hypervirulence traits, resulting in isolates capable of causing invasive and hard-to-treat infections. Although the study of such strains has been more extensive in *K. pneumoniae*, recent reports have identified hypervirulent and multidrug-resistant strains in other species of the genus, such as *K. variicola* and *K. quasipneumoniae* (Dong *et al*., 2022).

Moreover, accurate identification of *Klebsiella* species and genotypic characterization of isolates are essential for epidemiological understanding, outbreak control, and treatment guidance. Modern techniques such as whole-genome sequencing, multilocus sequence typing (MLST), and mass spectrometry (MALDI-TOF) have significantly contributed to advances in this field, enabling the distinction between species and lineages with varying resistance and virulence profiles (Dong *et al*., 2022; Russo *et al*., 2019).

In summary, the *Klebsiella* genus represents a group of bacteria with a high clinical impact, whose taxonomic complexity and evolutionary capacity contribute to the spread of antimicrobial resistance and the emergence of multidrug-resistant hypervirulent clones. Tackling this challenge requires integrated efforts in microbiological surveillance, the development of new therapies, and effective infection control policies.

2.3 *Klebsiella pneumoniae*

Klebsiella pneumoniae is the most frequently isolated species in clinical settings within the *Klebsiella* genus, accounting for approximately 85% of hospital isolates. This microorganism is a significant opportunistic pathogen and is part of the ESKAPE group—a set of six bacterial species recognized by the World Health Organization as public health priorities due to their high virulence and treatment challenges posed by antimicrobial resistance (Dong *et al*., 2022). Two subspecies, *K. pneumoniae* subsp. *ozaenae* and *K. pneumoniae* subsp. *rhinoscleromatis*, are linked to specific syndromes such as atrophic

rhinitis and rhinoscleroma, and are considered hypervirulent clones derived from the main species (Russo *et al*., 2019).

The adaptive success of *K. pneumoniae* is largely attributed to its remarkable genetic plasticity. This bacterium is highly proficient in acquiring mobile genetic elements—such as plasmids, transposons, and integrons—which carry resistance genes and virulence factors. This capability has led to the emergence of two major pathotypes: the classical (cKP, classical *K. pneumoniae*) and the hypervirulent (hvKp). The former is widely known for its capacity to develop resistance to multiple classes of antibiotics, including last-resort drugs (Zhu *et al*., 2021).

To date, more than 100 acquired resistance genes have been described in clinical isolates of *K. pneumoniae*, conferring resistance to several antibiotic classes, including β-lactams (such as carbapenems), aminoglycosides, quinolones, tigecycline, and polymyxins (Zhu *et al*., 2021). The most common resistance mechanisms include:

- Production of β-lactamases, such as extended-spectrum β-lactamases (ESBLs), particularly *bla_CTX-M*, *bla_TEM*, *bla_SHV*, and, in more severe cases, carbapenemases like *bla_KPC*, *bla_NDM*, and *bla_OXA-48*;
- Altered membrane permeability, through loss of porins (e.g., OmpK35/36), and overexpression of efflux pumps;
- Plasmid-mediated quinolone resistance (PMQR), including genes such as *qnr* and *oqxAB*, which also contribute to multidrug resistance.

The most prevalent resistant clones include the clonal complex CC258—especially ST258, ST11, and ST512—which are widely disseminated in hospital environments and associated with carbapenemase production. Other clonal groups such as CG14/15, CG101, and CG147 have also been reported globally with high levels of resistance (Russo *et al*., 2019).

Concurrently, the hypervirulent variant (hvKp) has received growing attention since its initial description in the 1980s in the Asia-Pacific region. Unlike cKP, this variant can cause severe infections in previously healthy individuals, including pyogenic liver abscesses, necrotizing pneumonia, meningitis, endophthalmitis, and necrotizing fasciitis. A striking feature of hvKp is its capacity for metastatic spread to various tissues and organs—a phenomenon uncommon among enteric Gram-negative bacilli (Zhu *et al*., 2021).

Genetically, hvKp strains typically harbor virulence plasmids such as pLVPK, which encode (Dong *et al*., 2022; Russo *et al*., 2019):

- Regulators of the hypermucoid phenotype (*rmpA*, *rmpA2*);
- Potent siderophores, such as aerobactin (*iucABCD*) and salmochelin (*iroBCDN*);
- Genes like *peg-344* and other transporters involved in iron uptake and nutrient acquisition essential for bacterial survival and invasion.

Although initially described as distinct entities, in recent years, convergent isolates have emerged that combine both hypervirulence and multidrug resistance traits. These hybrid clones, known as MDR-hvKp, represent a growing threat. The coexistence of resistance and virulence genes within the same bacterial genome significantly increases the clinical severity of infections and drastically reduces therapeutic options (Russo *et al*., 2019).

The detection of these emerging clones in hospital outbreaks and community-acquired infections further burdens healthcare systems. Studies have shown that infections caused by multidrug-resistant *K. pneumoniae* are associated with higher mortality rates, longer hospital stays, and increased healthcare costs. The convergence of resistance and virulence, particularly in environments with excessive antibiotic use, such as hospitals and intensive care units, underscores the urgent need for genomic surveillance and stricter infection control measures (Dong *et al*., 2022; Zhu *et al*., 2021).

Moreover, hvKp and MDR-hvKp clones have already been reported in non-hospital environments, including isolates from pigs, cattle, and food products. This expands the potential for zoonotic transmission and highlights the importance of the "One Health" approach in containing this global threat (Zhu *et al*., 2021).

2.4 *Klebsiella pneumoniae* in livestock

Klebsiella pneumoniae is traditionally recognized as an opportunistic pathogen of clinical relevance in humans, responsible for severe hospital- and community-acquired infections. According to the Chinese antimicrobial resistance surveillance system (CARSS), it is the second most commonly isolated Gram-negative bacterium (Yang *et al*., 2019). However, a growing number of studies have highlighted its increasing importance in veterinary medicine, where it has been associated with a wide range of diseases in various

animal species, including pneumonia, bacteremia, and septicemia (Yang *et al*., 2019; Wareth *et al*., 2020).

The intensive and often indiscriminate use of antimicrobials in animal production has driven the emergence of multidrug-resistant (MDR), hypervirulent, and even pan-resistant strains of *K. pneumoniae*. These strains present a significant challenge to the prevention, control, and treatment of infections in livestock, particularly in swine, where the bacterium is increasingly being detected (Yang *et al*., 2019).

In a long-term study conducted by Ribeiro *et al*. (2022), 697 *Klebsiella* isolates from various animal species, including pigs, were analyzed over a 22-year period. The findings revealed the clinical diversity of infections and the recurrent presence of *K. pneumoniae* in respiratory, urinary, enteric, and systemic conditions. In pigs, the bacterium has been predominantly isolated from respiratory samples, underscoring its role in the complex etiology of respiratory diseases in intensive production systems.

Previous studies have detected *K. pneumoniae* in up to 84% of healthy pigs, suggesting its endemic presence as part of the gut microbiota, although the resistance profile of these strains is not always characterized. This subclinical colonization represents a silent reservoir of resistance genes and a potential starting point for infectious outbreaks under stress or immunosuppressive conditions in animals (Wareth *et al*., 2020).

The transmission of resistant strains between food-producing animals and humans is an increasing concern. MDR and extended-spectrum β-lactamase (ESBL)-producing *K. pneumoniae* strains have been reported in dogs, cats, horses, and pigs, with resistance genes such as *bla_CTX-M-15* and *bla_OXA-48* widely distributed across isolates from different origins. These strains share genetic characteristics with human isolates, raising the hypothesis of interspecies exchange through direct contact, shared environments, or the consumption of animal-derived products (Wareth *et al*., 2020).

In pigs specifically, intensified production practices, confinement, and prophylactic antibiotic use create ideal conditions for the selection of resistant strains. The excretion of MDR *K. pneumoniae* in swine waste and its subsequent application as fertilizer in agriculture further amplifies the environmental spread of resistance genes, linking animal, human, and environmental health within the One Health framework (Zhu *et al*., 2021; Dong *et al*., 2022).

Therefore, the occurrence of *K. pneumoniae* in livestock—particularly in pigs—represents a phenomenon with profound public health implications. Its adaptability, capacity to acquire resistance genes, and ability to circulate among humans, animals, and the

environment demand continuous surveillance, genomic monitoring, and integrated policies for the rational use of antimicrobials in agriculture.

2.5 Bacteriophages

Bacteriophages, or phages, are viruses that exclusively infect bacterial cells, recognizing their targets through a wide range of surface receptors such as carbohydrates, lipopolysaccharides, and proteins. The specificity of this interaction determines the host range of each phage, which can be quite narrow—in some cases, restricted to a single bacterial species or strain. This selectivity makes phages promising agents for therapeutic and biocontrol applications, while also presenting challenges related to bacterial diversity and the variability of target receptors (Batinovic *et al*., 2019).

Phage life cycles, classified as lytic and lysogenic, are key to both their ecological role and therapeutic potential. In the lytic cycle, the phage binds to the bacterial cell, injects its genetic material, and hijacks the host's machinery to produce new virions. This replication culminates in the lysis of the host cell and the release of new phages, which can then infect other bacteria as shown in figure 3 (Kasman *et al*., 2022 and Gaitero *et al*., 2021). In contrast, in the lysogenic cycle, the viral genome integrates into the bacterial DNA or remains as a plasmid, replicating silently alongside the host cell's genome. This latent state is known as a prophage, and the host cell is termed lysogenic. Environmental stimuli such as stress, UV radiation, or temperature fluctuations can trigger the activation of the prophage and the resumption of the lytic cycle (Figure 3) (Kasman *et al*., 2022).

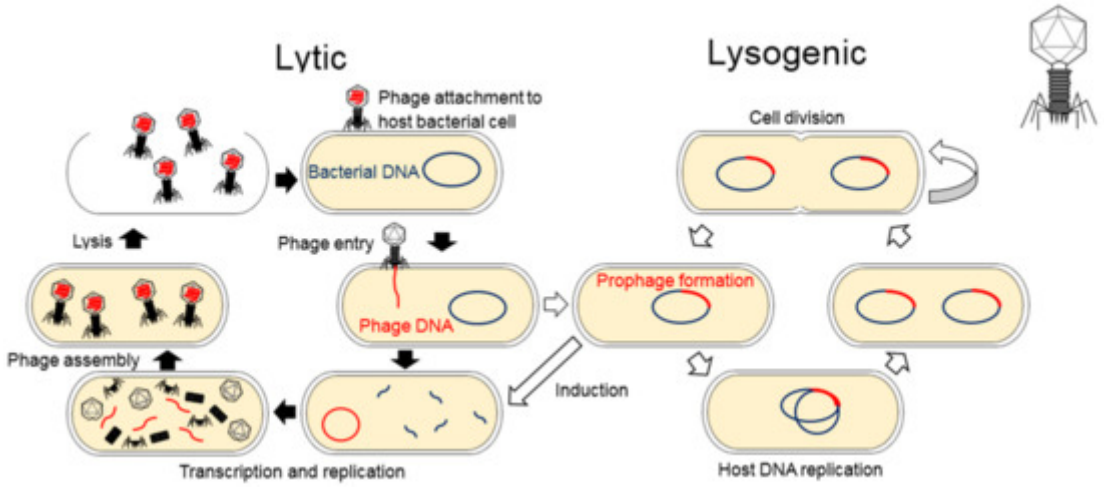

Figure 3. Lytic and lysogenic cycles of a bacteriophage. (Batinovic *et al*., 2019)

Beyond their direct impact on bacterial populations, phages play a critical role in horizontal gene transfer. Transduction, the process by which bacterial DNA fragments are transferred by phages to new cells, contributes significantly to bacterial genetic variability. Generalized transduction occurs during the lytic phase, when random fragments of bacterial DNA are mistakenly packaged into viral capsids. In specialized transduction, bacterial genes adjacent to the integrated viral genome are transferred during prophage excision. These processes not only facilitate bacterial adaptation but also reinforce the role of phages as evolutionary agents (Kasman *et al*., 2022).

In natural environments, phages are found in remarkable abundance and diversity. In the human body, they colonize various regions including the skin, oral cavity, intestines, urinary tract, and lungs. Outnumbering bacteria, phages help shape microbiota composition, particularly in mucosal regions where they can bind to mucin glycoproteins via the BAM mechanism (Bacteriophage Adherence to Mucus). This adhesion promotes protection against pathogens and helps maintain microbial balance. Studies suggest that phages can cross the epithelial barrier via transcytosis, directly influencing immune responses and regulating inflammatory processes. Alterations in the human virome have been associated with diseases such as type 1 diabetes and inflammatory bowel diseases, highlighting phages as potential biomarkers and emerging therapeutic agents (Batinovic *et al*., 2019 and Gaitero *et al*., 2021).

Outside the human body, phages are essential components of various ecosystems. In marine environments, they dominate the viral fraction. These phages regulate bacterial populations and influence biogeochemical cycles such as carbon and nitrogen. In deep ocean regions, where host diversity is lower, lysogenic phages are more common and perform specific ecological roles. In soil—though less studied—phages also play a critical role. They regulate microbial diversity, participate in nutrient cycling, and influence symbiotic interactions between roots and bacteria. Practical applications have been reported, such as the use of phages for controlling agricultural pathogens, evidenced in the case of *Dickeya solani* in potatoes. Advances in metagenomics have expanded our understanding of phage diversity and functional potential in these environments (Batinovic *et al*., 2019).

In the therapeutic field, bacteriophages have emerged as promising allies in addressing the crisis caused by bacterial resistance to antibiotics. Unlike conventional antimicrobials, phages exhibit high specificity, targeting only the pathogenic bacteria while preserving beneficial microbiota. This feature reduces side effects and dysbiosis commonly

associated with prolonged antibiotic use. Moreover, phages can replicate at the infection site, reducing the need for repeated doses and enhancing therapeutic efficacy. Even in hard-to-reach sites such as the central nervous system, phages have shown effectiveness, as demonstrated in neonatal meningitis models where early administration of a specific phage led to 100% survival in animals (Principi *et al*., 2019 and Gaitero *et al*., 2021).

Another notable advantage is their efficacy against biofilms - structures that confer resistance to bacterial antibiotics. Phages can be genetically engineered to express enzymes capable of degrading the biofilm matrix, improving their penetration and effectiveness. There are also efforts to modify phages to restore bacterial sensitivity to antibiotics. Furthermore, numerous studies have reported the safety of phage use in both humans and animals, with few or no significant side effects. Combining efficacy, specificity, safety, and lower cost, bacteriophages stand out as a realistic and complementary alternative to conventional antimicrobial therapy, particularly in a global context marked by the rise of multidrug-resistant bacteria (Principi *et al*., 2019).

3. MATERIALS AND METHODS

3.1 Experimental design

1. **Bacterial cultures:** Requirement for isolated cultures, confirmation of isolation, growth curves, CFU/ml, stock and minimum inhibitory concentration - MIC.
2. **Isolation of bacteriophages:** Collection of environmental samples, processing and enrichment, double-layer plaque assay, passages for isolation, propagation and titration.
3. **Selection of bacteriophages for the cocktail:** Host range, efficiency of plating (EOP), growth curves and biofilm prevention assay.
4. **Characterization:** Lysis plaque morphology, one-step growth curve, stability test and DNA extraction.
5. ***Galleria mellonella* model:** Median lethal dose - LD50, cocktail viability in larva, infection and cocktail.

The methodology for each experiment is described below.

3.2 Bacterial strains and their growth profiles

The bacterial cultures used in this study included *Klebsiella pneumoniae* (KPC+) and *Klebsiella oxytoca* (13182 ATCC), obtained from the collection of the Molecular Immunology Laboratory (LIVM). Cultures of *K. pneumoniae* (KP13, KP13-V, KP144, KP58B, KP220, KP39459, KP41061, KPcatheter, and KP5B), *K. oxytoca* (KO7170-2, KO3635), *Klebsiella variicola* (KV26E, KV7383), and *K. aerogenes* (KA38823) were also used, provided by the Laboratory of Bacterial Molecular Genetics (LGMB), the Veterinary Hospital of the Federal University of Viçosa, and the Brazilian Agricultural Research Corporation (Embrapa). In general, the isolates from these sources are of human and swine origin. All bacterial cultures were streaked on Chromagar medium for confirmation, grown in Luria-Bertani (LB) broth until reaching the exponential growth phase, and stored in glycerol at -80 °C for future use.

To determine the onset of bacterial proliferation and the logarithmic growth phase, bacterial growth curves were performed based on the protocol described by Sharma *et al.* (2021), with modifications. In 96-well polystyrene microplates, 200 µL of liquid Luria Bertani (LB) medium were added to the wells designated as controls. In the remaining wells, 180 µL of LB medium and 20 µL of bacterial suspension adjusted to an optical density (OD_{600}) of 0.1 were added, aiming for an initial OD_{600} of 0.01. The plates were incubated at 37 °C for 24 hours in a Multiskan Go microplate reader (Thermo Scientific), with optical density measurements taken every 15 minutes at a wavelength of 600 nm. All experiments were conducted in triplicate to ensure data reproducibility and analysis performed using GraphPad Prism.

3.3 Colony-forming unit (CFU) count

The colony-forming unit per milliliter (CFU/mL) counts were performed at two points in the bacterial growth curve, corresponding to optical densities at 600 nm (OD_{600}) of 0.1 and 0.3. An OD_{600} of 0.1 was selected to represent the early logarithmic phase, while an OD_{600} of 0.3 was chosen to represent a point during an exponential growth phase.

The bacteria were subjected to serial dilutions up to 10^5 and then plated using the spread-plate method. A volume of 100 µL from each dilution was spread onto Petri dishes containing solid LB agar. Inoculation was carried out using a Drigalski spatula, and the plates were incubated at 37 °C for 24 hours. CFU/mL counts were determined following the

methodology outlined in the 14th edition of Brock's Manual, utilizing two plates for each dilution.

3.4 Minimum inhibitory concentration (MIC)

For the determination of the minimum inhibitory concentration (MIC) of antibiotics against *Klebsiella pneumoniae* isolates, the microdilution method in 96-well plates was used, as described by Sani *et al*. (2023). Four commonly cited antibiotics in the literature were selected for testing: amikacin, ciprofloxacin, colistin, gentamicin, and tobramycin.

Initially, antibiotic dilutions were prepared based on the reference mentioned. In each well of the plate, 180 μL of LB medium were added, followed by 20 μL of the bacterial suspension. For the controls, 20 μL of the bacteria were used in the positive control, and only LB was used in the negative control. Then, 20 μL of the antibiotic dilutions in increasing concentrations were added until reaching the MIC.

After preparing the bacterial cultures, the plates were incubated in a Multiskan Go microplate reader (Thermo Scientific), with optical density (OD_{600}) measurements taken every 15 minutes. The incubation times were adjusted until the bacteria reached the start of the stationary phase, as determined by the previous growth data of the strains. The MIC was determined by the lowest antibiotic concentration that inhibited visible bacterial growth. Data were analyzed using GraphPad Prism (version 8.3.0), applying the multiple t-test – one per line – for group comparisons, as described in the software's statistical guide.

3.5 Environmental samples and bacteriophage isolation

Environmental samples were collected from various sources, including domestic and hospital sewage, frog farming systems, dairies, swine farms, lakes, and other aquatic and agro-industrial environments. The selection of these sources aimed to cover different ecological niches and enable the isolation of bacteriophages adapted to these diverse environments. After collection, the samples underwent a preliminary preparation process to concentrate the viral present. This process included centrifugation steps to remove larger solid particles and debris that could interfere with the analysis. Subsequently, the samples were subjected to filtration using filters with appropriate pore sizes to concentrate viruses, following the methodology described by Han *et al*. (2021), with adaptations performed to optimize the recovery of the agents of interest.

The bacteriophage isolation process was carried out as described by Horváth *et al*. (2020), with modifications. Briefly, 5 ml of processed environmental sample were added to 1 ml of bacterial culture in the logarithmic phase and 5 ml of concentrated LB medium, and the mixture was incubated at 37 °C for 24 hours with agitation at 100 rpm. Residual bacterial cells were removed by centrifugation (5000 rpm, 8 minutes), and the supernatant was sterile filtered using a 0.22 μm pore size filter. The phage suspensions were serially diluted in phosphate-buffered saline (PBS) and purified in three consecutive steps using the double agar overlay technique with 0.6% agar. Phage stocks were stored at +4 °C and used for subsequent characterization.

3.6 Lysis plaque morphology

The morphology of the lysis plaques was evaluated based on the protocol described by Li et al. (2021), using the double agar layer technique. For this, aliquots of previously titrated bacteriophages were inoculated into soft LB agar (0.7%). This mixture was poured onto plates containing previously prepared solid LB agar (1.5%). The plates were incubated at 37 °C for 24 hours. After incubation, the formation of lysis plaques was photographed, and morphological characteristics such as plaque size, border definition, and the presence of enzymatic halos—indicative of extracellular phage activity—were documented.

3.7 Host range

The host range of the isolated bacteriophages was determined using the spot test assay, as described by Liu *et al*. (2020), with modifications. Bacterial cultures in the logarithmic phase of growth were evenly spread on LB agar plates. Then, 10 μL of each phage suspension was carefully dropped onto the surface of the agar. Plates were incubated at 37 °C for 24 hours.

After incubation, the plates were examined for the presence of lysis zones. The appearance of clear halos indicated possible lytic activity against the tested bacterial strain. To confirm productive infection, a double-layer agar assay was performed, using 0.6% soft agar overlaid on a solid LB agar base. Only phage-host interactions that resulted in plaque formation in this confirmatory assay were considered effective infections.

3.8 Efficiency of plating (EOP)

To evaluate the infectivity of bacteriophages against non-host bacterial strains — i.e., those not originally used for phage isolation — the Efficiency of Plating (EOP) was determined. This analysis was performed for phages that produced visible lysis plaques on non-host strains using the double-layer agar method, as described by Mirzaei and Nilsson (2015), with adaptations.

Initially, phage titration was conducted on both the original host strains and the non-host test strains. The values of plaque-forming units per milliliter (PFU/mL) were used to calculate EOP using the following formula:

$$\text{EOP} = \frac{\text{PFU/mL on test strain}}{\text{PFU/mL on original host strain}}$$

In other words, the phage titer on the test strain was divided by the titer on the original host.

3.9 Growth curves with individual and combined bacteriophages

To evaluate the impact of bacteriophages on the growth dynamics of host and non-host bacteria, as well as to investigate potential interactions between different phages, bacterial growth curves were performed using six individually isolated phages against each bacterial strain, in addition to a combination of the most potential effective phages. The multiplicities of infection (MOIs) tested were 0.1, 1, and 10, following the protocol described by Sharma *et al*. (2021), with modifications.

The assays were conducted in 96-well microplates. For the control wells, 200 µL of sterile liquid LB medium was added. In the bacterial treatments, 180 µL of LB medium and 20 µL of a standardized bacterial suspension with an optical density (OD) of 0.1—corresponding to the early exponential growth phase as previously determined—were used. For the phage treatments, each well received 160 µL of LB medium, 20 µL of the bacterial suspension (OD 0.1), and 20 µL of bacteriophages, either individually or in combination.

The phage combination included KP4, KP6, KP7, and KP8, selected based on promising individual results against *Klebsiella pneumoniae* strains. After preparing the bacterial cultures, the plates were incubated in a Multiskan Go microplate reader (Thermo Scientific), with optical density (OD600) measurements taken every 15 minutes. The

incubation times were adjusted until the bacteria reached the onset of the stationary phase, as determined by previous growth data of the strains. The data were analyzed using GraphPad Prism (version 8.3.0) applying the multiple t test – one per row procedure for group comparisons, as described in the software's statistical guide.

3.10 Biofilm prevention assay

The biofilm prevention assays followed the protocol described by Liu *et al*. (2020), with adaptations. The experiment was carried out using 96-well microtiter plates. The control groups consisted of: (i) LB culture medium only and (ii) bacteria in LB medium without the addition of bacteriophages. For the treatment groups, individual bacteriophages or a cocktail (composed of KP4, KP6, KP7, and KP8) were used at three different multiplicities of infection (MOI): 0.1, 1, and 10, added together with the bacteria and LB medium. The plates were incubated at 37 °C for 24 hours.

After incubation, the biofilms formed in each well were fixed with 200 µL of 99% methanol for 15 minutes. The wells were then air-dried and stained with 1% crystal violet for 10 minutes. Excess dye was removed by washing with phosphate-buffered saline (PBS), and the plates were dried again. The bound crystal violet was then solubilized with 200 µL of a 80:20 acetone/ethanol solution for 10 minutes. Finally, absorbance was measured at 595 nm using a microplate reader.

Data analysis was performed using GraphPad Prism software. The graphs were generated based on absorbance values, and statistical comparisons between groups were conducted using Student's t-test, with a significance level of $p < 0.05$.

3.11 One-step growth curve

The one-step growth curve will be performed to determine the latency period, which corresponds to the time the bacteriophage takes to lyse the host cell after adsorption, and the burst size, i.e., the number of viral particles released during each bacterial lysis. The experiment will follow the protocol described by Horváth *et al*. (2020), with modifications.

Briefly, 5 mL of exponentially growing bacterial culture and 50 µL of phage suspension (10^7 PFU/mL) will be mixed (MOI 0.1). Phages will be allowed to adsorb for 10 minutes at 37 °C in a shaking incubator (100 RPM), and then the mixture will be centrifuged at 10,000 RPM for 10 minutes to remove unadsorbed phages. The pellet will be resuspended

in 5 mL of liquid LB medium and incubated at 37 °C in a shaking incubator (100 RPM). Samples of 100 µL will be collected at 10-minute intervals from 0 to 60 minutes. Phage titers will be estimated by spotting serial dilutions on agar plates using the double-layer agar (DLA) method and incubating overnight (24 h) at 37 °C. The resulting data will be analyzed using GraphPad Prism software for graph construction.

3.12 Phage tolerance to temperature and pH

Thermal and pH tolerance tests were performed based on the protocol described by Chen et al. (2023), with modifications. The thermal stability of the phage was assessed after incubation for 1 hour at -20 °C, 4 °C, 25 °C, 37 °C, 50 °C, and 60 °C, and for 5 minutes at 70 °C and 80 °C. Subsequently, the phage titer was determined using the double-layer agar method. The T-test was used to compare the treatment groups with the control group.

To evaluate stability at different pH levels, SM buffer was prepared and adjusted to pH values ranging from 2 to 12. For each pH condition, 100 µL of phage suspension was mixed with 900 µL of the corresponding SM buffer. The mixtures were incubated at 37 °C for 1 hour, and then the phage titer was determined using the double-layer agar method. The T-test was used to compare the treatment groups with the control group.

3.13 Viral DNA extraction and sequencing

DNA extraction was performed on all seven isolated bacteriophages; however, only the four phages composing the cocktail were sent for sequencing on the Illumina platform. The extraction followed the PCI/SDS protocol (phenol-chloroform/sodium dodecyl sulfate solution). After infecting bacterial cells, the phages were released into the culture medium, and the suspension was treated with SDS to denature proteins and disrupt the phage membranes. Phenol-chloroform was added to separate the aqueous phase (containing the DNA) from the organic phase, and the DNA was precipitated using ethanol or isopropanol. The quality of the extracted DNA was verified by agarose gel electrophoresis, and quantification was performed using the Nanodrop Lite and Qubit Fluorometer. Sequencing involved library preparation, including DNA fragmentation and adapter ligation, followed by high-throughput sequencing. The generated data were bioinformatically analyzed for genome assembly and sequence annotation, enabling a detailed study of the bacteriophages.

3.14 In vivo tests with *Galleria mellonella*

The experiments with *Galleria mellonella* followed the protocol of Nale *et al*., 2020 with modifications.

Median lethal dose (LD_{50}) determination

The first step involved calculating the median lethal dose (LD_{50}), defined as the bacterial inoculum concentration capable of killing approximately 50% of the larvae in each group within 24 hours. For this purpose, we selected larvae weighing approximately 0.25–0.30 g and surface-sterilized them using cotton swabs soaked in 70% ethanol. We then administered a single 10 µL dose containing 10^5, 10^4, 10^3, or 10^2 colony-forming units (CFU) of the bacterial strain KP58B to duplicated groups of ten larvae per dose, injected into the last left posterior proleg. The infected larvae were incubated at 37 °C for 24 hours. We assessed bacterial colonization impact using a live/dead evaluation, considering larvae that remained motionless and entirely black as dead. The concentration that killed approximately half of the larval population within this period was designated the LD_{50}. This dose was then used to initiate colonization of each bacterial strain in the in vivo phage therapy experiments.

Phage cocktail viability in larvae

To optimize the infection model, it was essential to verify the stability of phages within the larvae's hemolymph to ensure therapeutic efficacy. Phage stability and survival in the infection model were determined for the proposed experimental duration of 72 h. Each larva was treated with approximately 10^7 PFU of the phage cocktail suspension (10 µL), with ten larvae being analyzed at each time point: 0, 24, 48, and 72 hours. The treated insects were incubated as described. Larval survival and phage counts in the hemolymph were measured. The data were analyzed using GraphPad Prism, and all in vivo experiments were performed at least twice.

Infection and phage cocktail

For each of the three phage therapy regimens — coinfection, corrective, and prophylactic — we conducted separate experiments using the KP58B bacterial strain. Each

regimen involved 10 larvae per time point (0, 24, 48, and 72 hours) and included two controls: a bacterial control and a phage control. In the coinfection regimen, larvae received, simultaneously at time zero, 10 µL of the LD_{50} dose of KP58B and 10 µL of the phage cocktail (MOI 0.1). As controls, one group was treated only with the same dose of KP58B at time zero followed by 10 µL of PBS (bacterial control), and another group received only 10 µL of the phage cocktail at time zero followed by LB (phage control). In the prophylactic regimen, larvae received 10 µL of the phage cocktail at time zero and, after 2 hours, received 10 µL of the LD_{50} dose of KP58B. The same bacterial and phage controls were applied, with respective administration of KP58B + LB and phages + LB. In the corrective regimen, larvae received 10 µL of the LD_{50} dose of KP58B at time zero and, after 2 hours, received 10 µL of the phage cocktail. Controls were identical to those of the coinfection regimen, with the bacterial control receiving KP58B followed by LB, and the phage control receiving phages followed by LB. After each treatment, all larvae were incubated at 37 °C, without food, for up to 72 hours. At each time point, we recorded larval survival, and quantified bacteria (CFU/mL) and phages (PFU/mL). For this purpose, the hemolymph was homogenized, centrifuged at 5,000 g for 10 minutes at 4 °C, filtered, and subjected to double-layer plaque assays and spread-plating. The data were then analyzed using GraphPad Prism, and all experiments were performed with at least two independent replicates.

4. RESULTS

Bacterial strains and their growth profiles

All 16 selected bacterial strains were successfully recovered and showed characteristic growth on Chromagar medium, with colonies displaying a dark blue coloration, a typical pattern for the *Klebsiella* genus (CHROMagar, 2024). This result confirmed the viability and presumed identity of the isolates. Based on the growth curves established in this study, it was determined that a point corresponding to the exponential growth phase was an optical density (OD) of approximately 0.3, as shown in Figure 4 - A and B. This value was therefore adopted as a reference for preparing the bacterial stocks. The cultures were then stored in 20% glycerol at -80 °C for use in subsequent experimental procedures.

A. B.

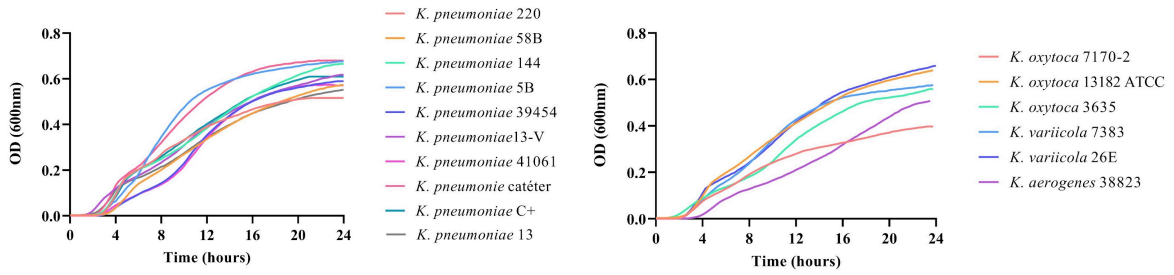

Figure 4. Growth curves obtained in 96-well plates using liquid LB medium at 37°C for 24 hours, with a ratio of 180µL of medium to 20µL of bacterial inoculum. The analyses were performed for strains of the *Klebsiella* genus: A. *Klebsiella pneumoniae* and B. *Klebsiella* sp.

Colony-forming unit (CFU) count

The colony-forming unit (CFU/mL) count was performed for all bacterial strains, as it was necessary for the subsequent bacterial growth curve assays in combination with bacteriophages. The measurements were taken at an optical density (OD) of 0.1 at 600 nm, with an average of approximately 10^7 CFU/mL. For the strains KP58B, KP13, and KP5B, the count was performed at an OD of 0.3 at 600 nm. This was done only for these three strains because they are the hosts of the phages selected to be part of the cocktail, and this OD was required for the characterization of those phages. This OD also showed an average close to 10^7 CFU/mL. The table below presents the results obtained.

Table 1. Colony-forming unit (CFU/mL) counts of the *Klebsiella* strains used in this study. The counts were performed under two conditions: for all strains at an optical density (OD) of 0.1, corresponding to the beginning of the exponential growth phase; and specifically for strains KP58B, KP13, and KP5B — which are hosts of the bacteriophages selected for the phage cocktail — also at an OD of 0.3, a value used in the phage characterization assays.

Strain	OD600 0.1 (Log phase start)	OD600 0.3 (Log phase)
K. pneumoniae 220	2,4 10^7 CFU/mL	-
K. pneumoniae 58B	9,4 10^6 CFU/mL	6,1 10^7 CFU/mL
K. pneumoniae 144	6,0 10^7 CFU/mL	-
K. pneumoniae 5B	8,5 10^6 CFU/mL	1,7 10^7 CFU/mL
K. pneumoniae 39459	3,6 10^7 CFU/mL	-
K. pneumoniae 13-V	1,9 10^7 CFU/mL	-
K. pneumoniae 41061	2,7 10^7 CFU/mL	-
K. pneumoniae catheter	2,4 10^7 CFU/mL	-
K. pneumoniae C+	2,8 10^7 CFU/mL	-
K. pneumoniae 13	2,0 10^7 CFU/mL	5,0 10^7 CFU/mL
K. oxytoca 7170-2	3,0 10^7 CFU/mL	-
K. oxytoca 13182 ATCC	2,3 10^7 CFU/mL	-
K. oxytoca 3635	3,8 10^7 CFU/mL	-
K. variicola 7383	3,9 10^7 CFU/mL	-
K. variicola 26E	2,6 10^7 CFU/mL	-
K. aerogenes 38823	7,0 10^7 CFU/mL	-

Minimum inhibitory concentration (MIC)

The MIC results for the *Klebsiella pneumoniae* isolates (KP58B, KP5B, and KP13) revealed varied resistance profiles. It is important to note that these isolates were the hosts of the phages composing the cocktail developed in this study, with direct implications for therapeutic decisions and bacteriophage cocktail development. First, all isolates showed universal resistance to tobramycin, with MICs ranging from 50 to 20,000 mg/L — values well above the EUCAST breakpoint (R > 2 mg/L) — making this aminoglycoside completely unsuitable for clinical use or phage–antibiotic combination therapies. Isolate KP13 also exhibited resistance to amikacin (MIC between 250–500 mg/L, EUCAST breakpoint R > 10 mg/L), while isolates KP58B and KP5B remained sensitive to this antibiotic. All three isolates were sensitive to ciprofloxacin, colistin, and gentamicin. The generated curves can be found in the appendix of this work, and the resistance and sensitivity results are shown in Table 2 below.

Table 2. Antibiotic resistance and sensitivity profiles of the *Klebsiella pneumoniae* strains KP13, KP58B, and KP5B tested. The table presents the minimum inhibitory concentration (MIC) results for each antibiotic evaluated, highlighting resistance and susceptibility patterns that are critical for guiding therapeutic strategies and the development of bacteriophage-based treatments.

Isolate	Antibiotic	MIC range (mg/L)	EUCAST breakpoints (mg/L)	Interpretation
K. pneumoniae 58B	Amikacin	3.12–6.25	S ≤ 8; R > 8	S (Sensitive)
	Ciprofloxacin	0.065–0.125	S ≤ 0.25; R > 0.5	S (Sensitive)
	Colistin	0.05–0.1	S ≤ 2; R > 2	S (Low)
	Gentamicin	0.00125–0.0025	S ≤ 2; R > 2	S (Sensitive)
	Tobramycin	50-100	S ≤ 2; R > 2	R (Resistant)
K. pneumoniae 5B	Amikacin	0.4–0.8	S ≤ 8; R > 8	S (Sensitive)
	Ciprofloxacin	0.008–0.015	S ≤ 0.25; R > 0.5	S (Sensitive)
	Colistin	0.05–0.1	S ≤ 2; R > 2	S (Low)
	Gentamicin	0.002–0.004	S ≤ 2; R > 2	S (Sensitive)
	Tobramycin	10000-20000	S ≤ 2; R > 2	R (Resistant)
K. pneumoniae 13	Amikacin	250–500	S ≤ 8; R > 8	R (Resistant)
	Ciprofloxacin	0.065–0.125	S ≤ 0.25; R > 0.5	S (Sensitive)
	Colistin	0.4–0.8	S ≤ 2; R > 2	S (Sensitive)
	Gentamicin	1–2	S ≤ 2; R > 2	S (Sensitive)
	Tobramycin	6-12	S ≤ 2; R > 2	R (Resistant)

S ≤: The MIC value is equal to or below the cutoff for sensitive and R >: The MIC value is above the cutoff for resistance.

Bacteriophage isolation

Seven bacteriophages were isolated for *Klebsiella* spp., named according to their host and isolation sequence: KO2 (host bacterium KO13182), KV3 (host bacterium KV26E), KP4 (host bacterium KP13), KP6 (host bacterium KP58B), KP7 (host bacterium KP58B), KP8 (host bacterium KP5B), and KP9 (host bacterium KP5B). Phages KO2, KV3, and KP4 were isolated from sewage collected in the São Bartolomeu River in the city of Viçosa, Minas Gerais. The remaining phages were isolated from samples from the pig farm of the Federal University of Viçosa.

Host range

Among the phages tested, two results were consistent in both assays. Phage KP4, originally isolated using the KP13 host strain, also lysed on the KP220 strain, as observed in both the spot test and the bilayer assay, confirming its infectivity. Similarly, phage KP6, whose host is the KP58B strain, was able to lyse the KP39459 strain in both tests. Other phages showed lysis halos in the spot test against non-host and nonspecific strains (Table 3 and 5), providing potential lytic activity. However, these results were not confirmed in the bilayer assay, suggesting that the observed lysis may have been due to nonspecific effects.

Table 3. Host range analysis of bacteriophages using the spot test method on various *Klebsiella* sp. strains. This table summarizes the ability of each phage to produce lysis zones on different bacterial strains, indicating their infectivity spectrum.

Strain	Phage KO2	Phage KV3	Phage KP4	Phage KP6	Phage KP7	Phage KP8	Phage KP9
K. pneumoniae 220	-	-	Yes	-	-	-	-
K. pneumoniae 58B	-	-	-	-	-	-	-
K. pneumoniae 144	-	-	-	Host strain	Host strain	-	-
K. pneumoniae 5B	-	-	-	-	-	Host strain	Host strain
K. pneumoniae 39459	-	-	-	Yes	-	-	-
K. pneumoniae 13-V	-	-	-	-	-	-	-
K. pneumoniae 41061	-	-	-	-	-	-	-
K. pneumoniae catheter	-	-	-	-	-	-	-
K. pneumoniae C+	-	-	-	-	-	-	-
K. pneumoniae 13	-	-	Host strain	-	-	-	-
K. oxytoca 7170-2	-	-	-	Yes	Yes	-	-
K. oxytoca 13182 ATCC	Host strain	-	-	-	-	-	-
K. oxytoca 3635	-	-	-	-	-	-	-
K. variicola 7383	-	-	-	-	-	-	-
K. variicola 26E	-	Host strain	Yes	-	-	-	-
K. aerogenes 38823	-	-	-	-	-	-	-

(+) positive result and (–) negative result.

Table 4. Confirmation of the host range of bacteriophages through the double-layer plating assay on *Klebsiella* sp. strains. This table presents results validating the ability of the phages to infect and lyse different bacterial strains, as evidenced by plaque formation in the assay. These data are essential to confirm the specificity and therapeutic potential of the selected phages.

Strain	Phage KO2	Phage KV3	Phage KP4	Phage KP6	Phage KP7	Phage KP8	Phage KP9
K. pneumoniae 220	-	-	Yes	-	-	-	-
K. pneumoniae 58B	-	-	-	-	-	-	-
K. pneumoniae 144	-	-	-	Host strain	Host strain	-	-
K. pneumoniae 5B	-	-	-	-	-	Host strain	Host strain
K. pneumoniae 39459	-	-	-	Yes	-	-	-
K. pneumoniae 13-V	-	-	-	-	-	-	-
K. pneumoniae 41061	-	-	-	-	-	-	-
K. pneumoniae catheter	-	-	-	-	-	-	-
K. pneumoniae C+	-	-	-	-	-	-	-
K. pneumoniae 13	-	-	Host strain	-	-	-	-
K. oxytoca 7170-2	-	-	-	-	-	-	-
K. oxytoca 13182 ATCC	Host strain	-	-	-	-	-	-
K. oxytoca 3635	-	-	-	-	-	-	-
K. variicola 7383	-	-	-	-	-	-	-
K. variicola 26E	-	Host strain	-	-	-	-	-
K. aerogenes 38823	-	-	-	-	-	-	-

(+) positive result and (–) negative result.

Table 5. Evaluation of the nonspecific host range of bacteriophages using the spot test on *Escherichia coli* and *Salmonella* sp. strains. This table presents the results regarding the

phages' ability to cause lysis in strains from genera different from *Klebsiella*, indicating possible nonspecific effects or a broad lytic activity spectrum. These data are important to assess the safety and specificity of the phages, especially in the context of therapeutic and biotechnological applications.

Strain	Phage KP4	Phage KP6	Phage KP7	Phage KP8
E. coli 20	-	-	-	-
E. coli 011	Yes	-	-	-
E. coli 8D	-	-	-	-
E. coli CDC	-	-	-	-
E. coli 29213	Yes	-	-	-
E. coli 246	Yes	-	-	-
E. coli 3010	-	-	-	-
E. coli SAN1	-	-	-	-
E. coli 29231	-	-	-	-
E. coli 4	-	-	-	-
E. coli K12	Yes	-	-	-
E. coli 304	-	-	-	-
E. coli 286	-	-	-	-
E. coli AY2	-	-	-	-
E. coli 8095	Yes	-	-	-
E. coli AY4	-	-	-	-
E. coli SAN3	-	-	-	-
E. coli 11C	Yes	-	-	-
E. coli 25293	-	-	-	-
E. coli 4A	-	-	-	-
E. coli 30	Yes	-	-	-
S. minnesota 64	-	-	-	-
S. minnesota 65	-	-	-	-
S. heidelberg 65	-	-	-	-
S. heidelberg 63	-	-	-	-
S. mbandaka 166	-	-	-	-
S. mbandaka 188	-	-	-	-
S. typhimurium	-	-	-	-
S. enteritidis	-	-	-	-

(+) positive result and (–) negative result.

Efficiency of plating (EOP)

The efficiency of plating (EOP) is a key parameter for assessing a bacteriophage's ability to infect different bacterial strains. According to Mirzaei and Nilsson (2015), an EOP equal to or below 0.001 (10^{-3}) is considered indicative of inefficient or limited infection, suggesting low replication efficiency of the phage in the test strain. In this study, both evaluated phages KP4 and KP6 exhibited EOP values well below this threshold. Phage KP4 showed an EOP of 3.6×10^{-5} against strain KP220, while KP6 showed an even lower EOP of

4.8×10^{-7} against strain KP39459. These results indicate that although plaque formation was observed on non-host strains, the infection was highly inefficient.

1. **Phage KP4**

Titer on host strain (KP13): 2.0×10^{9} PFU/mL
Titer on test strain (KP220): 7.2×10^{4} PFU/mL
EOP: 3.6×10^{-5}

2. **Phage KP6**

Titer on host strain (KP58B): 1.0×10^{9} PFU/mL
Titer on test strain (KP39459): 4.8×10^{2} PFU/mL
EOP: 4.8×10^{-7}

Growth Curves with Individual and Combined Bacteriophages

The lytic activity of individual and combined bacteriophages against *Klebsiella* strains was evaluated at different multiplicities of infection (MOIs). The results revealed distinct lytic profiles depending on the host strain and MOI (Figure 5 and 6). Phage KO2 showed consistent and significant lysis of its primary host (KO13182 ATCC) at all tested MOIs, with no effect on other strains, indicating a narrow host range. Phage KV3 did not induce statistically significant lysis in its host, possibly due to a temperate nature or assay variability. Phages KP4, KP6, KP7, KP8, and KP9 demonstrated significant lytic activity against their respective primary hosts across all MOIs. Some also affected non-primary strains at higher MOIs, suggesting varying degrees of host specificity. The phage cocktail composed of KP4, KP6, KP7, and KP8 exhibited broad and significant lytic activity against all tested host strains (KP13, KP5B, KP58B, KP220), in figure 7, at all MOIs over a 21-hour observation period. This highlights the potential advantage of combining phages with diverse host ranges and replication dynamics to enhance therapeutic efficacy. The growth curves supporting these findings are presented throughout the main text, while those that did not show significant differences between treatments are included in appendix.

A. B.

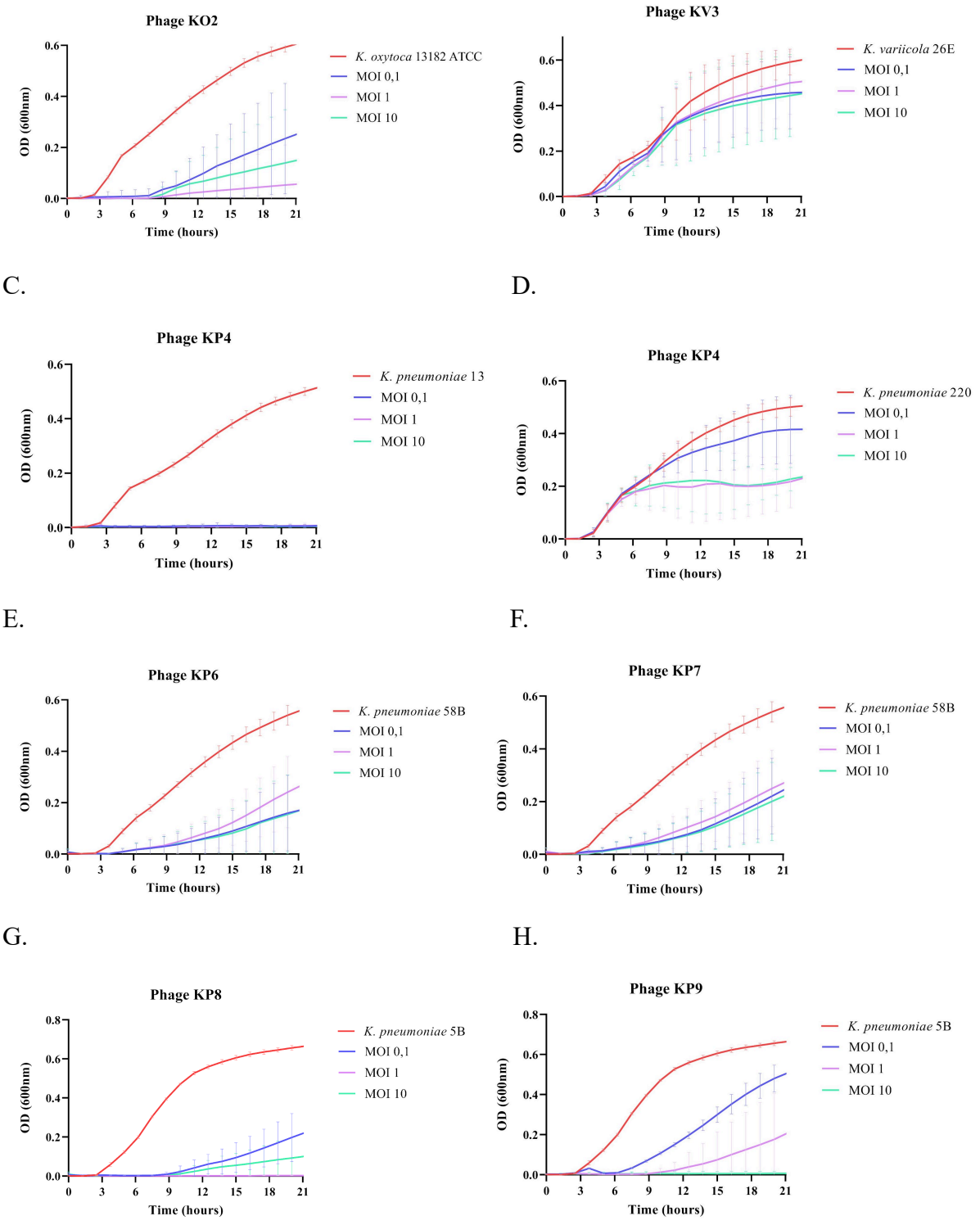

Figure 5. Bacterial growth curves in the presence and absence of bacteriophages, performed in 96-well plates using LB medium. The analyses were conducted with all *Klebsiella* strains, each combined with its respective host phage. The curves show the bacterial growth dynamics over time, highlighting the impact of phage infection on the reduction of optical density (OD600), indicating the lytic activity of the phages against their host strains.

A.

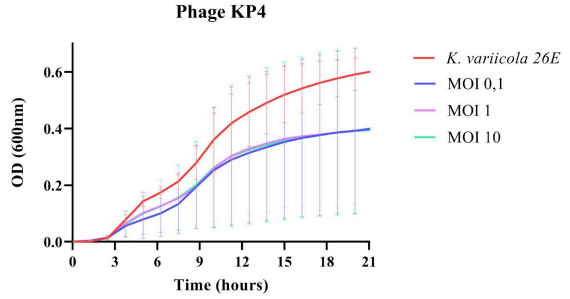

B.

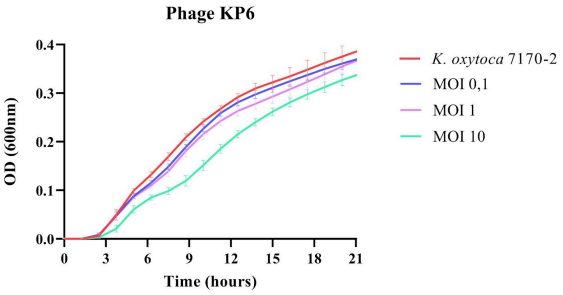

C.

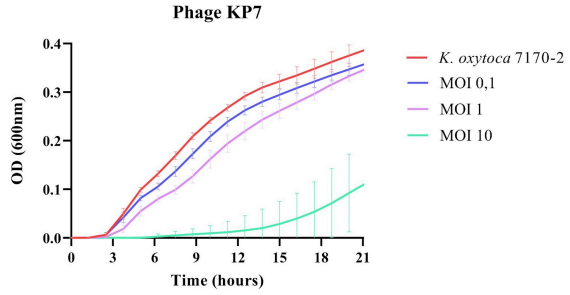

Figure 6. Bacterial growth curves in the presence and absence of bacteriophages, performed in 96-well plates using LB medium. The analyses were conducted with *Klebsiella* strains that showed only nonspecific effects, without plaque formation in previous plating assays. The curves demonstrate a reduction in bacterial growth over time, suggesting a possible inhibitory effect, although without confirmation of typical lytic activity. Only the graphs showing this type of response are presented in this figure; the remaining growth curves are included in appendix of this work.

A.

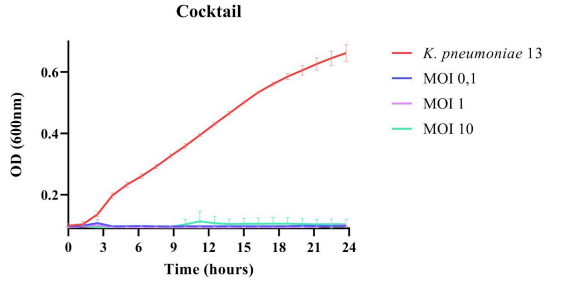

B.

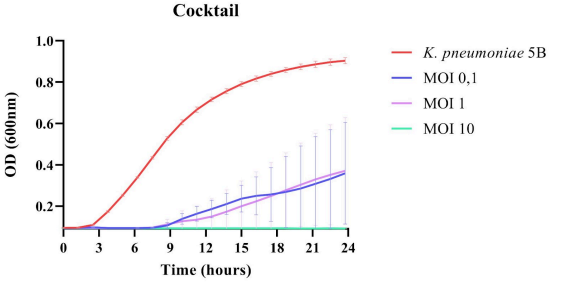

C.

D.

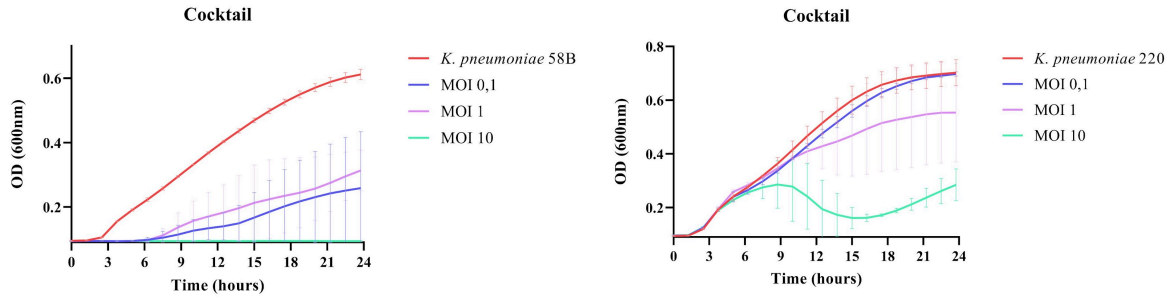

Figure 7. Bacterial growth curves in the presence and absence of the phage cocktail composed of KP4, KP6, KP7, and KP8, performed in 96-well plates using LB medium. The analyses were conducted with all *Klebsiella* strains used in the study, evaluating the cocktail's ability to inhibit bacterial growth over time. The graphs presented in this figure correspond to positive results, where a significant reduction in optical density (OD600) compared to the bacterial control was observed. Curves that did not show significant differences compared to the control are included in appendix of this work.

Biofilm prevention assay

The seven bacteriophages isolated (KO2, KV3, KP4, KP6, KP7, KP8, and KP9) surpassed the ability to reduce biofilm formation in at least two of the 16 bacterial strains tested. Detailed results are presented in the accompanying graphs (Figure 8). The most significant impact on biofilm reduction was generally distributed across the host strains of the respective phages, providing greater efficacy against the target bacteria from which they were originally isolated. Therefore, taking advantage of the growth curves and results of this test, the following experiments were performed with those with the greatest potential: KP4, KP6, KP7, and KP8 (Figure 9). The other graphs that showed no statistically significant difference compared to the control are included in the appendix of this work.

A. B. C.

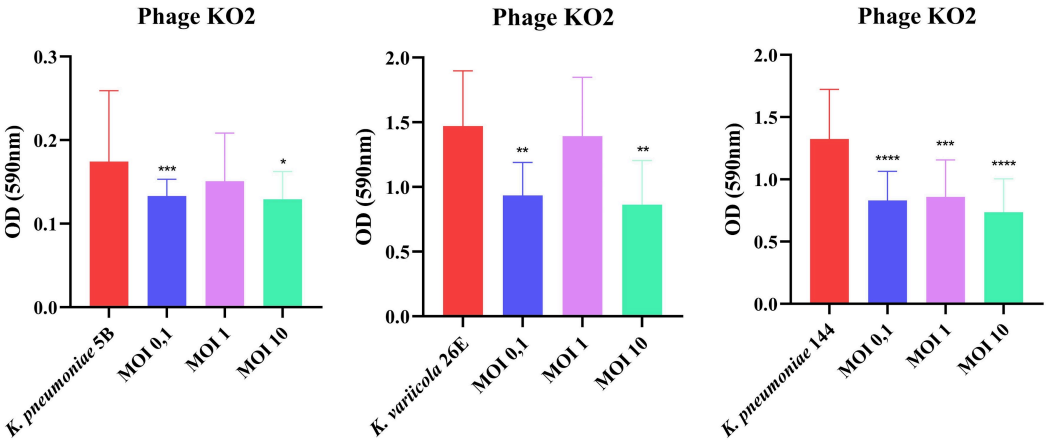
Phage KO2
OD (590nm)
0.3
0.2
0.1
0.0
***
*
K. pneumoniae 5B
MOI 0,1
MOI 1
MOI 10

D.

Phage KO2
OD (590nm)
2.0
1.5
1.0
0.5
0.0
**
**
K. varicola 26E
MOI 0,1
MOI 1
MOI 10

E.

Phage KO2
OD (590nm)
2.0
1.5
1.0
0.5
0.0
****
***
****
K. pneumoniae 144
MOI 0,1
MOI 1
MOI 10

F.

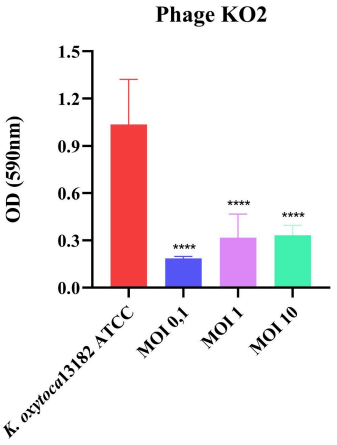
Phage KO2
OD (590nm)
1.5
1.2
0.9
0.6
0.3
0.0
****
****
K. oxytoca13182 ATCC
MOI 0,1
MOI 1
MOI 10

G.

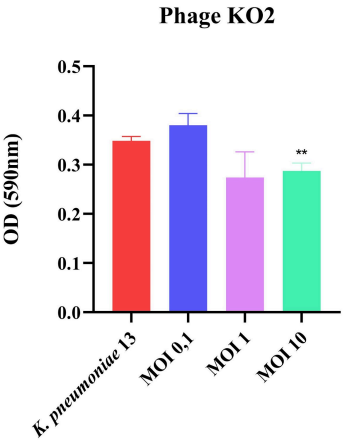
Phage KO2
OD (590nm)
0.5
0.4
0.3
0.2
0.1
0.0
**
K. pneumoniae 13
MOI 0,1
MOI 1
MOI 10

H.

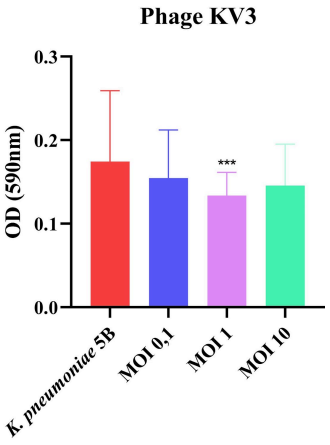
Phage KV3
OD (590nm)
0.3
0.2
0.1
0.0
***
K. pneumoniae 5B
MOI 0,1
MOI 1
MOI 10

I.

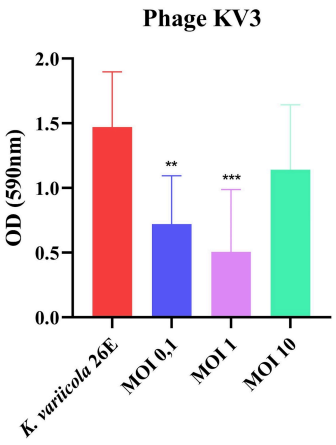
Phage KV3
OD (590nm)
2.0
1.5
1.0
0.5
0.0
**
***
K. varicola 26E
MOI 0,1
MOI 1
MOI 10

J.

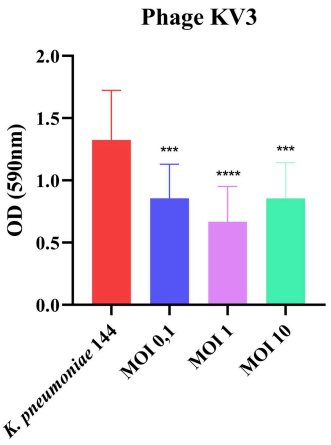
Phage KV3
OD (590nm)
2.0
1.5
1.0
0.5
0.0
***
****
***
K. pneumoniae 144
MOI 0,1
MOI 1
MOI 10

K.

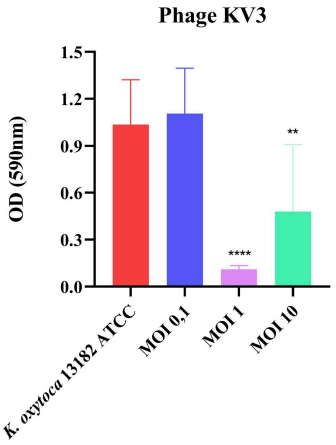
Phage KV3
OD (590nm)
1.5
1.2
0.9
0.6
0.3
0.0
**
****
K. oxytoca 13182 ATCC
MOI 0,1
MOI 1
MOI 10

L.

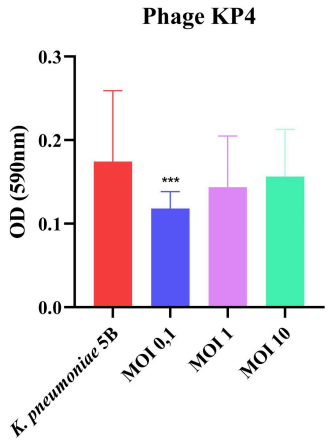
Phage KP4
OD (590nm)
0.3
0.2
0.1
0.0
***
K. pneumoniae 5B
MOI 0,1
MOI 1
MOI 10

M.

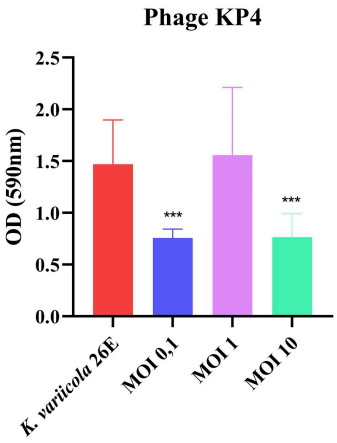
Phage KP4
OD (590nm)
2.5
2.0
1.5
1.0
0.5
0.0
***
***
K. variicola 26E
MOI 0,1
MOI 1
MOI 10

N.

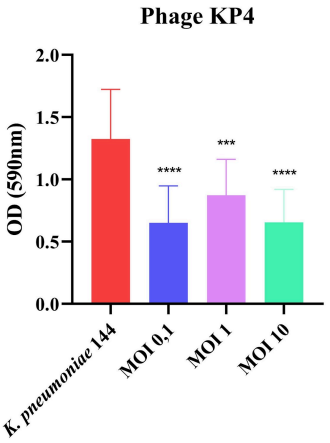
Phage KP4
OD (590nm)
2.0
1.5
1.0
0.5
0.0
****
***
****
K. pneumoniae 144
MOI 0,1
MOI 1
MOI 10

O.

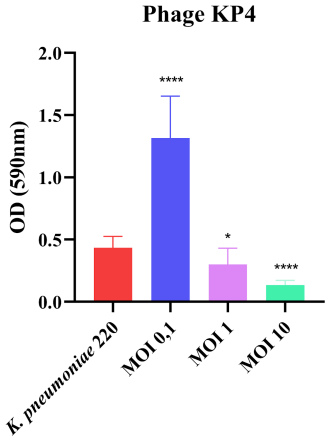
Phage KP4
OD (590nm)
2.0
1.5
1.0
0.5
0.0
****
*
****
K. pneumoniae 220
MOI 0,1
MOI 1
MOI 10

P.

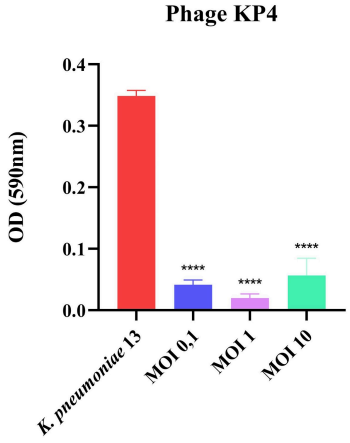
Phage KP4
OD (590nm)
0.4
0.3
0.2
0.1
0.0
****
****
****
K. pneumoniae 13
MOI 0,1
MOI 1
MOI 10

Q.

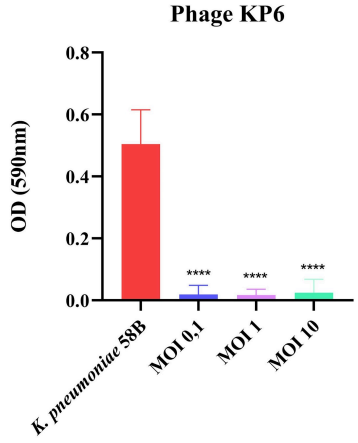
Phage KP6
OD (590nm)
0.8
0.6
0.4
0.2
0.0
****
****
****
K. pneumoniae 58B
MOI 0,1
MOI 1
MOI 10

R.

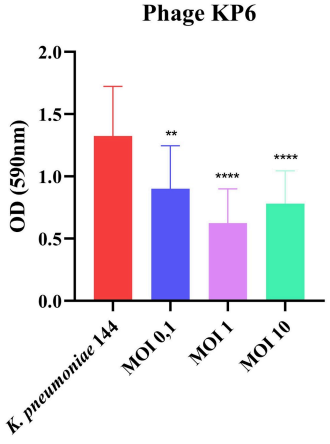
Phage KP6
OD (590nm)
2.0
1.5
1.0
0.5
0.0
**
****
****
K. pneumoniae 144
MOI 0,1
MOI 1
MOI 10

S.

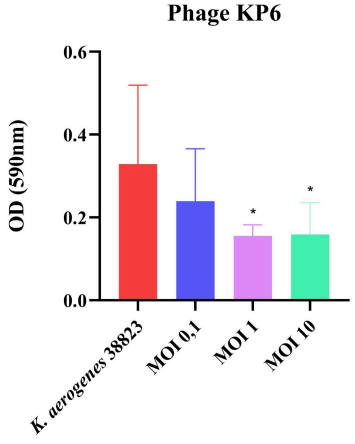
Phage KP6
OD (590nm)
0.6
0.4
0.2
0.0
*
*
K. aerogenes 38823
MOI 0,1
MOI 1
MOI 10

T.

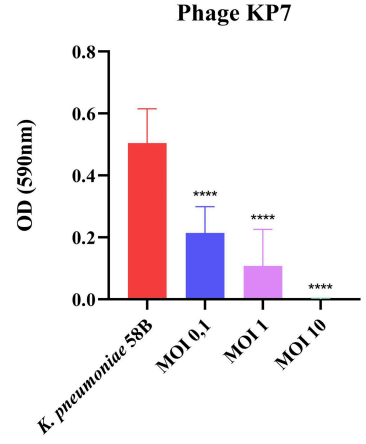
Phage KP7
OD (590nm)
0.8
0.6
0.4
0.2
0.0
****
****
****
K. pneumoniae 58B
MOI 0,1
MOI 1
MOI 10

U.

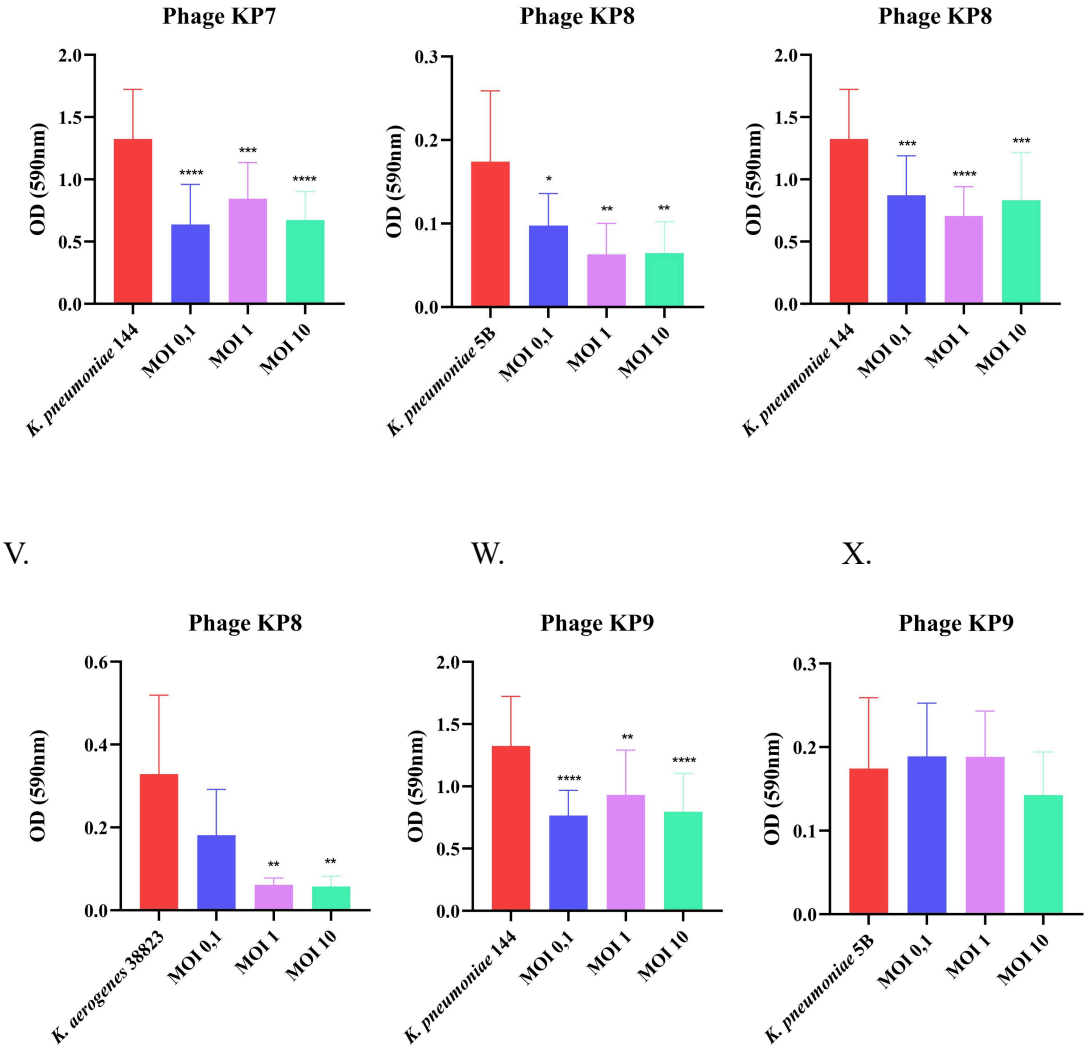

Figure 8. Evaluation of biofilm prevention performed in 96-well plates using Luria Bertani medium and crystal violet staining. The figure presents the graphs that showed statistically significant differences, assessed by the T-test, between treatments with different multiplicities of infection of the bacteriophages and the untreated bacterial control. These results indicate the effect of the phages in inhibiting biofilm formation by the tested bacterial strains.

A. B. C.

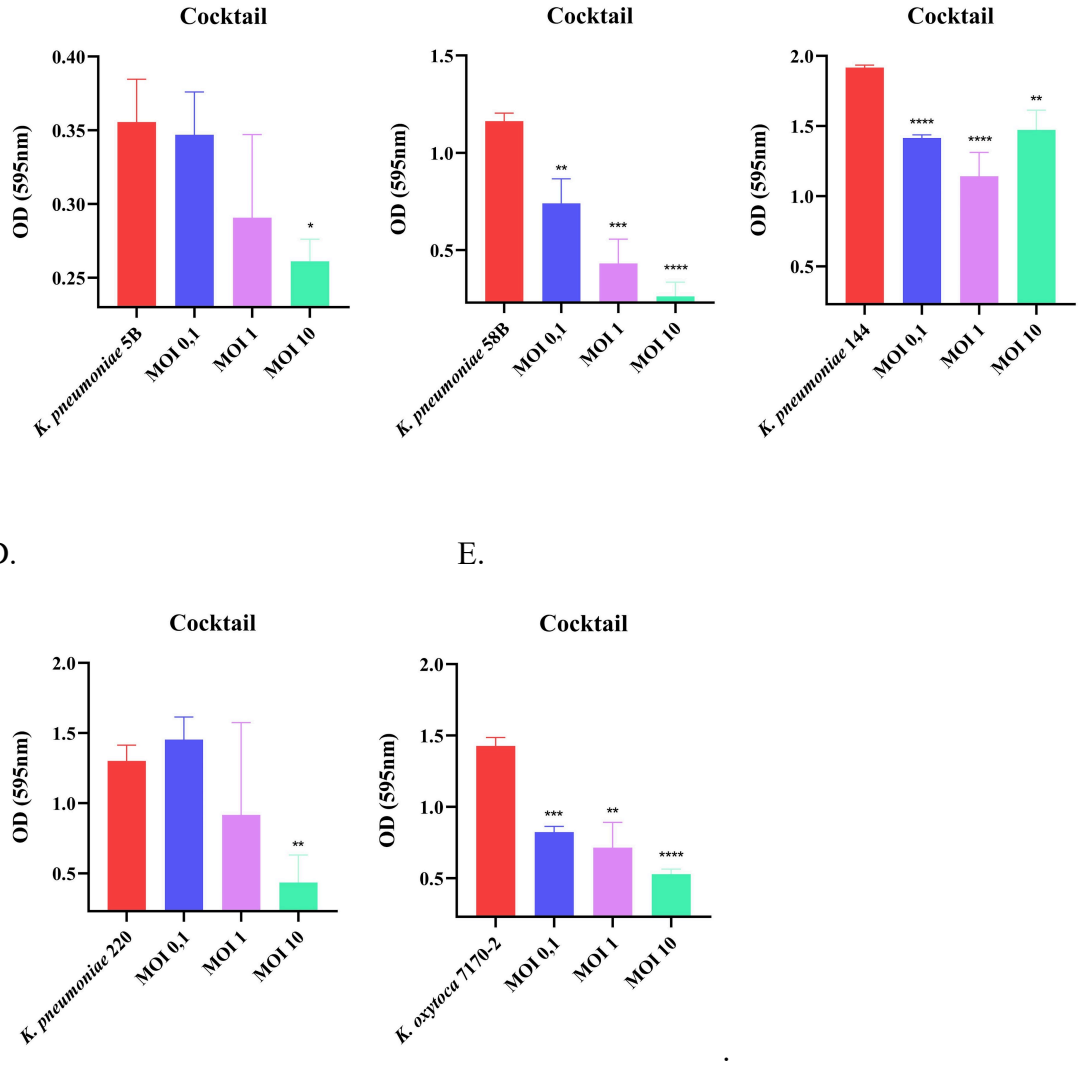

Figure 9. Evaluation of biofilm prevention performed in 96-well plates using Luria Bertani medium and crystal violet staining. The figure presents the graphs that showed statistically significant differences, assessed by the T-test, between the treatment with the phage cocktail composed of KP4, KP6, KP7, and KP8 and the untreated bacterial control. These results indicate the efficacy of the cocktail in inhibiting biofilm formation by the tested bacterial strains.

Lysis plaque morphology

The phages KP4 and KP6 formed large lysis plaques (Figure 10. A and B). KP4 exhibited irregular borders and a granular appearance, while KP6 produced large, well-defined plaques. The phages KP7 and KP8 formed small plaques, with KP8 also displaying irregular borders (Figure 10. C and D). All phages showed the presence of halos

around the plaques, suggesting the production of extracellular enzymes, possibly depolymerases, associated with the degradation of bacterial structures such as capsules or biofilms. The following images illustrate these morphological differences observed among the phages.

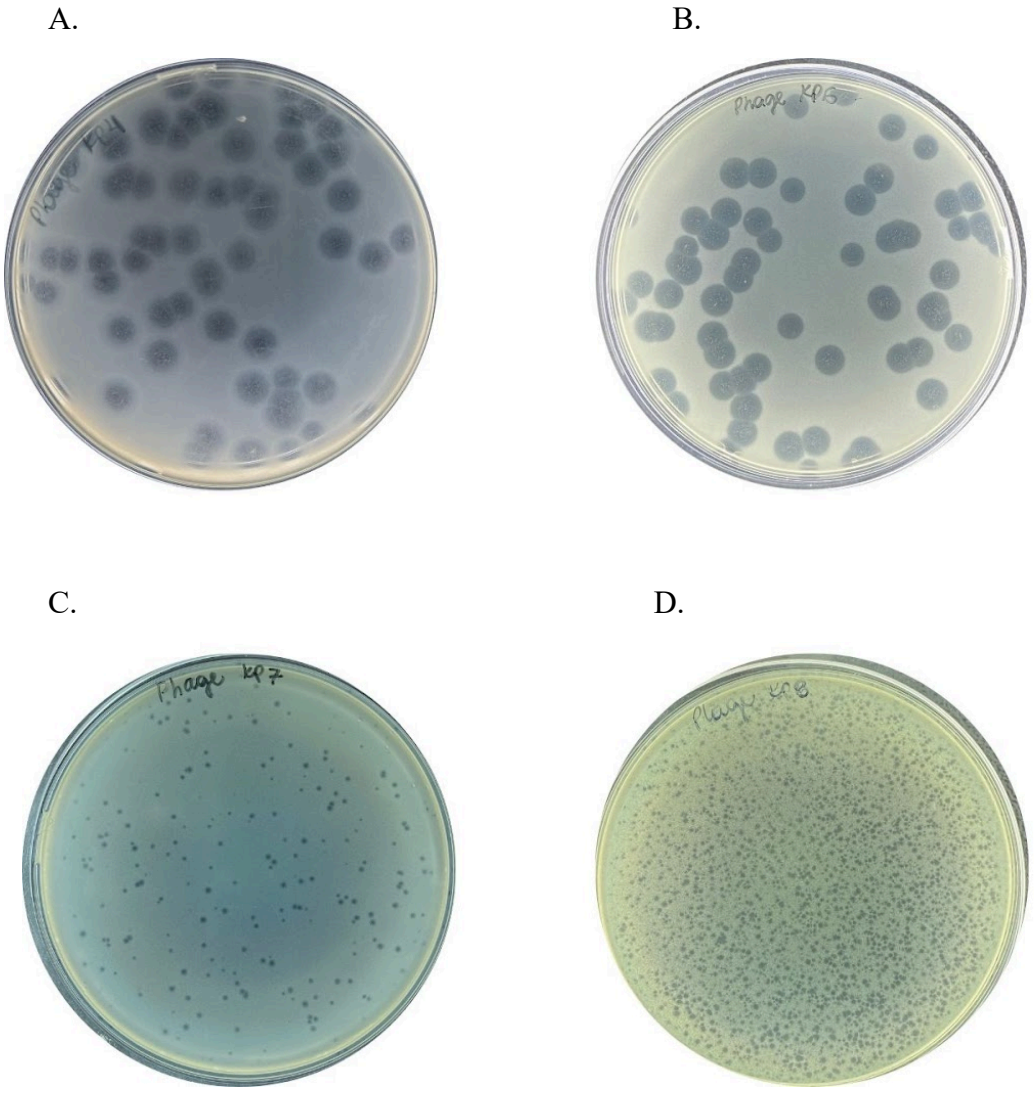

Figure 10. Morphological characterization of lysis plaques formed by the four bacteriophages included in the phage cocktail. Panel A shows plaques produced by phage KP4, panel B by KP6, panel C by KP7, and panel D by KP8. The images were obtained from double-layer agar assays, where the bacteriophages were plated on their respective *Klebsiella* host strains. The plaques differ in size, clarity, and edge definition, indicating possible variations in diffusion, replication rate, and lytic activity among the phages. These

morphological features support their individual contribution to the effectiveness of the phage cocktail.

One-Step growth curve

In the one-step growth curve analysis, phages KP4, KP6, KP7, and KP8 (Figure 11. A–D) exhibited varying latent periods and burst sizes. KP4 and KP6 both showed a latent period of approximately 15 minutes, with burst sizes of 23 and 83 PFU/cell, respectively. KP7 had a longer latent period of about 35 minutes and a burst size of 34 PFU/cell. Meanwhile, KP8 displayed a latent period of 30 minutes and the lowest burst size among them, with only 14 PFU/cell.

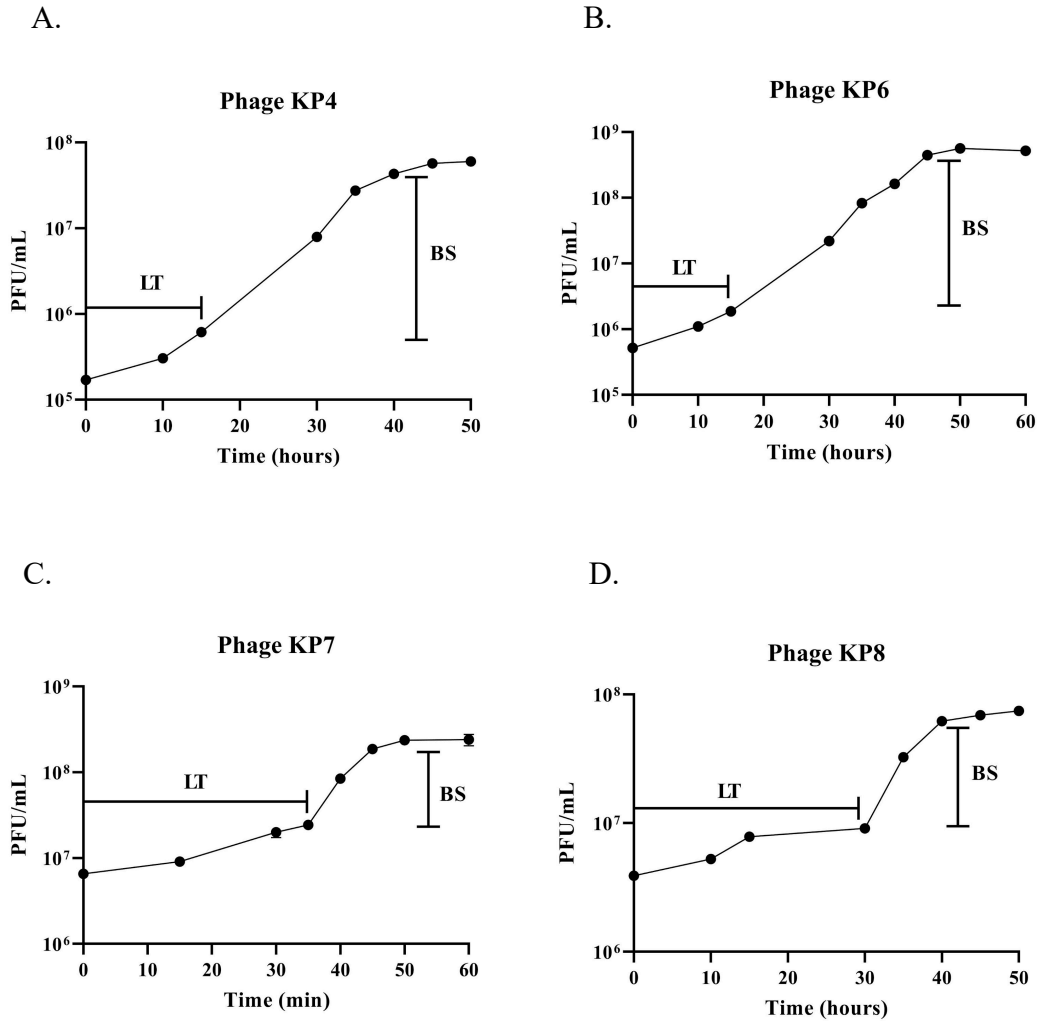

Figure 11. One-step growth curves of bacteriophages A- KP4, B- KP6, C- KP7, and D- KP8. The analyses were performed to determine key parameters of the lytic cycle of each phage: latent period and burst size.

Phage tolerance to temperature and pH

Phage KP4 showed a significant loss of viability at 70 °C and complete inactivation at 80 °C. Phage KP6 displayed a similar pattern but began to show a decrease in viral titer at 60 °C. Phage KP7 maintained viability at all temperatures except 80 °C, where complete inactivation was observed. Lastly, phage KP8 showed a reduction in titer at 70 °C, but still retained active viral particles at 80 °C (Figure 12. A-D).

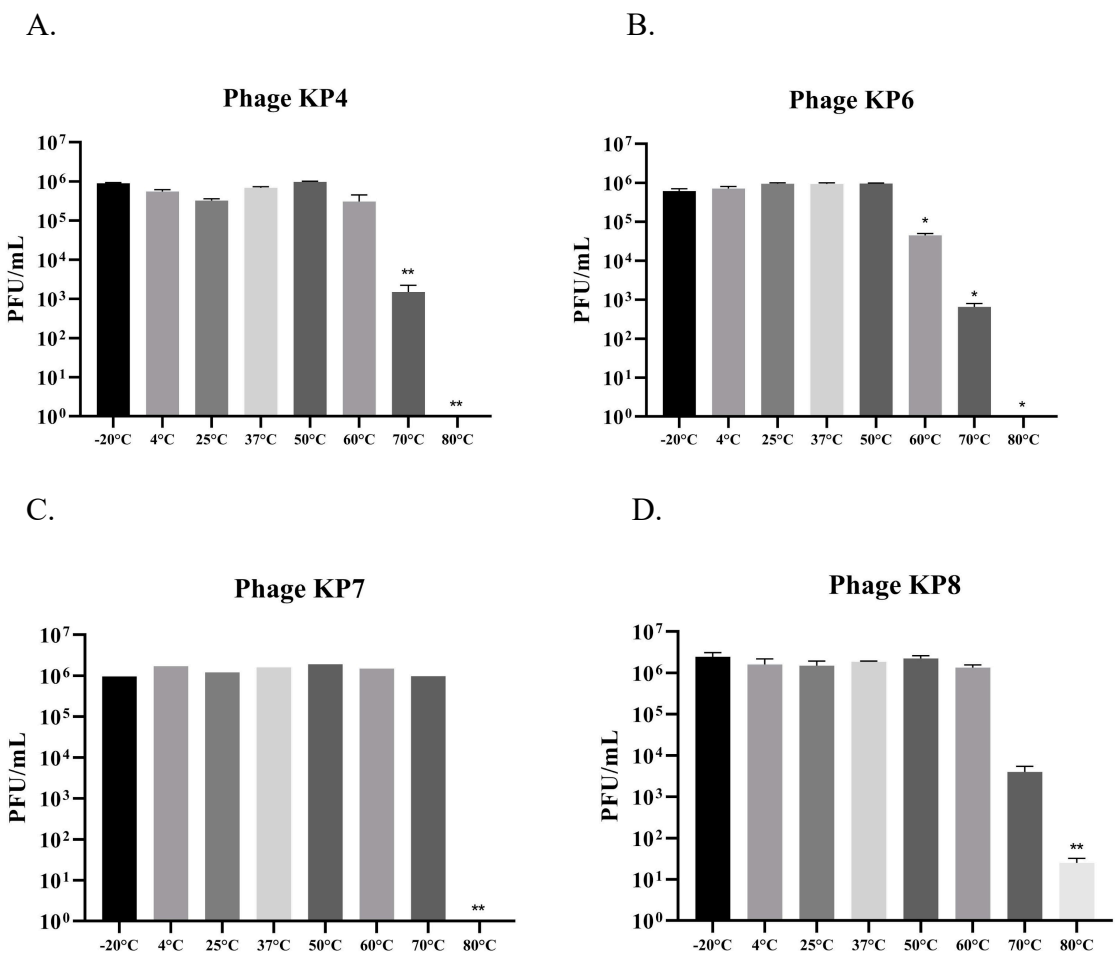

Figure 12. Thermal stability test of the cocktail phages. Bacteriophages KP4, KP6, KP7, and KP8 were subjected to different temperatures for a defined period to assess their stability and viability after thermal exposure. Following incubation, lytic activity was measured through

plaque-forming unit (PFU) assays, allowing the observation of potential losses in phage infectivity as temperature increased. These data are essential for determining the optimal storage and application conditions of the phage cocktail in therapeutic or industrial settings.

The four phages evaluated showed a similar pattern of stability across different pH levels (Figure 13. A-D). All phages completely lost viability at extreme pH values of 2, 3, and 12. At the other pH values tested, the phages maintained their original titers, indicating good stability under those conditions.

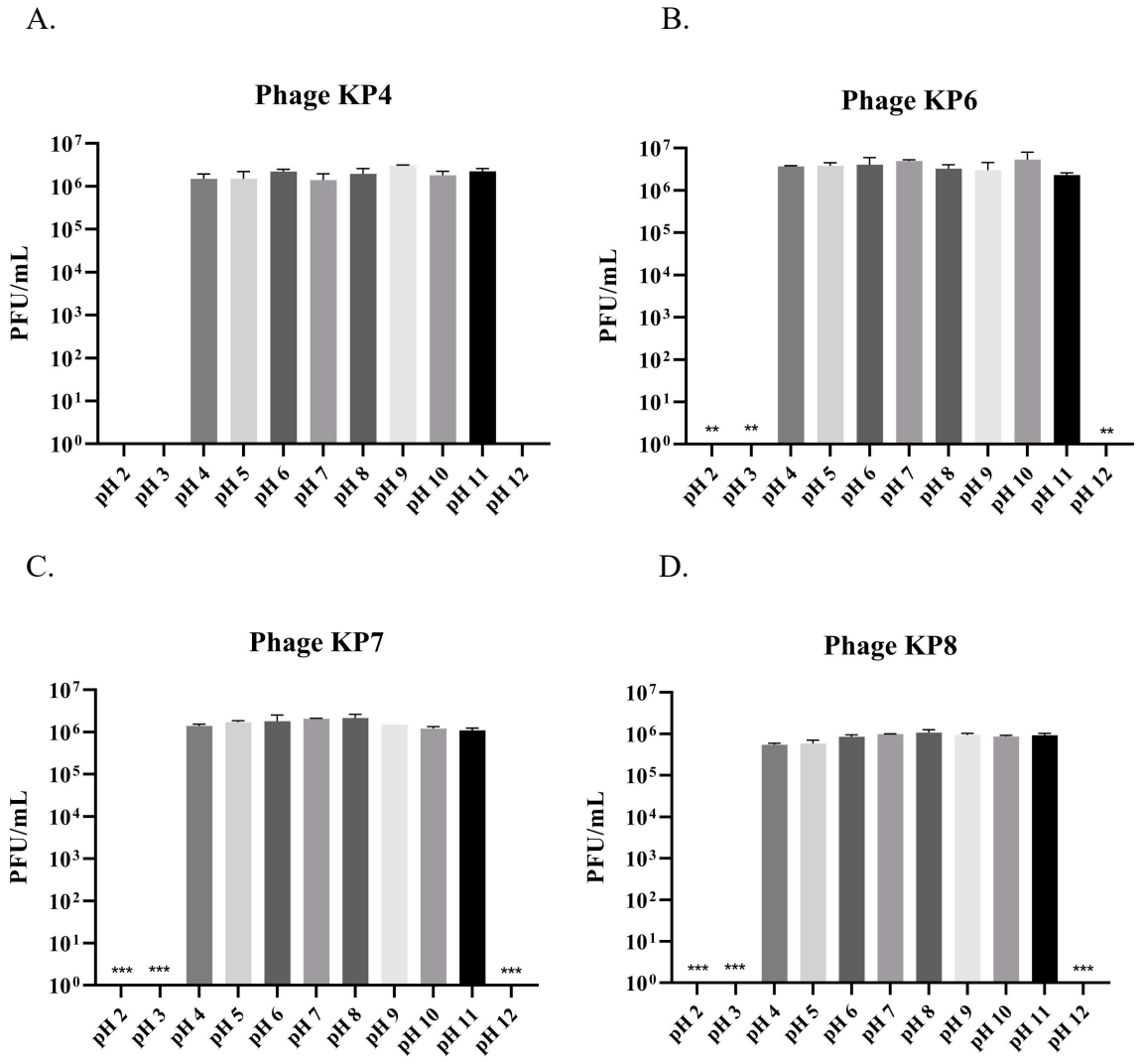

Figure 13. pH stability test of the cocktail phages. Bacteriophages KP4, KP6, KP7, and KP8 were exposed to solutions with different pH ranges for a defined period to assess their stability and infectivity under varying acidic and alkaline conditions. After incubation, lytic activity was evaluated through plaque-forming unit (PFU) assays, allowing the identification

of possible losses in phage viability. These data are essential for determining the suitability of the phage cocktail for different application environments, such as biological or industrial systems.

Viral DNA extraction and sequencing

In the analysis of the obtained results, it was observed that the DNA bands extracted from the bacteriophages were larger than 10 kb, which is significant considering that the molecular marker used for the agarose gel electrophoresis had a maximum resolution of 10 kb (Figure 10. A-B). This result indicates that the extracted DNA was of good integrity and did not show significant degradation, which is essential to ensure the quality of the genetic material for subsequent sequencing and genomic analysis steps.

Furthermore, DNA quantification performed using the Qubit Fluorometer yielded values above 20 ng/µL, which is the minimum required to ensure efficient sequencing on the Illumina platform. This concentration confirms that the amount of DNA obtained was sufficient for library preparation and successful high-throughput sequencing. The good quality and adequate quantity of the extracted DNA enabled the material to be sent for sequencing, which produced high-quality data.

Based on these results, the sequencing was successfully completed, providing the necessary information to begin the genomic analysis phase of the study. From this stage forward, it will be possible to assemble the phage genomes, annotate the sequences, and conduct a detailed analysis of the genetic characteristics of the bacteriophages, contributing to a better understanding of their properties and potential applications.

A. B.

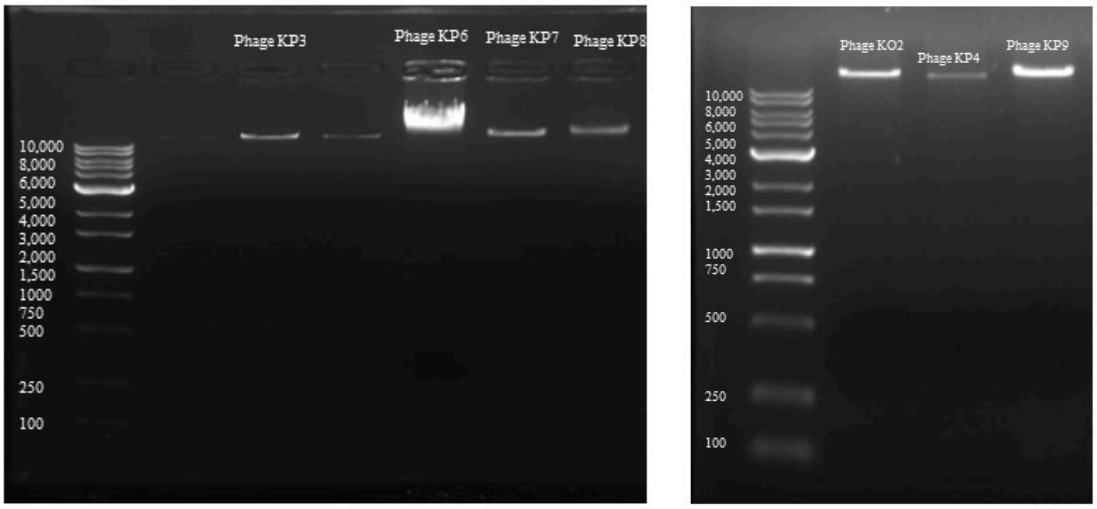

Figure 14. Agarose gel with bands resulting from viral DNA extraction.

In vivo assays using *Galleria mellonella*

Dose-response curve for the KP58B strain in *Galleria mellonella* larvae. The graph shows larval mortality as a function of bacterial inoculum concentration. The LD_{50} was determined as the concentration of 10^5 CFU of KP58B, which caused approximately 50% mortality in the larval population after 24 hours of exposure. The sigmoidal curve (Figure 2) was fitted to the experimental data, with mortality recorded as the percentage of dead larvae at each administered dose.

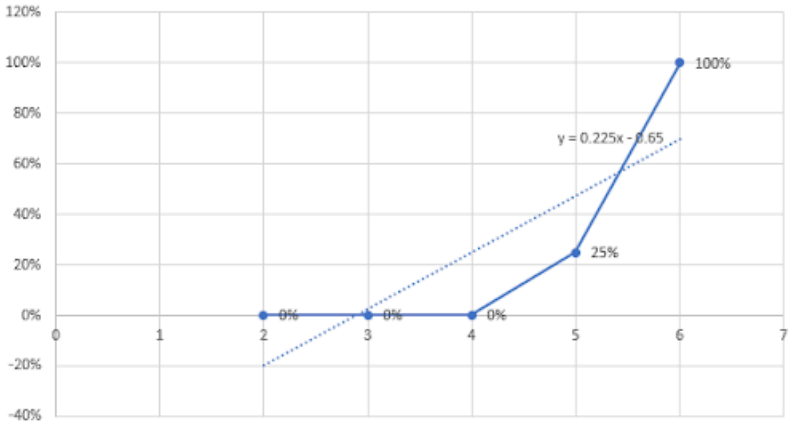

Figure 15. Linear regression graph used to determine the lethal dose 50 (LD50) in *Galleria mellonella*. The analysis shows the relationship between the *Klebsiella pneumoniae*

concentration and the larval mortality rate, allowing estimation of the dose required to kill 50% of the tested population.

In vivo experiments using *Galleria mellonella* revealed high efficacy of the phage cocktail, especially in prophylactic and coinfection treatment regimens. The cocktail remained stable over 72 hours, with consistent recovery of infectious particles (PFU/mL) even at the end of the observation period (Figure 16).

Prophylactic therapy was the most effective, resulting in nearly 100% survival of larvae infected with the KP58B strain. The coinfection regimen also maintained high survival rates throughout the 72-hour period. In contrast, the curative regimen - where the phage cocktail was administered two hours post-infection - was less effective, with most larvae succumbing within the first 24 hours (Figure 17).

Survival outcomes were further supported by CFU/mL quantification in larval hemolymph. Bacterial loads were virtually undetectable in both the prophylactic and coinfection groups, and phages remained recoverable throughout the entire observation period.

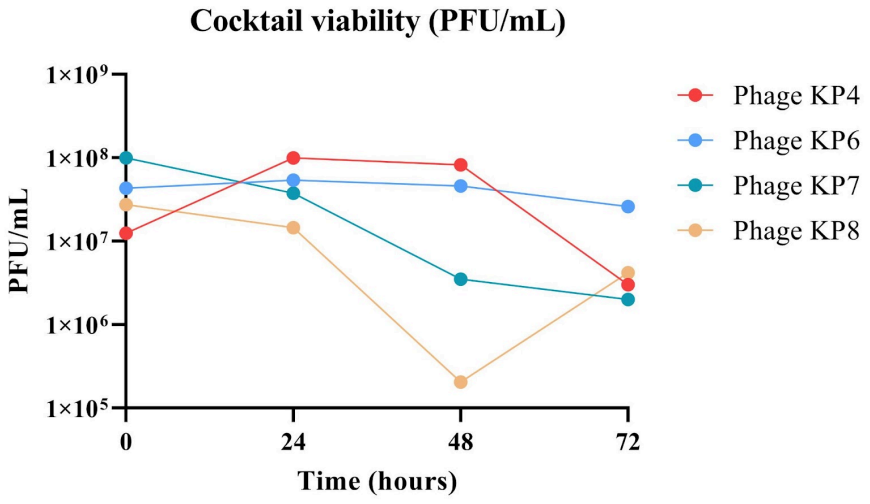

Figure 16. Viability of the phage cocktail in *Galleria mellonella* larvae. The figure shows the quantification of plaque-forming units per milliliter (PFU/mL) of the cocktail after inoculation in the larvae, assessing the phages ability to remain active and viable throughout the experimental period.

A. Larval mortality rate

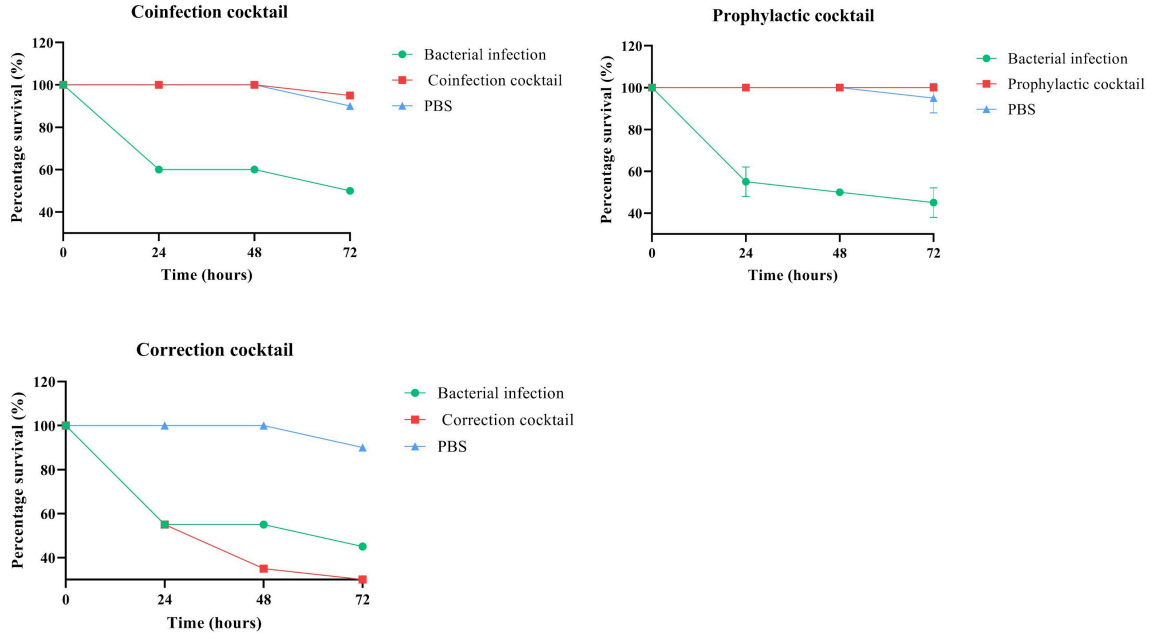

B. PFU/mL of the phage cocktail

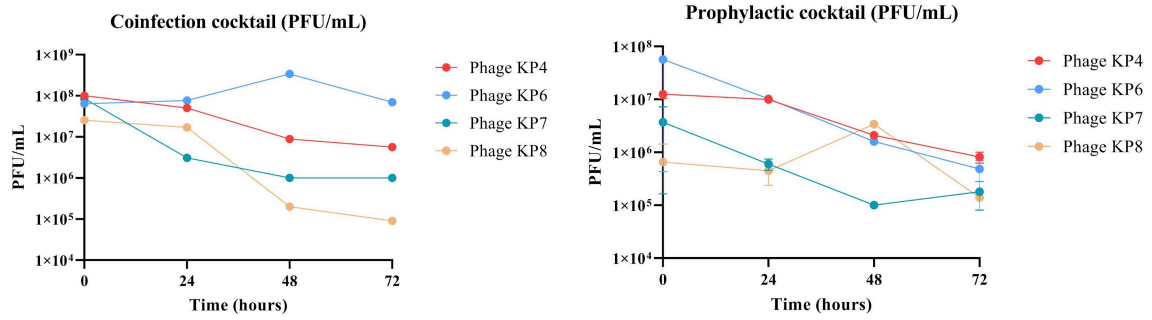

Figure 17. Infection assays with *Klebsiella pneumoniae* 58B and treatment with phage cocktail in *Galleria mellonella* larvae. (A) Larval mortality rates under different treatment protocols: prophylaxis, correction, and coinfection. (B) Quantification of plaque-forming units per milliliter (PFU/mL) of the phage cocktail recovered from larvae under the same treatments.

5. DISCUSSION

The bacterial growth observed in the experiment followed a pattern consistent with previous studies, such as Zhang *et al*. (2019), who reported a 4-hour adaptation phase

followed by an exponential phase lasting 16 to 20 hours, and Wang *et al*. (2021) and Narimisa *et al*. (2019), who observed a 2-hour adaptation phase followed by an exponential phase lasting 20 to 22 hours. The variation in the duration of the adaptation phase among studies can be explained by differences in the strains used or the presence of additives in the medium.

The CFU/mL count at different optical densities (OD_{600}) provides valuable information about bacterial viability and metabolic activity at various growth stages. The selection of OD_{600} values of 0.1 and 0.3 was based on previously established growth curves, where an OD_{600} of 0.1 corresponds to the beginning of the logarithmic phase, and an OD_{600} of 0.3 represents a more advanced stage of the same phase. These variations can be attributed to intrinsic differences between strains, such as growth rates, nutrient utilization efficiency, and resistance to adverse conditions. Additionally, technical factors - such as the accuracy in OD_{600} measurements and consistency in dilution preparation - may also influence the results. In this context, the data obtained provide a detailed view of the viability and metabolic activity of different *Klebsiella* strains at various points during the logarithmic phase.

The MIC results for the *Klebsiella pneumoniae* strains (KP58B, KP5B, and KP13) revealed distinct resistance profiles, with direct implications for therapeutic choices and the development of a bacteriophage cocktail. All strains exhibited universal resistance to tobramycin, with extremely high MIC values (ranging from 50 to 20,000 mg/L), rendering its clinical use or application in phage combination therapies unfeasible. Strain KP13 was also resistant to amikacin, while KP58B and KP5B remained susceptible. On the other hand, all strains were sensitive to ciprofloxacin, colistin, and gentamicin, with ciprofloxacin efficacy consistent with previous studies (Grillon *et al*., 2020). The observed resistance to aminoglycosides may be related to the presence of modifying genes, as described by Li *et al*. (2023). These findings support the exclusion of tobramycin - and amikacin in the case of KP13 - from treatment considerations, while reinforcing the preferential use of ciprofloxacin, colistin, and gentamicin, including in combination with phages. Combining phages with antibiotics to which the bacteria are susceptible may enhance treatment efficacy, provided that MICs are continuously monitored during therapy, given the risk of acquired resistance. Thus, the integration of quantitative MIC data, EUCAST breakpoints, and current evidence underpins a promising therapeutic strategy against *K. pneumoniae* infections, especially in multidrug-resistant contexts.

From environmental samples, seven bacteriophages with lytic activity against different *Klebsiella* strains were isolated, highlighting the presence and diversity of these

bacterial viruses in the analyzed environments. The successful recovery of phages specific to different species and strains reinforces the potential of aquatic and agro-industrial environments as promising sources for the isolation of phages with therapeutic or prophylactic applications, as also reported by Li *et al*. (2021) and Townsend *et al*. (2021). The identification of two distinct phages (KP6 and KP7) targeting the same host strain (KP58B) suggests the coexistence of different phage profiles within the same environment, which can be leveraged in the formulation of cocktails with broader spectra and greater efficacy. Additionally, the isolation of a phage active against *K. variicola* - a species rarely addressed in the phage therapy literature - expands the prospects for developing alternative approaches aimed at controlling emerging strains within the *Klebsiella* complex.

Determining the host range is a crucial step in the biological characterization of bacteriophages, especially when aiming to formulate therapeutic cocktails. The fact that some phages produced lysis halos in the spot test that were not confirmed in the double-layer agar assay is possibly due to the action of extracellular lytic enzymes, such as endolysins, or the degradation of the bacterial cell wall without effective phage replication (Denyes *et al*., 2019). These findings highlight the importance of using complementary methods, such as the double-layer assay and EOP analysis, for accurate assessment of phage infectivity. The performance of phages KP4 and KP6, which showed confirmed activity against a non-host strain, stands out as a promising result within the proposal to broaden the therapeutic spectrum of the developed cocktail.

The efficiency of plating (EOP) is a key parameter for assessing the infectivity of bacteriophages across different bacterial strains. According to Mirzaei and Nilsson (2015), EOP values equal to or below 0.001 (10^{-3}) indicate low or limited infection efficiency. In this study, phages KP4 and KP6 exhibited EOPs well below this threshold. These data suggest that, despite plaque formation on non-host strains, the infections were highly inefficient - possibly due to barriers in adsorption, intracellular replication restrictions, or the action of bacterial defense mechanisms such as CRISPR-Cas or restriction-modification systems (Labrie *et al*., 2010). Nevertheless, the presence of lytic activity, even with low efficiency, may still be relevant in the formulation of broad-spectrum phage cocktails. Phages with reduced EOP can contribute to the reduction of target strain populations when used in combination with more potent and specific phages.

The isolated phages exhibited distinct lytic activity profiles against their host strains and non-host bacteria, varying according to the multiplicity of infection (MOI). Phage KO2 demonstrated statistically significant lysis of its host strain at all tested MOIs, with no

differences among them, suggesting high affinity and efficient replication. However, it showed no effect on the other 15 strains tested, indicating a narrow host range. In contrast, phage KV3 did not show a statistically significant effect on its target strain (KV26E); if this phage is temperate or exhibits slow adsorption, it may display low lytic activity and a tendency toward lysogeny, especially at high MOIs, as previously described for phage λ (Mitarai *et al*., 2016). Phage KP4 showed robust and consistent lysis of strain KP13 across all tested MOIs, with no significant differences among them, indicating rapid and effective replication. It also affected two secondary strains, suggesting that at higher viral loads, it may infect non-host strains (Zheng *et al*., 2025). Phage KP6 exhibited significant lysis of its host strain at all MOIs and also lysed KO7170-2 (a non-host strain); no effect was observed at MOI 0.1, but lysis was statistically significant at MOIs 1 and 10, indicating moderate specificity dependent on viral load. KP7 also demonstrated strong lytic activity against KP58B, its host strain, at all MOIs. Notably, it induced significant lysis of KO7170-2 (a non-host strain) at all MOIs, with earlier onset at higher MOIs, reinforcing an intermediate specificity profile. Phage KP8 showed consistent lytic activity against its target strain, KP5B. Phage KP9, also targeting KP5B, induced significant lysis at MOIs 0.1 and 1 from time 0 h, and at MOI 10 from 2 h onward, suggesting that higher MOIs may delay lysis onset but prolong its duration (Dressman *et al*., 2020). The cocktail containing KP4, KP6, KP7, and KP8 demonstrated significant lytic activity against all target strains at all MOIs over a 21-hour period, highlighting the potential of combining phages with complementary spectra and mechanisms to enhance therapeutic efficacy. Few studies have applied this approach to phages targeting *Klebsiella*, as it is more commonly used with coliphages or vibriophages (Benela *et al*., 2021). Therefore, the use of bacterial growth assays in 96-well plates with different MOIs represents an innovative and promising strategy for investigating the therapeutic application of phages against *Klebsiella pneumoniae*.

Several studies have shown that bacteriophages can prevent biofilm formation by *Klebsiella pneumoniae*, particularly due to the action of phage-associated depolymerase enzymes. Hala *et al*. (2025) demonstrated that phage GBH014 significantly reduced biofilm formation in host strains ($P < 0.005$), while GBH019 and GBH010 were also effective, though with some variation. Part of this activity was attributed to the presence of capsule type (K)-specific enzymes capable of degrading the bacterial capsule. Interestingly, these phages also affected non-host strains, suggesting a nonspecific enzymatic action. Similarly, Askoura *et al*. (2021) observed that phages applied at high MOIs (>5) significantly enhanced biofilm prevention ($P < 0.05$), reinforcing the role of depolymerases in degrading the extracellular

matrix and capsule. Li *et al*. (2024) also reported biofilm reduction by phages even in the absence of visible plaque formation, supporting the hypothesis of enzymatic activity independent of traditional lytic infection. Our results (Appendix 2) support these findings: phages KP4, KP6, KP7, and KP8, both individually and in cocktail form, reduced biofilm formation in all tested strains, with varying statistical significance, depending on the MOI and strain. The use of phage cocktails broadened the spectrum of preventive activity. We observed that some strains, such as KP144, were more susceptible to non-specific phages, while others, like KP220 and KP13, may exhibit resistance or even increased biofilm production under phage pressure. Future assays focusing on the degradation of already-formed biofilms will be essential to determine whether the observed reduction results from early cell lysis or direct enzymatic action by phages.

The lysis plaques obtained in this study revealed marked differences among the analyzed phages. KP4 and KP6 formed large plaques, while KP7 and KP8 produced small ones. Irregular edges were observed in plaques formed by KP4 and KP8, and all phages exhibited halos around the plaques, suggesting extracellular enzymatic activity. These findings are consistent with Zurabov *et al*. (2021), who associated halos and large plaques with the presence of polysaccharide depolymerases in phages isolated against *Klebsiella pneumoniae*. These enzymes facilitate phage penetration into bacterial extracellular matrices, such as capsules and biofilms, and hold therapeutic value, including in formulations with broader action. On the other hand, the small and irregular plaques observed for phages KP7 and KP8 are similar to those described by Fayez *et al*. (2023) and may indicate lower infection rates, limited diffusion in agar, or reduced production of extracellular enzymes. Thus, the morphological diversity among KP4, KP6, KP7, and KP8 reflects potential differences in infection mechanisms and therapeutic potential. KP4 and KP6 stand out as promising candidates due to their well-defined halos and large plaques, features often associated with higher lytic efficiency and greater ability to act on complex bacterial structures.

Several studies have explored the biological characteristics of phages specific to *Klebsiella pneumoniae*, with particular focus on the latent period and burst size, key parameters for assessing replication potential and bacterial lysis efficiency. Chen *et al*. (2023) reported a latent period of 10 minutes and a burst size of 183 PFU/cell for phage HS106. Bai *et al*. (2022) observed a 30-minute latent phase in phage *vB_kpnM_17-11*, with a burst size of 31.7 PFU/cell. Fang *et al*. (2023) investigated three different phages, with latent periods ranging from 7 to 9 minutes and burst sizes between 6.25 and 13.26 PFU/cell. Senhaji-Kacha

et al. (2024) described latent periods of 20 to 30 minutes and burst sizes of 56 to 87 PFU/cell for phages F13 and F14. In the present study, the isolated phages also showed variation in these parameters. These results indicate that while the latent periods fall within the expected range for phages targeting *K. pneumoniae*, the burst sizes varied considerably. Such differences may be related to the phages' replication cycles, experimental conditions, or specific features of the host strains. Overall, phages with larger burst sizes and shorter latent periods are generally considered more promising for therapeutic applications, although other biological factors must also be taken into account.

The results obtained demonstrate that the analyzed phages exhibit stability across a wide pH range, maintaining viability between pH 4 and 11, with complete loss of activity only under extreme conditions such as pH 2, 3, and 12. These findings are consistent with those of Chen *et al*. (2023), who reported similar stability for phage HS106, which remained viable between pH 4 and 12 but was inactivated at more extreme values. This level of tolerance is considered a relevant criterion when selecting phages for practical applications, especially in environments with significant pH fluctuations, such as the gastrointestinal tract or fermented foods. Regarding thermal stability, phages KP4, KP6, KP7, and KP8 showed varying degrees of heat tolerance. These results align with those of Chen *et al*. (2023), who found that phage HS106 remained stable between 4 °C and 50 °C, with gradual loss of activity at higher temperatures. The ability to retain infectivity within this range supports the potential of these phages as biocontrol agents, particularly in food or clinical settings that demand some level of thermal resistance. Additionally, Pertics *et al*. (2021) conducted a long-term study on phage thermal stability. While immediate results also indicated stability up to 40 °C, prolonged monitoring over several months revealed a gradual decline in phage titers beginning at that temperature. This highlights the importance of evaluating not only the immediate thermal tolerance of phages but also their long-term stability, an essential factor that can directly impact the formulation and storage of phage-based products. Therefore, the findings of this study, supported by literature data, indicate that the evaluated phages possess promising physicochemical characteristics, particularly in terms of pH stability and, to a lesser extent, thermal tolerance. These properties strengthen the potential of the isolates as candidates for use in biocontrol strategies, provided their stability is matched to the specific requirements of each application.

In vivo experiments using *Galleria mellonella* demonstrated that the tested phage cocktail exhibited high efficacy, particularly in the prophylactic and co-infection treatment regimens. The LD_{50} determined for strain KP58B was 10^5 CFU, a value similar to that

reported by Nale *et al.* (2021) for one of their *Salmonella* isolates, indicating a comparable virulence profile between the tested strains. Regarding the viability of the phage cocktail, viral stability was observed over the 72-hour period, with recovery of infectious particles (PFU/mL) even after that time. As also reported by Nale *et al*. (2021), the number of phages recovered from the hemolymph remained consistent, although the variable volume of hemolymph collected per larva (0–20 µL) may have influenced the fluctuations in the values obtained. This factor was also mentioned by the authors as a common technical limitation of the *Galleria* model. The prophylactic treatment proved to be the most effective, promoting nearly 100% survival of larvae infected with the KP58B strain. These results are consistent with those reported by Nale *et al*. (2021), who also observed complete protection under prophylactic treatment, and with findings by Kelly *et al*. (2024), who achieved similar outcomes even using a longer interval (4 hours) between phage and bacterial administration. These findings reinforce the preventive potential of phage therapy, possibly due to early colonization of the hemolymph by the phages, which prevents the establishment of infection. In the co-infection regimen, survival rates also remained high throughout the 72-hour observation period, contrasting with the results of Nale *et al*. (2021), who reported larval mortality starting at 48 hours under the same condition. This more favorable outcome may be related to the characteristics of the phage cocktail used, the phage dose (MOI 10), or the lower virulence of the tested bacterial strain. Kelly *et al*. (2024) also reported excellent results with co-infection by *Klebsiella* sp., supporting the data presented here. On the other hand, the corrective treatment regimen, in which the phage cocktail was administered two hours after infection, was less effective: most larvae had already died within the first 24 hours. This result contrasts with that of Jeon *et al*. (2019), who used a 30-minute interval after infection for phage treatment against *Acinetobacter baumannii* and achieved over 90% survival. This suggests that the time interval between bacterial infection and phage therapy is a critical factor for therapeutic success. Future studies using shorter intervals (e.g., 30–60 minutes) may help define a more appropriate therapeutic window. Similarly, Kelly *et al*. (2024) observed that the success of corrective therapy varied depending on the virulence of the bacterial strains used, which may also explain the more drastic results observed in the present study. The quantification of CFU/mL and PFU/mL in the larval hemolymph supported the survival data. Bacterial counts were virtually nonexistent in the prophylactic and co-infection groups, and phage recovery remained consistent throughout the 72-hour period. These findings are in line with those of Quispe-Villegas *et al*. (2025), who reported 100% survival in *Salmonella* co-infection for 96 hours, although they did not test prophylactic or corrective

regimens in their study. Finally, Jeon *et al*. (2019), in a study with *Pseudomonas aeruginosa*, did not use an LD_{50} but instead applied a fully lethal dose, which may explain the lower survival rates even after phage treatment. This highlights the importance of calibrating the experimental infection based on LD_{50}, especially in therapeutic efficacy studies. Taken together, the results of this study indicate that prophylactic and co-infection approaches using the phage cocktail are promising strategies against *Klebsiella pneumoniae* infection in the *Galleria mellonella* model. However, the limited efficacy of the corrective regimen underscores the need to optimize treatment timing and reinforces the importance of additional assays to better understand the limitations of phage therapy in this model.

6. CONCLUSION AND FUTURE PERSPECTIVES

In this study, bacteriophages with lytic activity against *Klebsiella pneumoniae* were isolated and characterized through biological and genomic analyses, revealing the potential of some phages for therapeutic applications. Growth data showed that the phages exhibit characteristics consistent with those reported in the literature, with latent periods ranging from 10 to 30 minutes and varying burst sizes. The observed differences between isolates may be associated with variations in replication cycles, host strains, and experimental conditions. The phage cocktail formulated based on these isolates showed high efficacy in the *Galleria mellonella* larvae model, especially in prophylactic and co-infection assays, promoting a significant increase in larval survival rates and a reduction in bacterial load in the hemolymph. These results indicate that the application of the cocktail may be a viable strategy in combating antimicrobial resistance, particularly in veterinary contexts.

Future perspectives include detailed functional analysis of the sequenced phage genomes, biological testing of the remaining isolated phages, and evaluation of new cocktail combinations to broaden the spectrum of activity and prevent the emergence of resistance. It is also essential to test the cocktail's efficacy against different bacterial strains in *Galleria mellonella* and more complex in vivo models, such as livestock animals. Final product formulation, focusing on stability and practical applicability, along with safety and efficacy trials under real-world conditions, will be crucial for enabling its use as a therapeutic alternative for controlling *K. pneumoniae* infections in livestock production.

7. REFERENCES

AHMADI, M.; KARIMI TORSHIZI, M. A.; RAHIMI, S.; DENNEHY, J. J. Prophylactic bacteriophage administration more effective than post-infection administration in reducing *Salmonella enterica* serovar *Enteritidis* shedding in quail. Frontiers in Microbiology, v. 7, p. 1253, 2016. DOI: https://doi.org/10.3389/fmicb.2016.01253.

AJULO, S.; AWOSILE, B. Global antimicrobial resistance and use surveillance system (GLASS 2022): investigating the relationship between antimicrobial resistance and antimicrobial consumption data across the participating countries. PLoS One, v. 19, n. 2, p. e0297921, 5 fev. 2024. DOI: 10.1371/journal.pone.0297921.

ALI, Hala R.; VALDIVIA, Carlos; NEGUS, David. Bacteriophage-embedded and coated alginate layers inhibit biofilm formation by clinical strains of *Klebsiella pneumoniae*. Journal of Applied Microbiology, v. 136, n. 5,, maio 2025.

ASKOURA, M.; SAED, N.; ENAN, G.; et al. Characterization of polyvalent bacteriophages targeting multidrug-resistant *Klebsiella pneumoniae* with enhanced anti-biofilm activity. Applied Biochemistry and Microbiology, v. 57, p. 117–126, 2021.

BAI, J. *et al*. Isolation and characterization of vB_kpnM_17-11, a novel phage efficient against carbapenem-resistant *Klebsiella pneumoniae*. Frontiers in Cellular and Infection Microbiology, [S.l.], v. 12, p. 897531, 5 jul. 2022. DOI: https://doi.org/10.3389/fcimb.2022.897531.

BATINOVIC, S. et al. Bacteriophages in natural and artificial environments. Pathogens, v. 8, n. 3, p. 100, 2019. Disponível em: https://doi.org/10.3390/pathogens8030100.

BEETON, M. L.; ALVES, D. R.; ENRIGHT, M. C.; JENKINS, A. T. A. Assessing phage therapy against Pseudomonas aeruginosa using a Galleria mellonella infection model. International Journal of Antimicrobial Agents, v. 46, p. 196–200, 2015. DOI:

https://doi.org/10.1016/j.ijantimicag.2015.04.005.

BENELA, M.; VAIYAPURI, M.; VISNUVINAYAGAM, S.; GEORGE, J. C.; RAVEENDRAN, K.; GEORGE, I.; MOTHADAKA, M. P.; BADIREDDY, M. R. A revisited two-step microtiter plate assay: optimization of in vitro multiplicity of infection (MOI) for Coliphage and Vibriophage. Journal of Virological Methods, Amsterdam, v. 294, p. 114177, Aug. 2021. DOI: 10.1016/j.jviromet.2021.114177.

BRISSE, S.; GRIMONT, F.; GRIMONT, P. A. D. The genus *Klebsiella.* In: DWORKIN, M.; FALKOW, S.; ROSENBERG, E.; SCHLEIFER, K. H.; STACKEBRANDT, E. (eds.). The Prokaryotes. New York: Springer, 2006. DOI: 10.1007/0-387-30746-X_8.

CHEN, C. et al. Isolation and characterization of novel bacteriophage vB_KpP_HS106 for *Klebsiella pneumoniae* K2 and applications in foods. Frontiers in Microbiology, v. 14, p. 1227147, 16 ago. 2023. DOI: https://doi.org/10.3389/fmicb.2023.1227147. Disponível em: https://www.ncbi.nlm.nih.gov/pmc/articles/PMC10466807/. Acesso em: 20 jul. 2025.

CHIȘ, A. A. et al. Microbial resistance to antibiotics and effective antibiotherapy. Biomedicines, v. 10, n. 5, p. 1121, 2022. DOI: https://doi.org/10.3390/biomedicines10051121.

CHROMagar. CHROMagar Orientation Medium – Instructions for Use. Paris, France: CHROMagar, 2024. Disponível em: https://www.chromagar.com. Acesso em: jun. 2025.

DENYES, J. M.; LABRIE, S. J.; SIPOS, R. G.; MOINEAU, S. Phage-based assay for the rapid detection of viable Listeria monocytogenes cells. Applied and Environmental Microbiology, v. 80, n. 2, p. 626–633, 2014. DOI: https://doi.org/10.1128/AEM.03230-13.

DHINGRA, S. et al. Microbial resistance movements: an overview of global public health threats posed by antimicrobial resistance, and how best to counter. Frontiers in Public Health,

v. 8, p. 535668, 2020. DOI: https://doi.org/10.3389/fpubh.2020.535668.

DONG, N.; YANG, X.; CHAN, E. W.; ZHANG, R.; CHEN, S. *Klebsiella* species: taxonomy, hypervirulence and multidrug resistance. EBioMedicine, v. 79, p. 103998, maio 2022. DOI: 10.1016/j.ebiom.2022.103998.

DRESSMAN, H. K.; DRAKE, J. W. Lysis and lysis inhibition in bacteriophage T4: rV mutations reside in the holin t gene. Journal of Bacteriology, Washington, DC, v. 181, n. 14, p. 4391–4396, 15 jul. 1999. DOI: 10.1128/JB.181.14.4391-4396.1999.

FANG, C. *et al*. Isolation and characterization of three novel lytic phages against K54 serotype carbapenem-resistant hypervirulent *Klebsiella pneumoniae*. Frontiers in Cellular and Infection Microbiology, [S.l.], v. 13, p. 1265011, 12 dez. 2023. DOI: https://doi.org/10.3389/fcimb.2023.1265011.

FAYEZ, M. S.; HAKIM, T. A.; ZAKI, B. M. et al. Morphological, biological, and genomic characterization of *Klebsiella pneumoniae* phage vB_Kpn_ZC2. Virology Journal, v. 20, n. 86, 2023. Disponível em: https://doi.org/10.1186/s12985-023-02034-x. Acesso em: 19 jul. 2025.

GAITERO, M.; SEOANE-BLANCO, M.; VAN RAAIJ, M. J. Structure and function of bacteriophages. In: HARPER, D. R.; ABEDON, S. T.; BURROWES, B. H.; MCCONVILLE, M. L. (eds.). Bacteriophages. Cham: Springer, 2021. Disponível em: https://doi.org/10.1007/978-3-319-41986-2_1.

GORODNICHEV, R. B. et al. Novel *Klebsiella pneumoniae* K23-specific bacteriophages from different families: similarity of depolymerases and their therapeutic potential. Frontiers in Microbiology, v. 12, p. 669618, 2021. DOI: 10.3389/fmicb.2021.669618.

GRILLON, A.; SCHRAMM, F.; KLEINBERG, M.; JEHL, F. Comparative Activity of Ciprofloxacin, Levofloxacin and Moxifloxacin against *Klebsiella pneumoniae*, Pseudomonas aeruginosa and Stenotrophomonas maltophilia Assessed by Minimum Inhibitory

Concentrations and Time-Kill Studies. PLoS ONE, v. 11, n. 6, e0156690, 3 jun. 2016. DOI: 10.1371/journal.pone.0156690.

JEON, J.; PARK, J. H.; YONG, D. Efficacy of bacteriophage treatment against carbapenem-resistant *Acinetobacter baumannii* in *Galleria mellonella* larvae and a mouse model of acute pneumonia. BMC Microbiology, v. 19, p. 70, 2019. DOI: https://doi.org/10.1186/s12866-019-1443-5.

JEON, J.; YONG, D. Two novel bacteriophages improve survival in *Galleria mellonella* infection and mouse acute pneumonia models infected with extensively drug-resistant *Pseudomonas aeruginosa*. Applied and Environmental Microbiology, v. 85, e02900-18, 2019. DOI: https://doi.org/10.1128/AEM.02900-18.

KASMAN, L. M.; PORTER, L. D. Bacteriophages. \[Updated 2022 Sep 26]. In: StatPearls\[Internet]. Treasure Island (FL): StatPearls Publishing; 2025 Jan–. Disponível em: https://www.ncbi.nlm.nih.gov/books/NBK493185/.

KELLY, L.; JAMESON, E. Bacteriophage cocktail shows no toxicity and improves the survival of *Galleria mellonella* infected with *Klebsiella* spp. Journal of Virology, v. 98, e00272-24, 2024. DOI: https://doi.org/10.1128/jvi.00272-24.

KUMAR, M.; CURTIS, A.; HOSKINS, C. Application of nanoparticle technologies in the combat against anti-microbial resistance. Pharmaceutics, v. 10, n. 1, p. 11, 2018. DOI: https://doi.org/10.3390/pharmaceutics10010011.

LABRIE, S. J.; SAMSON, J. E.; MOINEAU, S. Bacteriophage resistance mechanisms. Nature Reviews Microbiology, v. 8, n. 5, p. 317–327, 2010. DOI: https://doi.org/10.1038/nrmicro2315.

LI, N. *et al*. Isolation and characterization of novel phages targeting pathogenic *Klebsiella pneumoniae*. Frontiers in Cellular and Infection Microbiology, Lausanne, v. 11, p. 792305, 3 dez. 2021. DOI: 10.3389/fcimb.2021.792305.

LI, Pei; ZHOU, Yu; GUO, Genglin; QIN, Xiayan; HU, Zimeng; LI, Min; TAN, Zhongming; LIU, Yuqing; HAN, Xiangan; MA, Jiale; DU, Hong; ZHANG, Wei. Efficacy of a new K3-specific bacteriophage for controlling *Klebsiella pneumoniae* in milk and its potential to disrupt biofilm formation. Food Control, v. 163, p. 110519, 2024.

LI, Yanping; KUMAR, Suresh; ZHANG, Lihu; WU, Hongjie; WU, Hongyan. Characteristics of antibiotic resistance mechanisms and genes of Klebsiella pneumoniae. Open Medicine, v. 18, n. 1, p. 1–12, 2023. DOI: 10.1515/med-2023-0707. Disponível em: https://www.degruyter.com/document/doi/10.1515/med-2023-0707/html. Acesso em: 16 jul. 2025.

LIU, Y.; ZHANG, C.; LIU, Y.; WANG, Y. Phage cocktail therapy: multiple strategies for a complex problem. Virologica Sinica, v. 35, n. 5, p. 539–550, 2020. DOI: https://doi.org/10.1007/s12250-020-00254-4.

MIRZAEI, M. K.; NILSSON, A. S. Isolation of phages for phage therapy: A comparison of spot tests and efficiency of plating analyses for determination of host range and efficacy. PLoS ONE, v. 10, n. 3, p. e0118557, 2015. DOI: https://doi.org/10.1371/journal.pone.0118557.

MITARAI, N.; BROWN, S.; SNEPPEN, K. Population dynamics of phage and bacteria in spatially structured habitats using phage λ and Escherichia coli. Journal of Bacteriology, Washington, DC, v. 198, n. 12, p. 1783–1793, 27 maio 2016. DOI: 10.1128/JB.00965-15.

MORENO SWITT, A. I. et al. Genomic characterization provides new insight into *Salmonella* phage diversity. BMC Genomics, v. 14, p. 481, 17 jul. 2013. DOI: https://doi.org/10.1186/1471-2164-14-481.

NALE, J. Y.; CHUTIA, M.; CARR, P.; HICKENBOTHAM, P.; CLOKIE, M. R. J. ‘Get in early’: biofilm and wax moth (*Galleria mellonella*) models reveal new insights into the

therapeutic potential of *Clostridium difficile* bacteriophages. Frontiers in Microbiology, v. 7, p. 1383, 2016. DOI: https://doi.org/10.3389/fmicb.2016.01383.

NALE, J. Y. et al. An optimized bacteriophage cocktail can effectively control *Salmonella* in vitro and in *Galleria mellonella*. Frontiers in Microbiology, v. 11, p. 609955, 2021. DOI: https://doi.org/10.3389/fmicb.2020.609955.

NARIMISA, N. et al. Effects of sub-inhibitory concentrations of antibiotics and oxidative stress on the expression of type II TA system genes in *Klebsiella pneumoniae*. Journal of Global Antimicrobial Resistance, 2019. DOI: 10.1016/j.jgar.2019.09.005.

PERTICS, B. Z. et al. Isolation and characterization of a novel lytic bacteriophage against the K2 capsule-expressing hypervirulent *Klebsiella pneumoniae* strain 52145, and identification of its functional depolymerase. Microorganisms, v. 9, n. 3, p. 650, 2021. DOI: https://doi.org/10.3390/microorganisms9030650. Disponível em: https://www.mdpi.com/2076-2607/9/3/650. Acesso em: 20 jul. 2025.

PRINCIPI, N.; SILVESTRI, E.; ESPOSITO, S. Advantages and limitations of bacteriophages for the treatment of bacterial infections. Frontiers in Pharmacology, v. 10, p. 513, 8 maio 2019. DOI: 10.3389/fphar.2019.00513.

QUISPE-VILLEGAS, G.; ALCÁNTARA-LOZANO, G. I.; CUICAPUZA, D.; LAUREANO, R.; AYZANOA, B.; TSUKAYAMA, P.; TAMARIZ, J. In vivo evaluation of phage therapy against *Klebsiella pneumoniae* using the *Galleria mellonella* model and molecular characterization of a novel *Drulisvirus* phage species. Microbiology Spectrum, v. 13, e01145-24, 2025. DOI: https://doi.org/10.1128/spectrum.01145-24.

RIBEIRO, M. G.; DE MORAIS, A. B. C.; ALVES, A. C. et al. *Klebsiella*-induced infections in domestic species: a case-series study in 697 animals (1997–2019). Brazilian Journal of Microbiology, v. 53, p. 455–464, 2022. DOI: 10.1007/s42770-021-00667-0.

RUSSO, T. A.; MARR, C. M. Hypervirulent *Klebsiella pneumoniae*. Clinical Microbiology Reviews, v. 32, n. 3, 2019. DOI: 10.1128/cmr.00001-19.

SANI, G.S.; GHANE, M.; BABAEEKHOU, L. Fluoroquinolone-resistance mechanisms and molecular epidemiology of ciprofloxacin-resistant Klebsiella pneumoniae isolates in Iran. Folia Microbiologica, v. 68, p. 633–644, 2023. DOI: https://doi.org/10.1007/s12223-023-01042-2.

SENHAJI-KACHA, A. et al. Isolation and characterization of two novel bacteriophages against carbapenem-resistant *Klebsiella pneumoniae*. Frontiers in Cellular and Infection Microbiology, [S.l.], v. 14, p. 1421724, 29 ago. 2024. DOI: https://doi.org/10.3389/fcimb.2024.1421724.

TOWNSEND, E. M. et al. Isolation and characterization of *Klebsiella* phages for phage therapy. Phage (New Rochelle), New Rochelle, v. 2, n. 1, p. 26–42, 1 mar. 2021. DOI: 10.1089/phage.2020.0046.

TOWNSEND, Eleanor et al. Isolation and characterisation of *Klebsiella* phages for phage therapy. PHAGE: Therapy, Applications, and Research, v. 1, n. 3, p. 127–136, 2020. DOI: https://doi.org/10.1089/phage.2020.0046.

WARETH, G.; NEUBAUER, H. The animal-foods-environment interface of *Klebsiella pneumoniae* in Germany: an observational study on pathogenicity, resistance development and the current situation. Veterinary Research, v. 52, p. 16, 2021. DOI: 10.1186/s13567-020-00875-w.

WANG, Z. et al. Antioxidant and antibacterial study of 10 flavonoids revealed rutin as a potential antibiofilm agent in *Klebsiella pneumoniae* strains isolated from hospitalized patients. Microbial Pathogenesis, v. 159, p. 105121, 2021. DOI: 10.1016/j.micpath.2021.105121.

WYRES, K. L.; LAM, M. M. C.; HOLT, K. E. Population genomics of *Klebsiella pneumoniae*. Nature Reviews Microbiology, London, v. 18, p. 344–359, 2020. DOI: 10.1038/s41579-019-0315-1.

YANG, F. et al. High rate of multiresistant *Klebsiella pneumoniae* from human and animal origin. Infection and Drug Resistance, v. 12, p. 2729–2737, 2019. DOI: 10.2147/IDR.S219155.

ZHANG, Y. et al. Chlorhexidine exposure of clinical strains of *Klebsiella pneumoniae* leads to acquired resistance to this disinfectant and colistin. International Journal of Antimicrobial Agents, 2019. DOI: 10.1016/j.ijantimicag.2019.02.

ZHENG, X.; WANG, X.; LI, P. et al. The change of long tail fibers expanded the host range of a T5-like Salmonella phage and its application in milk. BMC Microbiology, London, v. 25, article 169, 2025. DOI: 10.1186/s12866-025-03895-8.

ZHU, J.; WANG, T.; CHEN, L.; DU, H. Virulence factors in hypervirulent *Klebsiella pneumoniae*. Frontiers in Microbiology, v. 12, p. 642484, 8 abr. 2021. DOI: 10.3389/fmicb.2021.642484.

ZURABOV, F.; ZHILENKOV, E. Characterization of four virulent *Klebsiella pneumoniae* bacteriophages, and evaluation of their potential use in complex phage preparation. Virology Journal, v. 18, n. 9, 2021. Disponível em: https://doi.org/10.1186/s12985-020-01485-w. Acesso em: 19 jul. 2025.

8. APPENDIX

This appendix presents the graphs related to the complementary experiments conducted during the development of this work. It includes the bacterial growth curves used for the determination of the minimum inhibitory concentration (MIC), as well as the graphical results of the growth and biofilm prevention assays performed with the bacterial strains in the presence of bacteriophages. Although these tests were conducted with experimental rigor, the results did not show statistically significant differences compared to the bacterial control group.

Minimum inhibitory concentration (MIC)

1. *K. pneumoniae* 58B

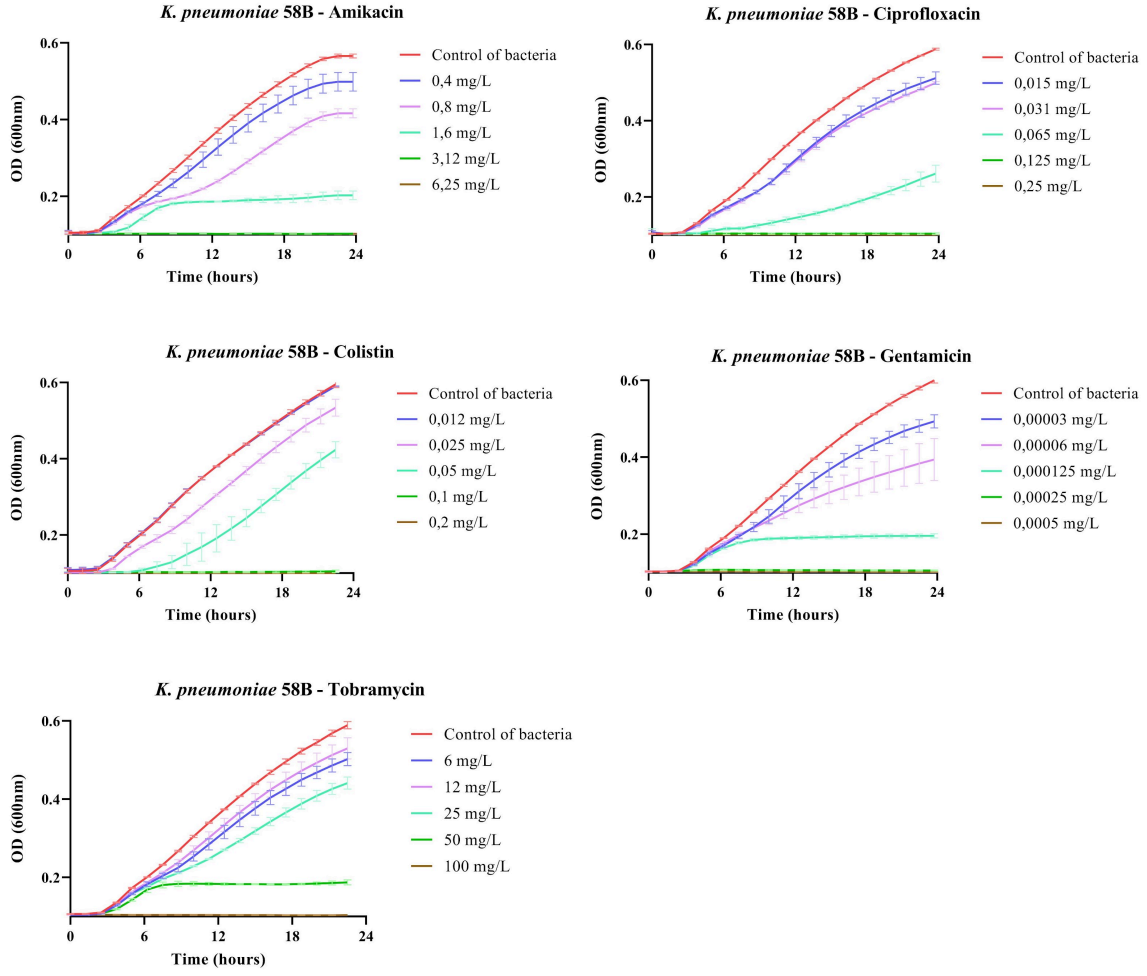

2. *K. pneumoniae* 5B

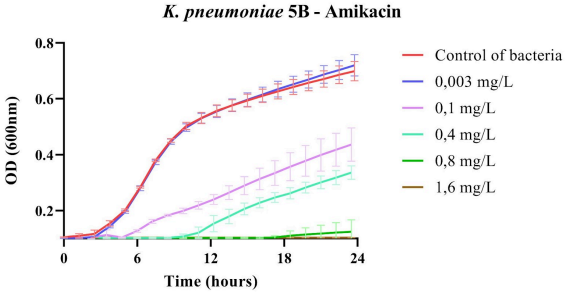

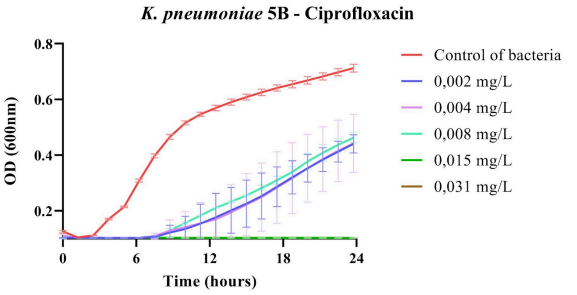

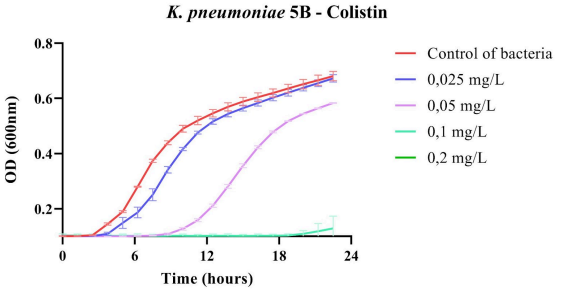

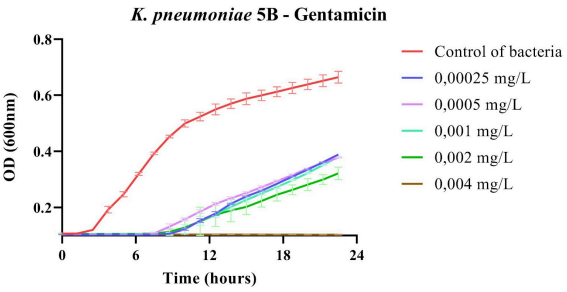

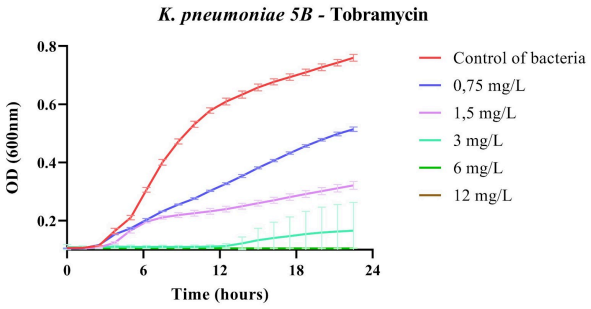

3. *K. pneumoniae* 13

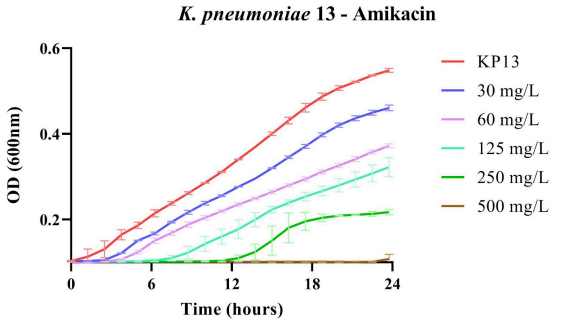

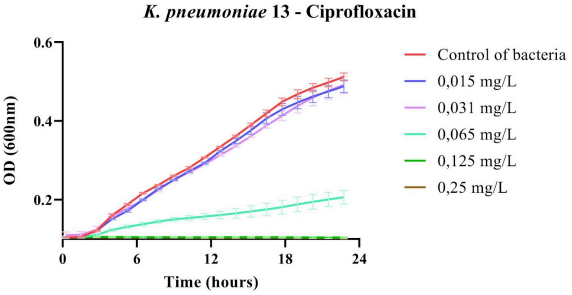

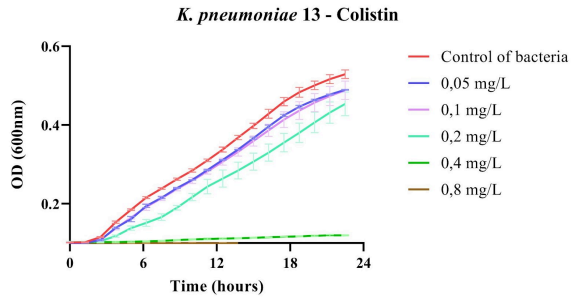

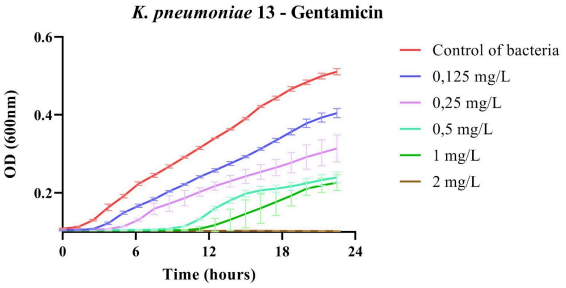

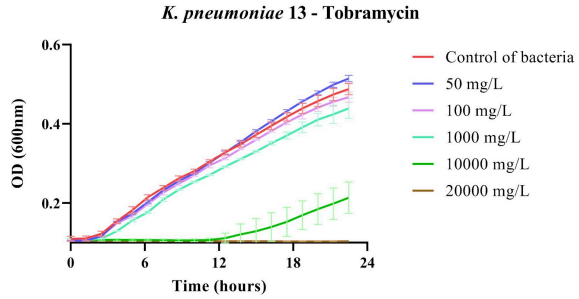

Growth curves

1. Phage KO2 - Host bacterium *K. oxytoca* 13182 ATCC

A.

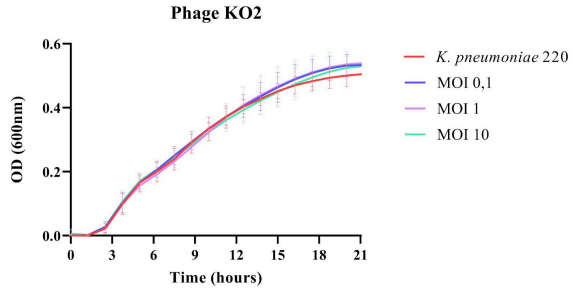

B.

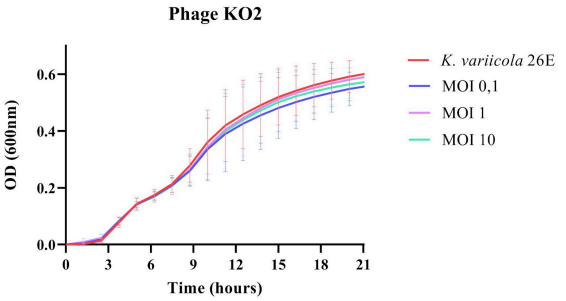

C.

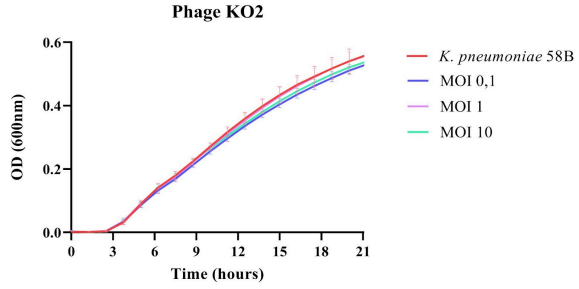

D.

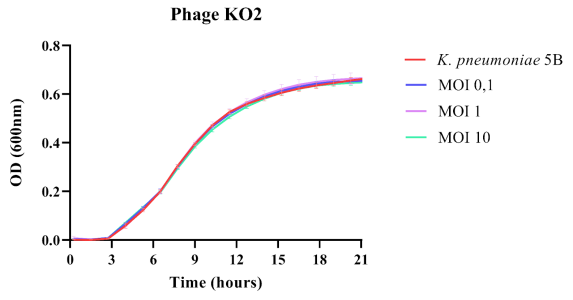

E.

F.

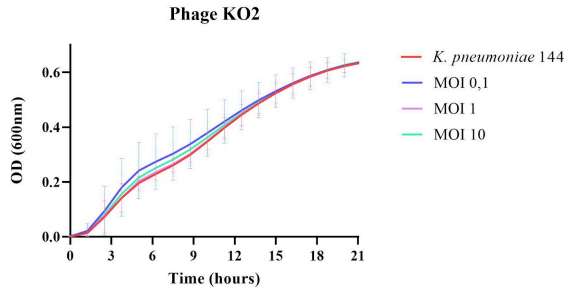
Phage KO2
OD (600nm)
Time (hours)
K. pneumoniae 144
MOI 0,1
MOI 1
MOI 10

G.

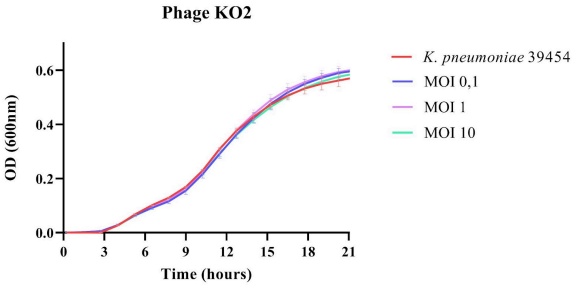
Phage KO2
OD (600nm)
Time (hours)
K. pneumoniae 39454
MOI 0,1
MOI 1
MOI 10

H.

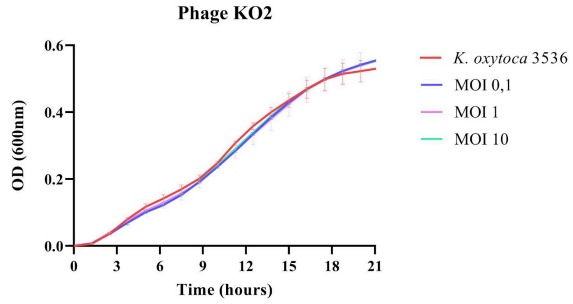
Phage KO2
OD (600nm)
Time (hours)
K. oxytoca 3536
MOI 0,1
MOI 1
MOI 10

I.

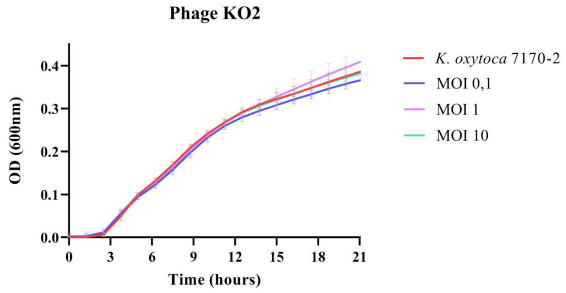
Phage KO2
OD (600nm)
Time (hours)
K. oxytoca 7170-2
MOI 0,1
MOI 1
MOI 10

J.

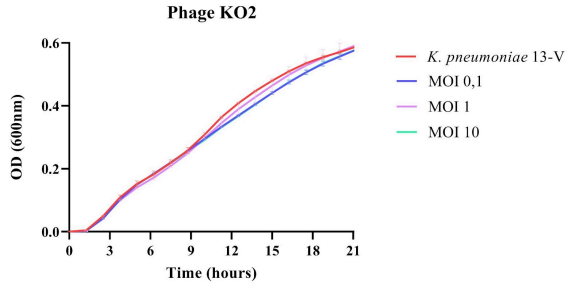
Phage KO2
OD (600nm)
Time (hours)
K. pneumoniae 13-V
MOI 0,1
MOI 1
MOI 10

K.

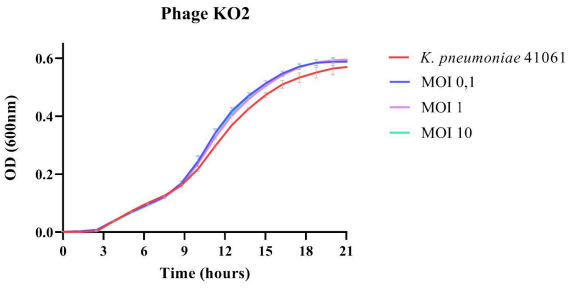
Phage KO2
OD (600nm)
Time (hours)
K. pneumoniae 41061
MOI 0,1
MOI 1
MOI 10

L.

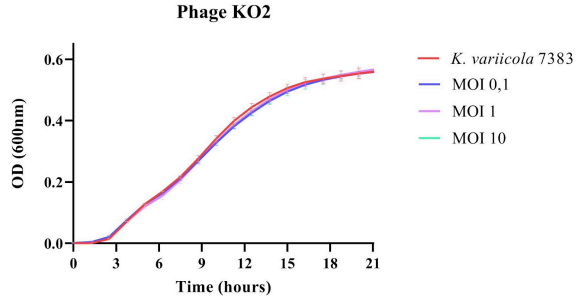
Phage KO2
OD (600nm)
Time (hours)
K. variicola 7383
MOI 0,1
MOI 1
MOI 10

M.

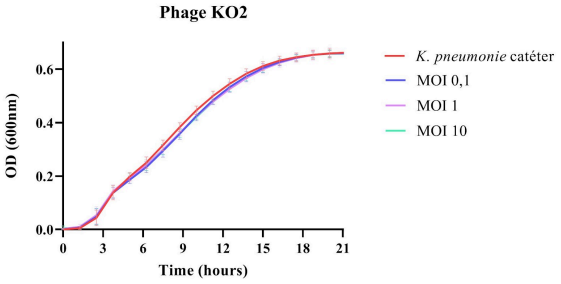
Phage KO2
OD (600nm)
Time (hours)
K. pneumonie catéter
MOI 0,1
MOI 1
MOI 10

N.

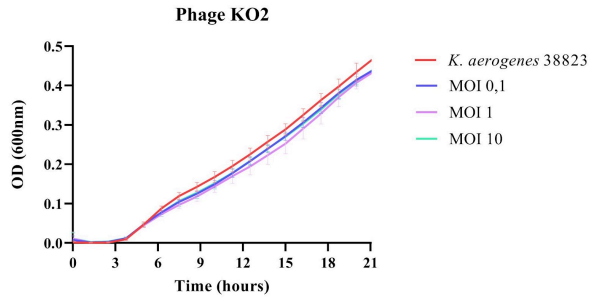

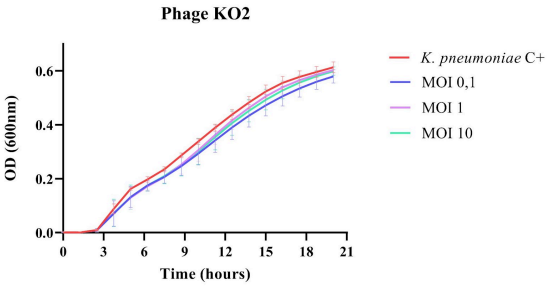

O.

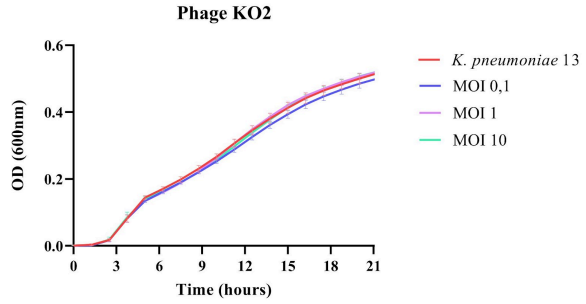

2. Phage KV3 - Host bacterium *K. variicola* 26E

A.

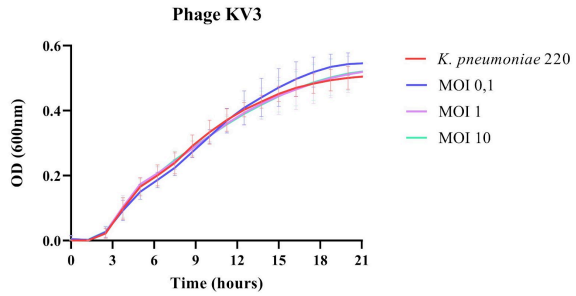

B.

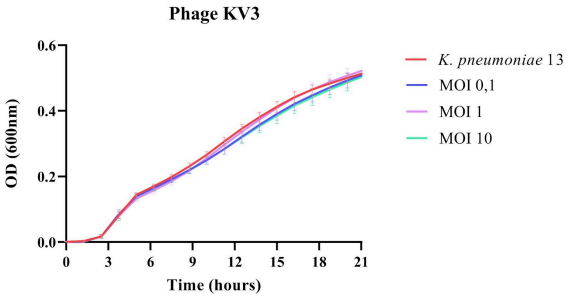

C.

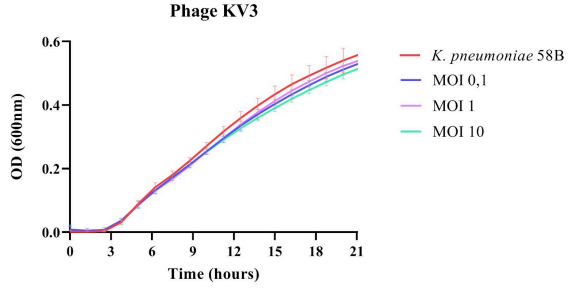

D.

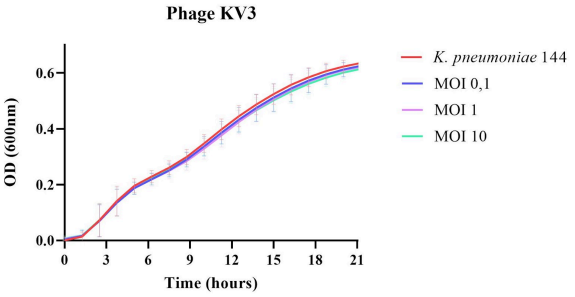

E.

F.

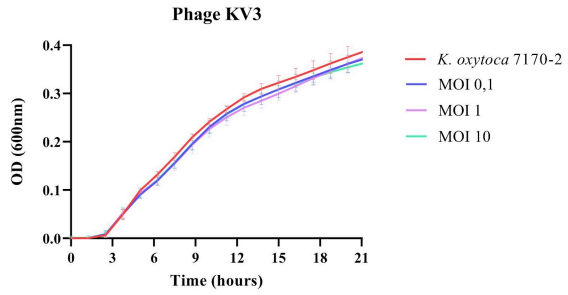
Phage KV3
OD (600nm)
Time (hours)
K. oxytoca 7170-2
MOI 0,1
MOI 1
MOI 10

G.

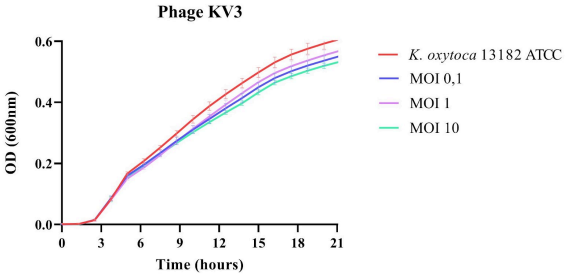
Phage KV3
OD (600nm)
Time (hours)
K. oxytoca 13182 ATCC
MOI 0,1
MOI 1
MOI 10

H.

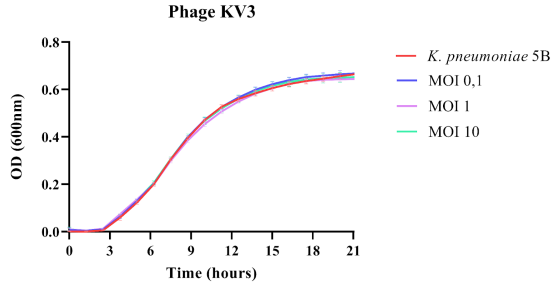
Phage KV3
OD (600nm)
Time (hours)
K. pneumoniae 5B
MOI 0,1
MOI 1
MOI 10

I.

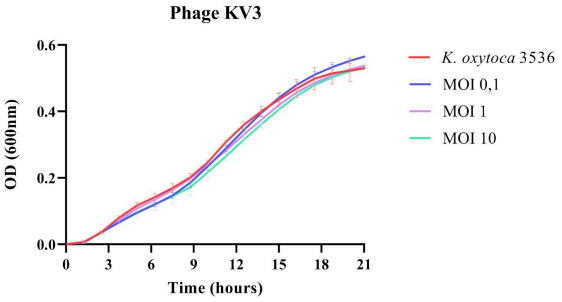
Phage KV3
OD (600nm)
Time (hours)
K. oxytoca 3536
MOI 0,1
MOI 1
MOI 10

J.

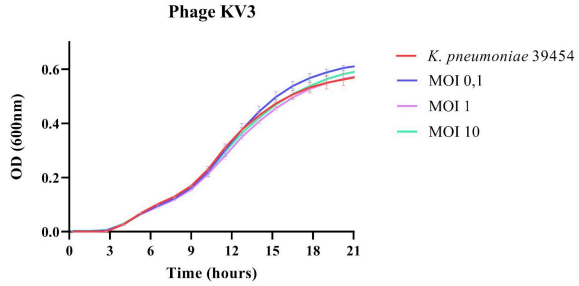
Phage KV3
OD (600nm)
Time (hours)
K. pneumoniae 39454
MOI 0,1
MOI 1
MOI 10

K.

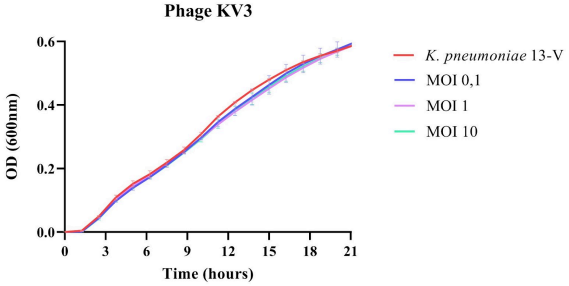
Phage KV3
OD (600nm)
Time (hours)
K. pneumoniae 13-V
MOI 0,1
MOI 1
MOI 10

L.

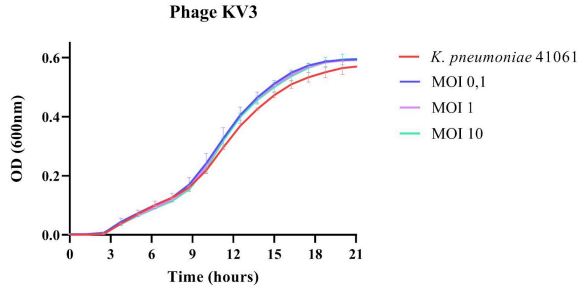
Phage KV3
OD (600nm)
Time (hours)
K. pneumoniae 41061
MOI 0,1
MOI 1
MOI 10

M.

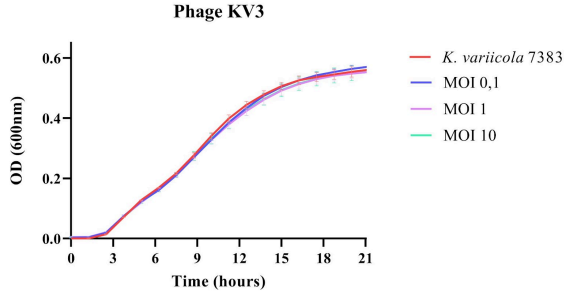
Phage KV3
OD (600nm)
Time (hours)
K. variicola 7383
MOI 0,1
MOI 1
MOI 10

N.

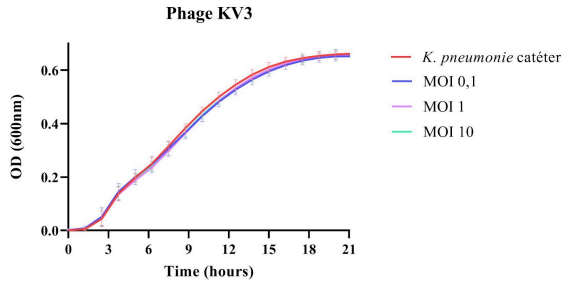

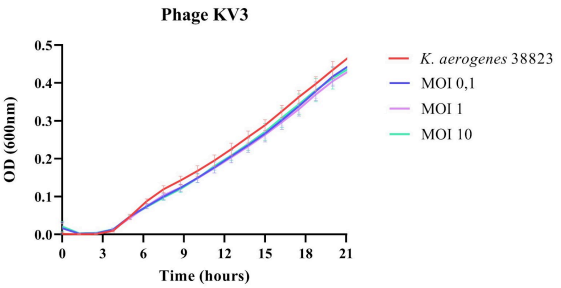

O.

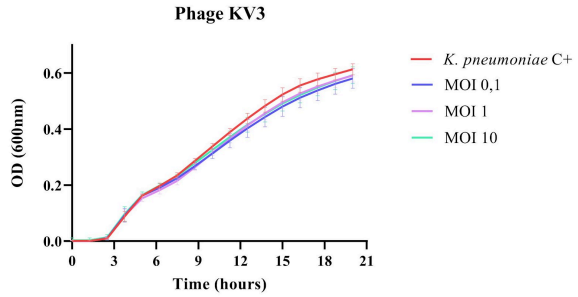

3. Phage KP4 - Host bacterium *K. pneumoniae* 13

A.

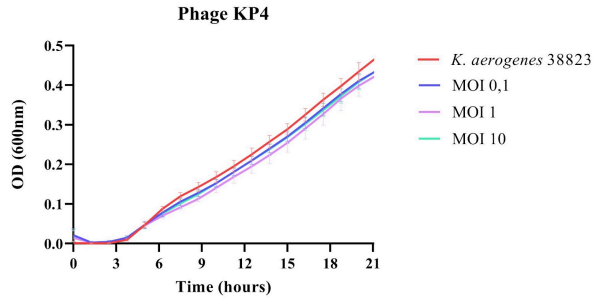

B.

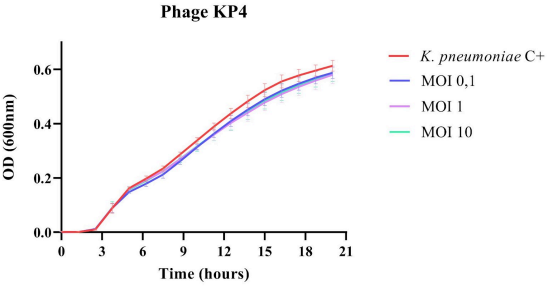

C.

D.

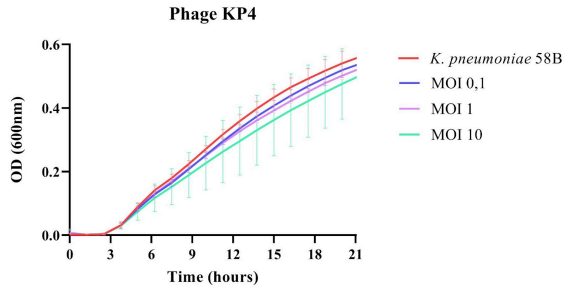

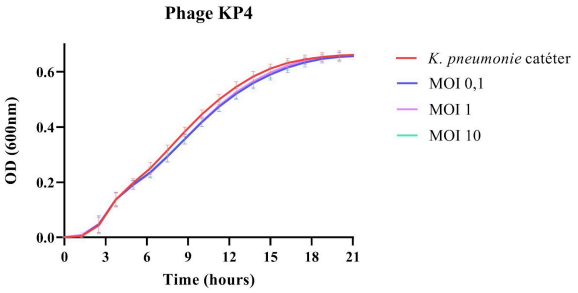

E.

F.

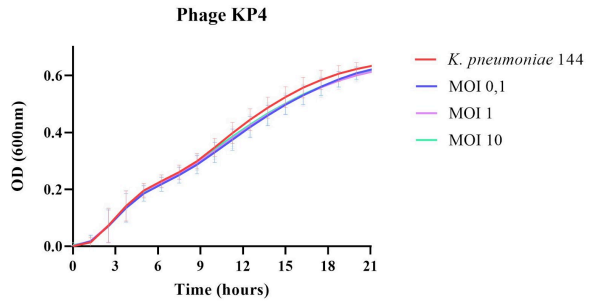
Phage KP4
OD (600nm)
Time (hours)
K. pneumoniae 144
MOI 0,1
MOI 1
MOI 10

G.

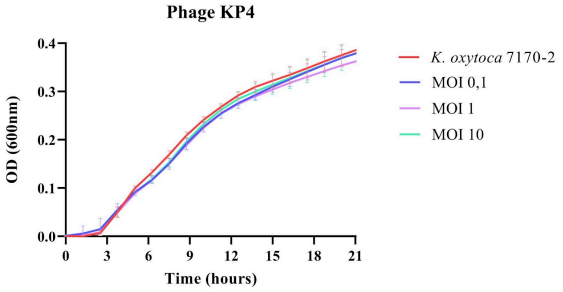
Phage KP4
OD (600nm)
Time (hours)
K. oxytoca 7170-2
MOI 0,1
MOI 1
MOI 10

H.

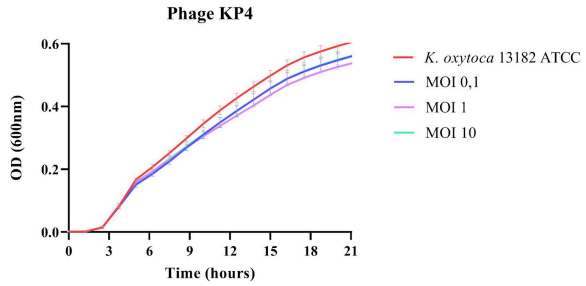
Phage KP4
OD (600nm)
Time (hours)
K. oxytoca 13182 ATCC
MOI 0,1
MOI 1
MOI 10

I.

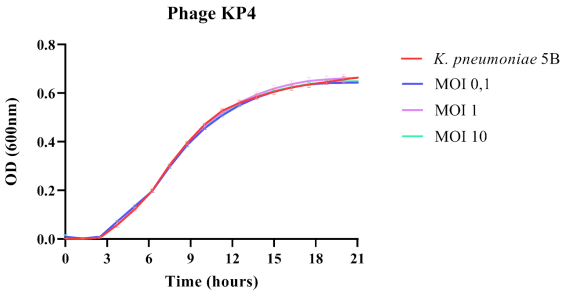
Phage KP4
OD (600nm)
Time (hours)
K. pneumoniae 5B
MOI 0,1
MOI 1
MOI 10

J.

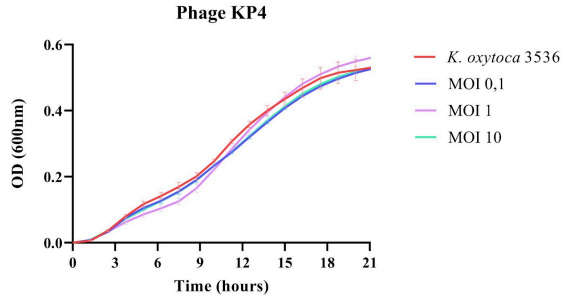
Phage KP4
OD (600nm)
Time (hours)
K. oxytoca 3536
MOI 0,1
MOI 1
MOI 10

K.

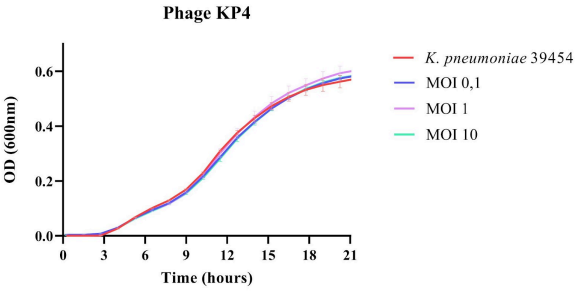
Phage KP4
OD (600nm)
Time (hours)
K. pneumoniae 39454
MOI 0,1
MOI 1
MOI 10

L.

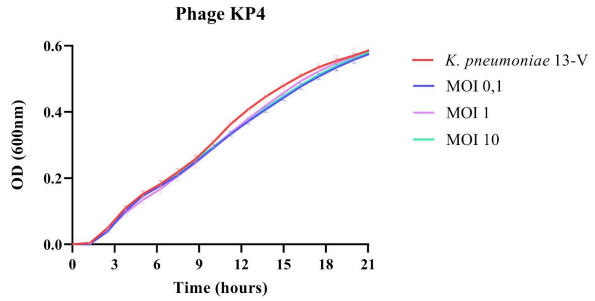
Phage KP4
OD (600nm)
Time (hours)
K. pneumoniae 13-V
MOI 0,1
MOI 1
MOI 10

M.

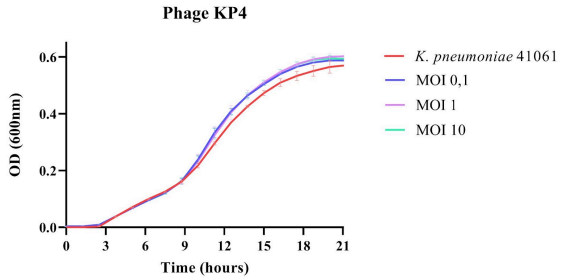
Phage KP4
OD (600nm)
Time (hours)
K. pneumoniae 41061
MOI 0,1
MOI 1
MOI 10

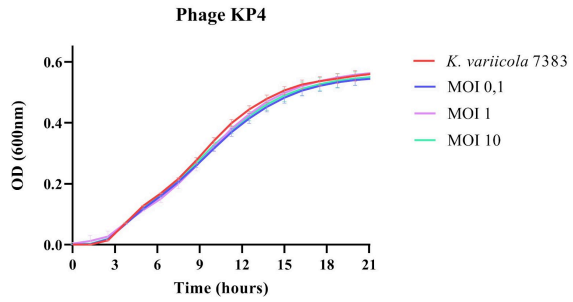

4. Phage KP6 - Host bacterium *K. pneumoniae* 58B

A.

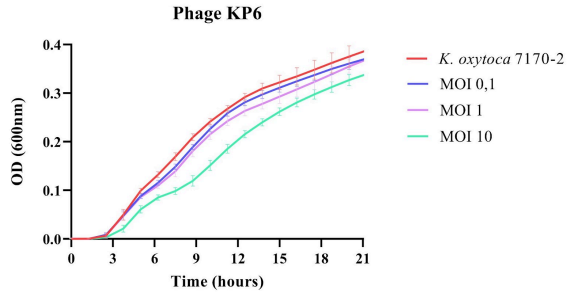

B.

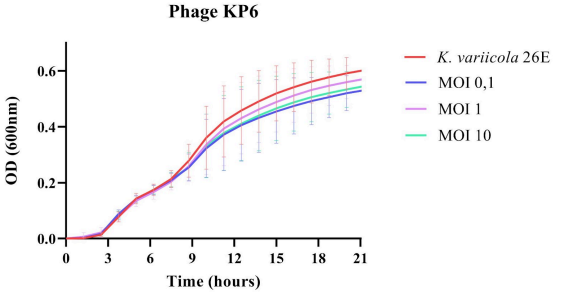

C.

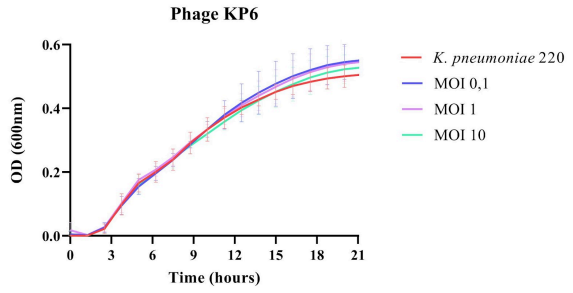

D.

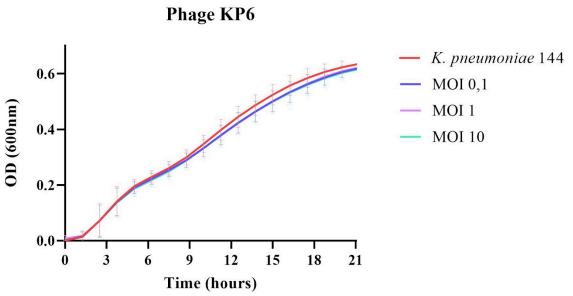

E.

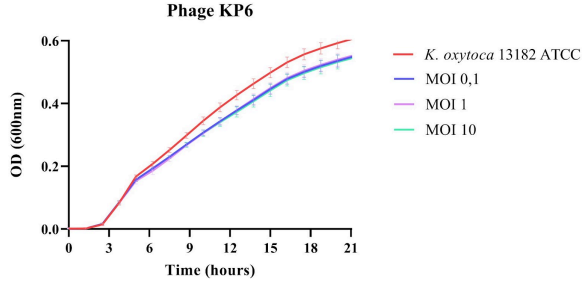

F.

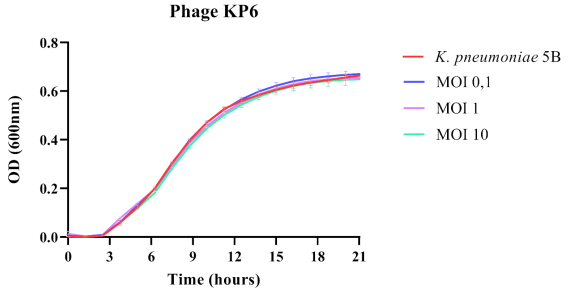

G.

H.

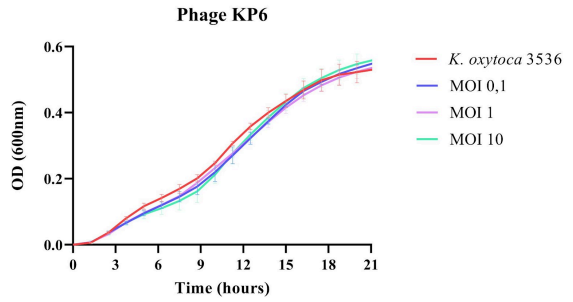
Phage KP6
OD (600nm)
Time (hours)
K. oxytoca 3536
MOI 0,1
MOI 1
MOI 10

I.

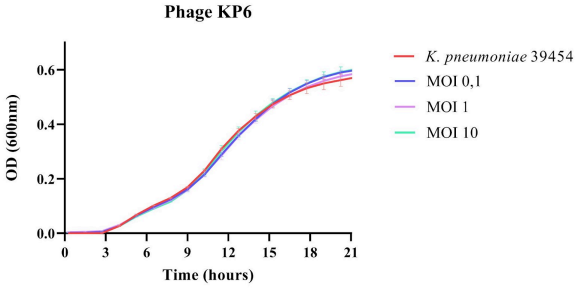
Phage KP6
OD (600nm)
Time (hours)
K. pneumoniae 39454
MOI 0,1
MOI 1
MOI 10

J.

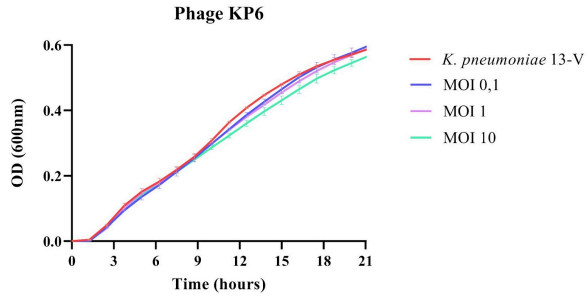
Phage KP6
OD (600nm)
Time (hours)
K. pneumoniae 13-V
MOI 0,1
MOI 1
MOI 10

K.

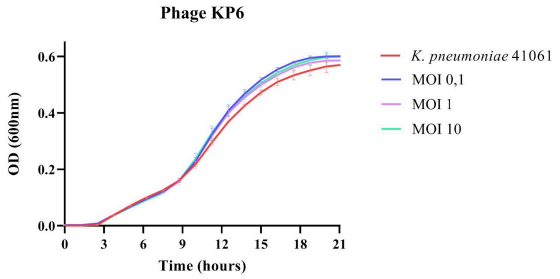
Phage KP6
OD (600nm)
Time (hours)
K. pneumoniae 41061
MOI 0,1
MOI 1
MOI 10

L.

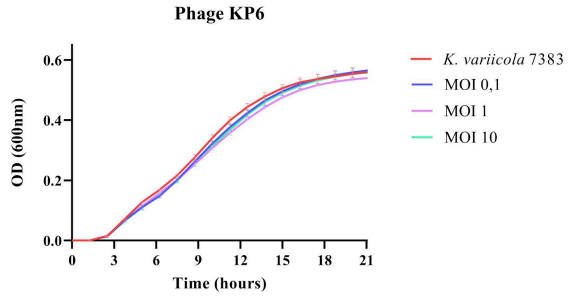
Phage KP6
OD (600nm)
Time (hours)
K. variicola 7383
MOI 0,1
MOI 1
MOI 10

M.

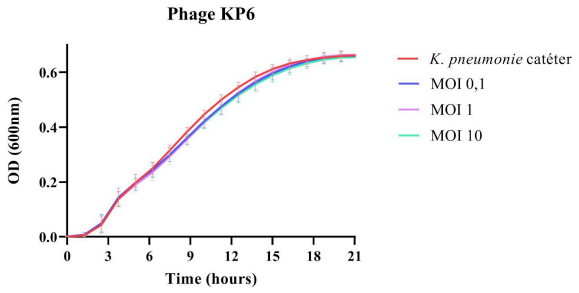
Phage KP6
OD (600nm)
Time (hours)
K. pneumonie catéter
MOI 0,1
MOI 1
MOI 10

N.

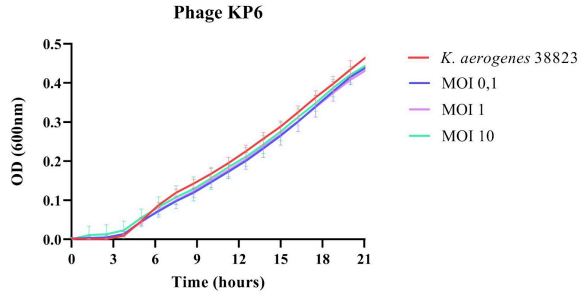
Phage KP6
OD (600nm)
Time (hours)
K. aerogenes 38823
MOI 0,1
MOI 1
MOI 10

O.

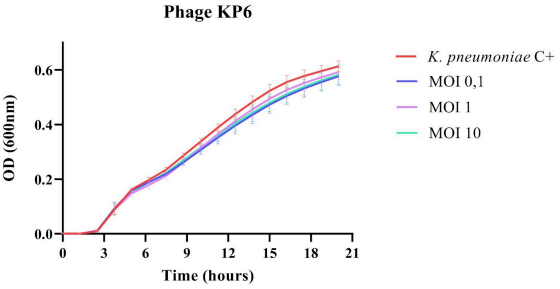
Phage KP6
OD (600nm)
Time (hours)
K. pneumoniae C+
MOI 0,1
MOI 1
MOI 10

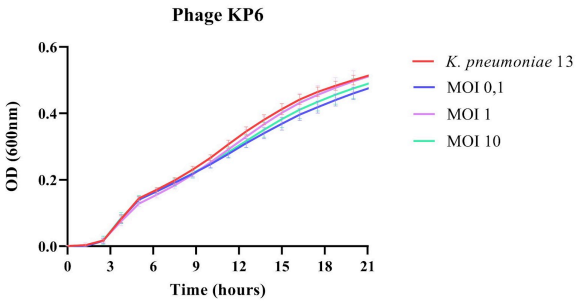

5. Phage KP7 - Host bacterium *K. pneumoniae* 58B

A.

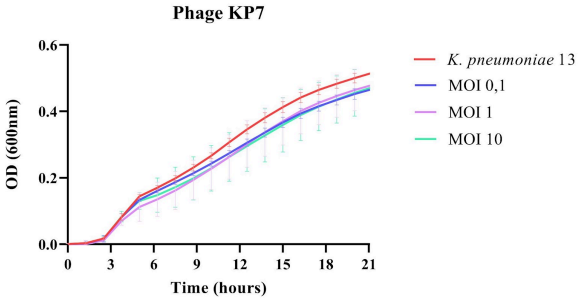

B.

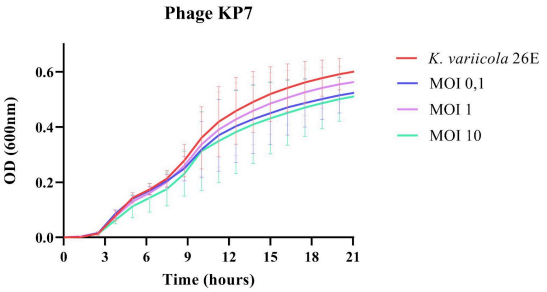

C.

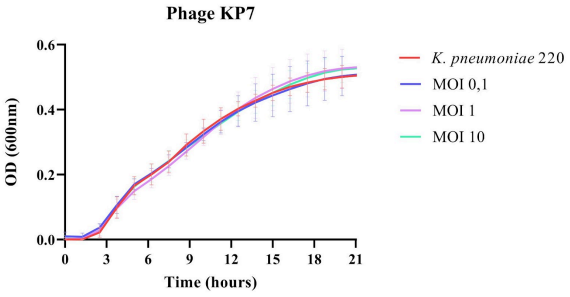

D.

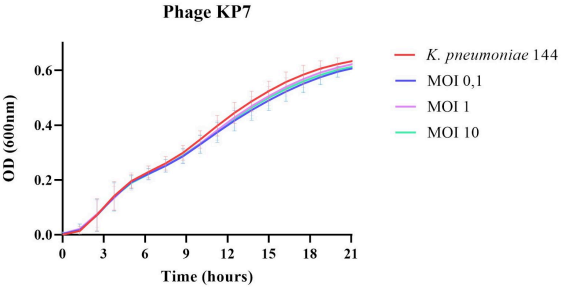

E.

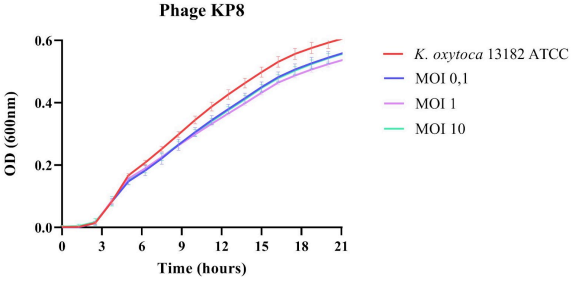

F.

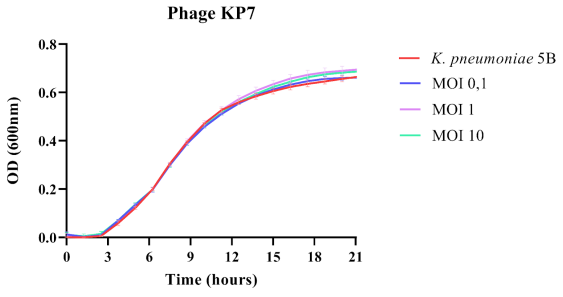

G.

H.

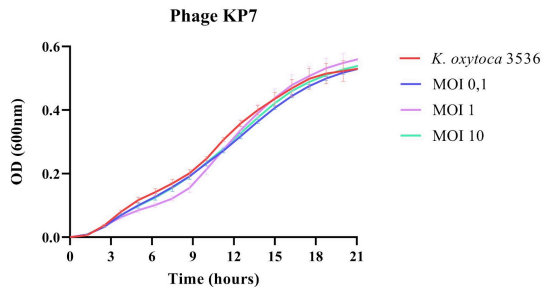

I.

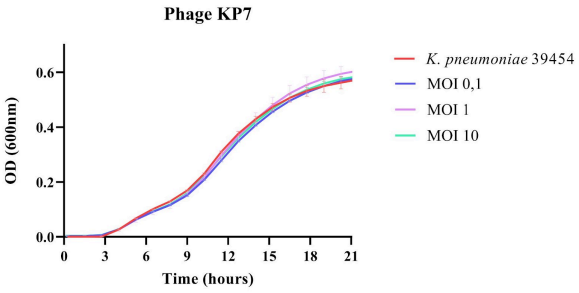

J.

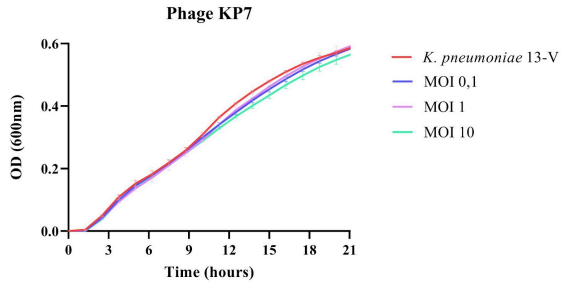

K.

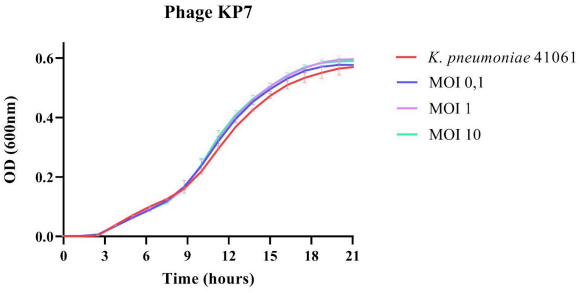

L.

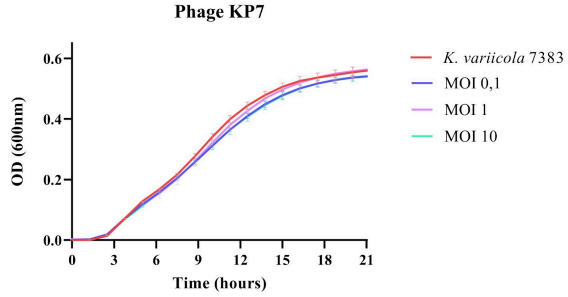

M.

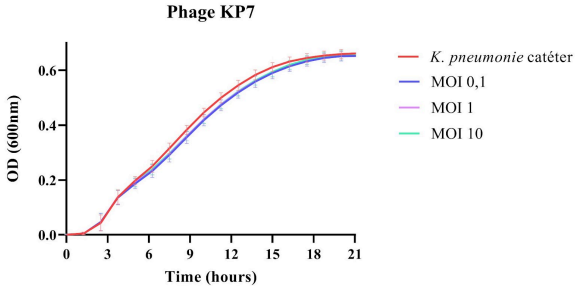

N.

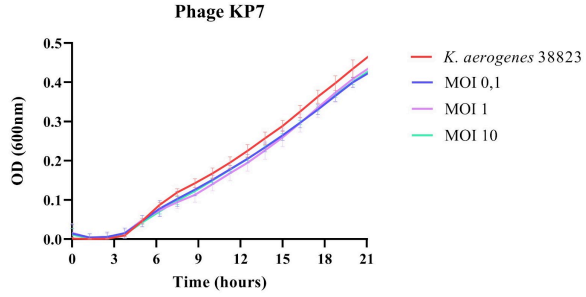

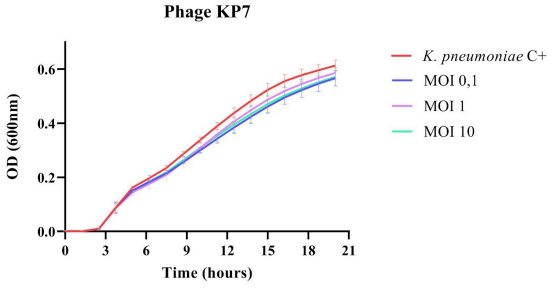

6. Phage KP8 - Host bacterium *K. pneumoniae* 5B

A.

B.

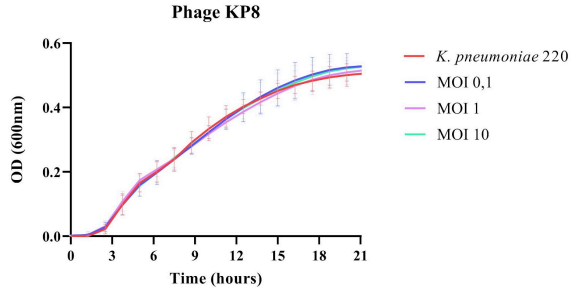
Phage KP8
OD (600nm)
Time (hours)
K. pneumoniae 220
MOI 0,1
MOI 1
MOI 10

C.

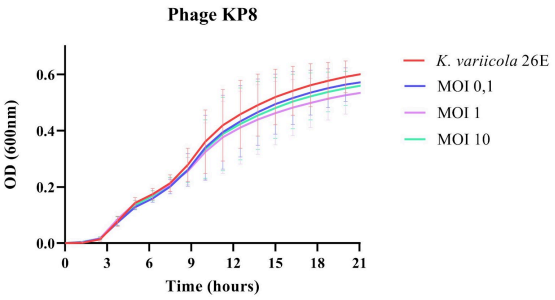
Phage KP8
OD (600nm)
Time (hours)
K. variicola 26E
MOI 0,1
MOI 1
MOI 10

D.

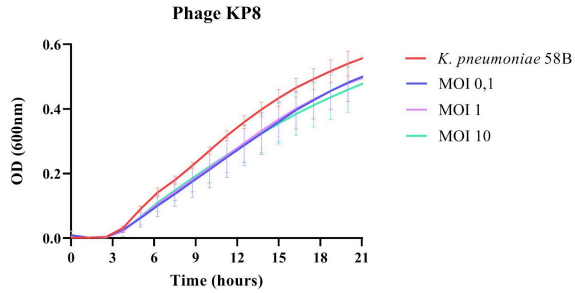
Phage KP8
OD (600nm)
Time (hours)
K. pneumoniae 58B
MOI 0,1
MOI 1
MOI 10

E.

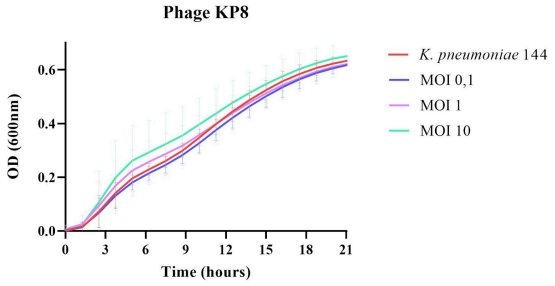
Phage KP8
OD (600nm)
Time (hours)
K. pneumoniae 144
MOI 0,1
MOI 1
MOI 10

F.

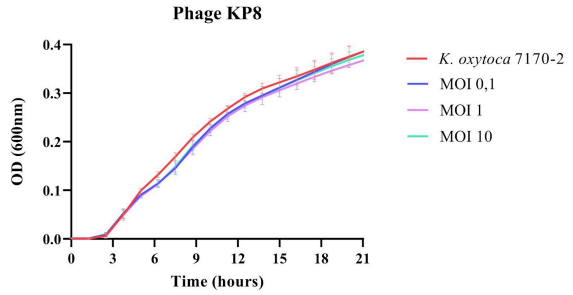
Phage KP8
OD (600nm)
Time (hours)
K. oxytoca 7170-2
MOI 0,1
MOI 1
MOI 10

G.

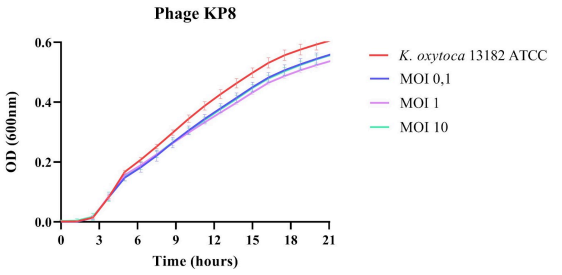
Phage KP8
OD (600nm)
Time (hours)
K. oxytoca 13182 ATCC
MOI 0,1
MOI 1
MOI 10

H.

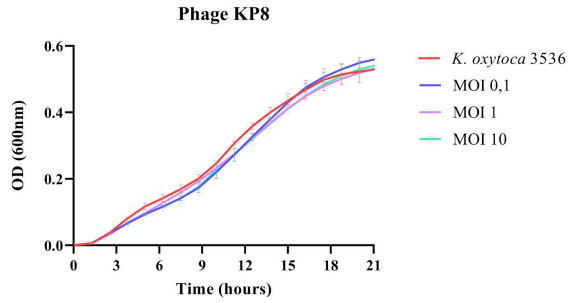
Phage KP8
OD (600nm)
Time (hours)
K. oxytoca 3536
MOI 0,1
MOI 1
MOI 10

I.

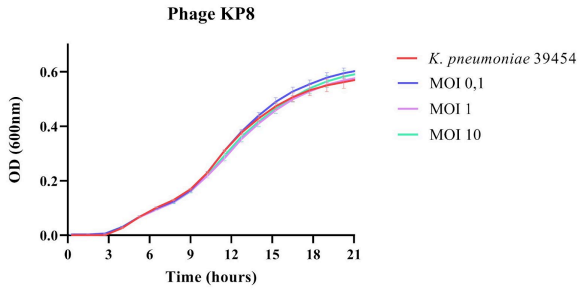
Phage KP8
OD (600nm)
Time (hours)
K. pneumoniae 39454
MOI 0,1
MOI 1
MOI 10

J.

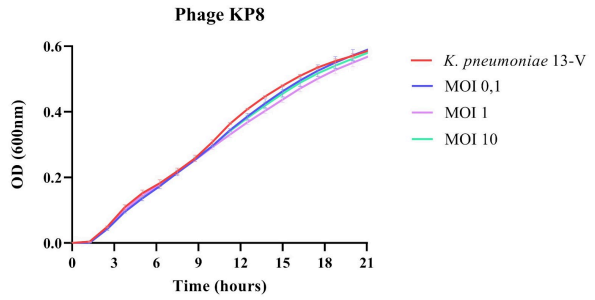

K.

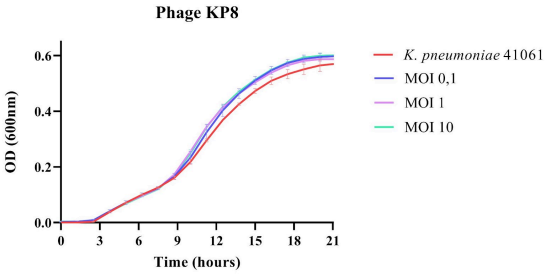

L.

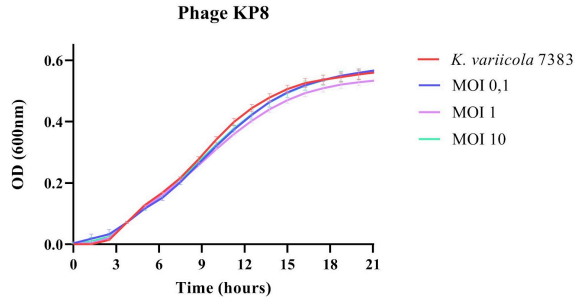

M.

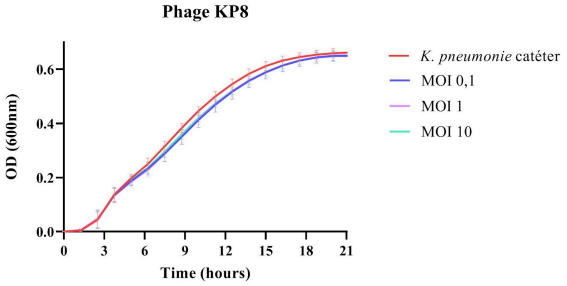

N.

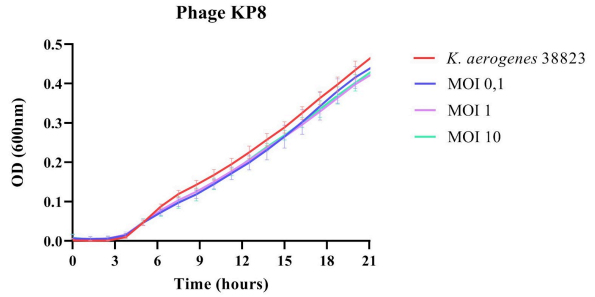

O.

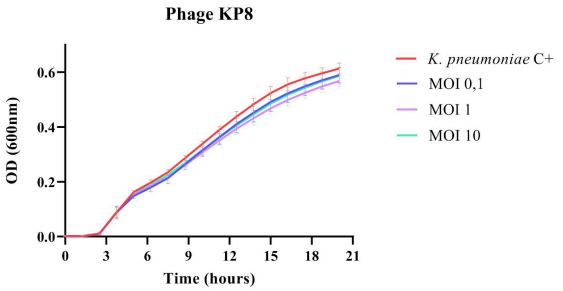

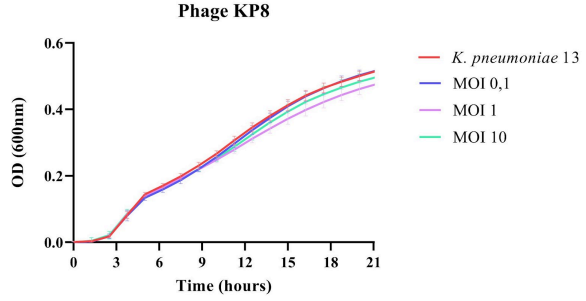

7. Phage KP9 - Host bacterium *K. pneumoniae* 5B

A.

B.

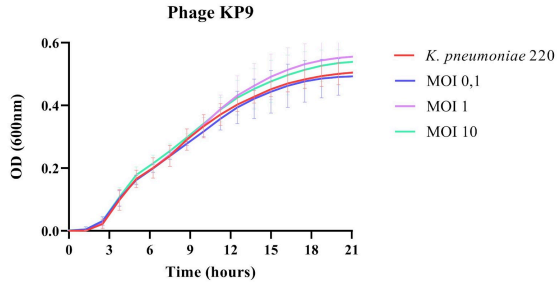
Phage KP9
OD (600nm)
Time (hours)
K. pneumoniae 220
MOI 0,1
MOI 1
MOI 10

C.

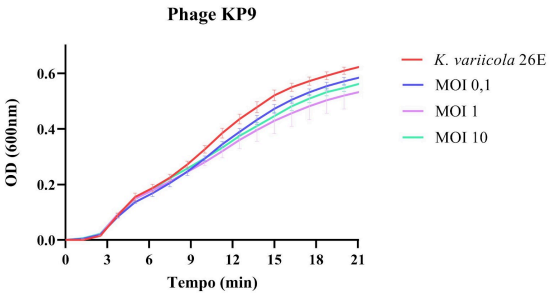
Phage KP9
OD (600nm)
Tempo (min)
K. variicola 26E
MOI 0,1
MOI 1
MOI 10

D.

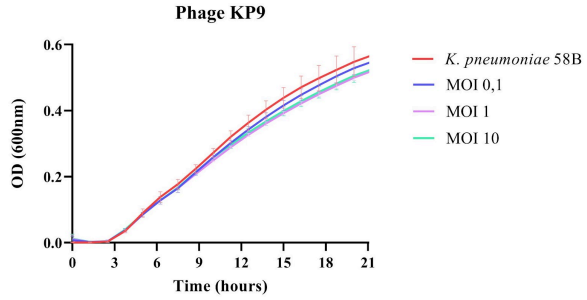
Phage KP9
OD (600nm)
Time (hours)
K. pneumoniae 58B
MOI 0,1
MOI 1
MOI 10

E.

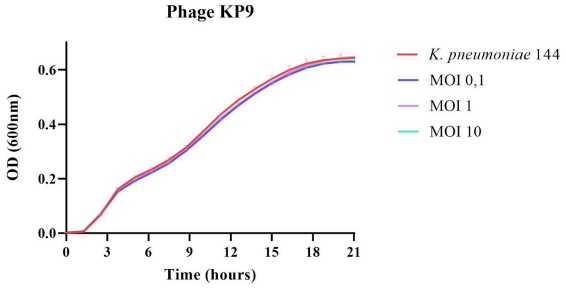
Phage KP9
OD (600nm)
Time (hours)
K. pneumoniae 144
MOI 0,1
MOI 1
MOI 10

F.

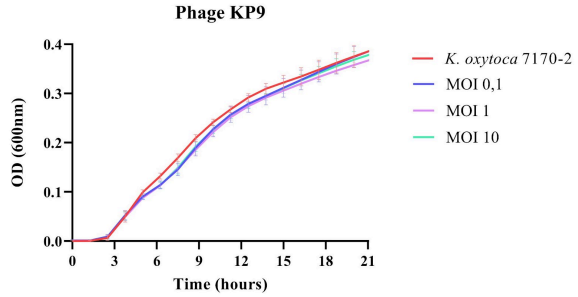
Phage KP9
OD (600nm)
Time (hours)
K. oxytoca 7170-2
MOI 0,1
MOI 1
MOI 10

G.

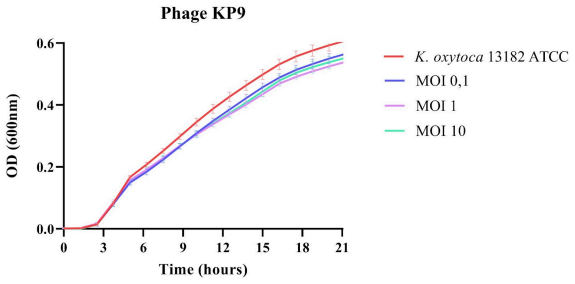
Phage KP9
OD (600nm)
Time (hours)
K. oxytoca 13182 ATCC
MOI 0,1
MOI 1
MOI 10

H.

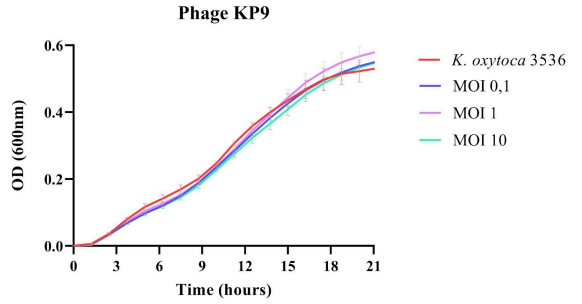
Phage KP9
OD (600nm)
Time (hours)
K. oxytoca 3536
MOI 0,1
MOI 1
MOI 10

I.

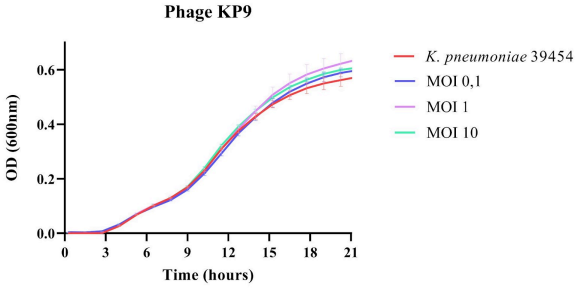
Phage KP9
OD (600nm)
Time (hours)
K. pneumoniae 39454
MOI 0,1
MOI 1
MOI 10

J.

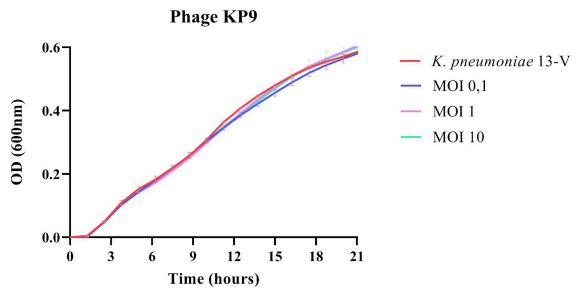

K.

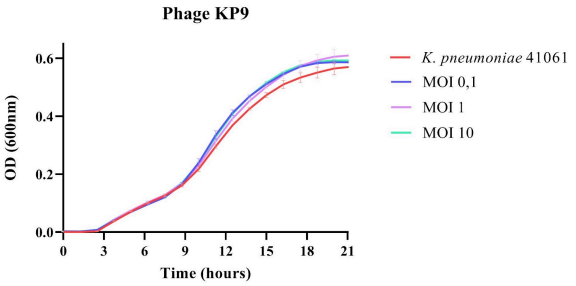

L.

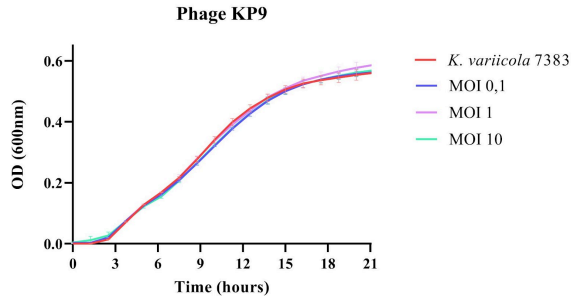

M.

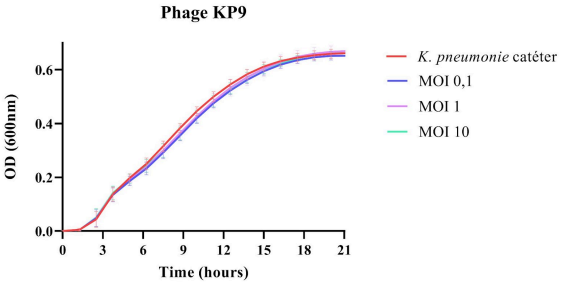

N.

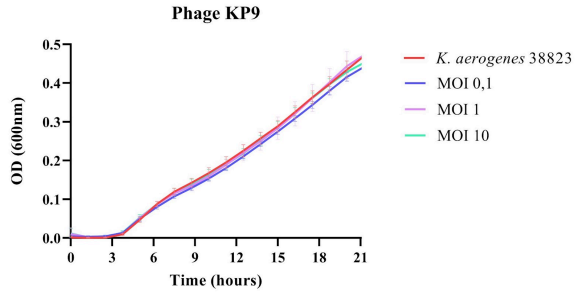

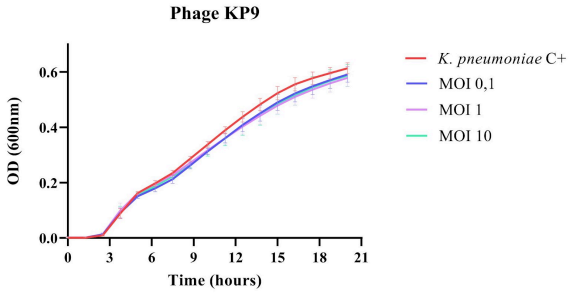

O.

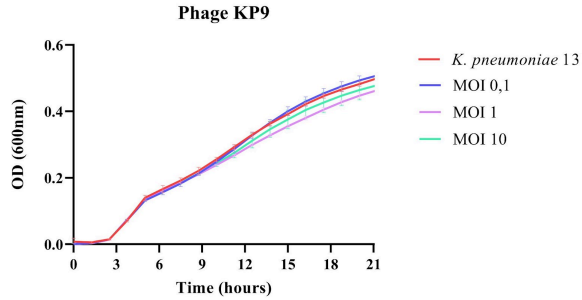

8. Cocktail (Phages KP4, KP6, KP7, and KP8)

A.

B.

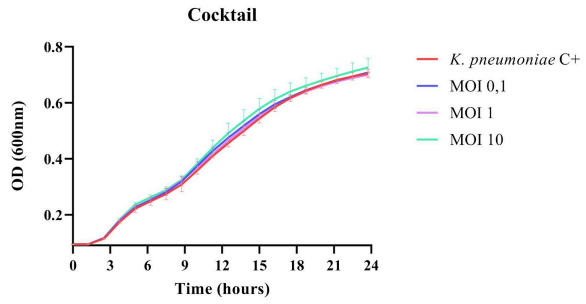
Cocktail
OD (600nm)
Time (hours)
K. pneumoniae C+
MOI 0,1
MOI 1
MOI 10

C.

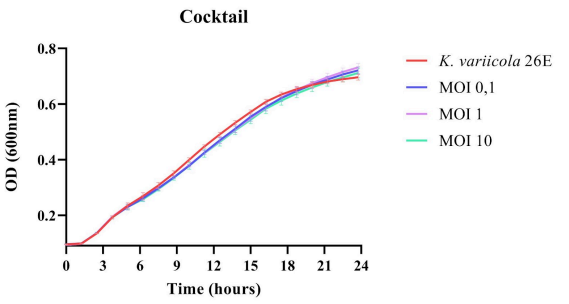
Cocktail
OD (600nm)
Time (hours)
K. variicola 26E
MOI 0,1
MOI 1
MOI 10

D.

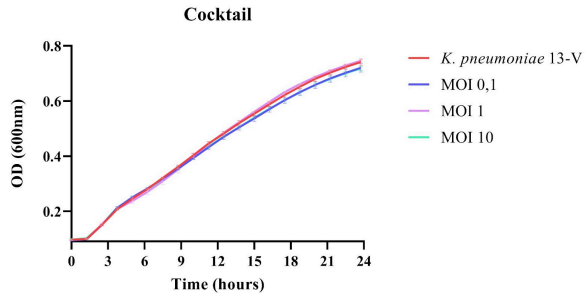
Cocktail
OD (600nm)
Time (hours)
K. pneumoniae 13-V
MOI 0,1
MOI 1
MOI 10

E.

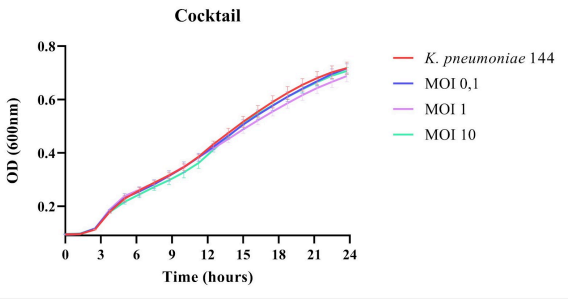
Cocktail
OD (600nm)
Time (hours)
K. pneumoniae 144
MOI 0,1
MOI 1
MOI 10

F.

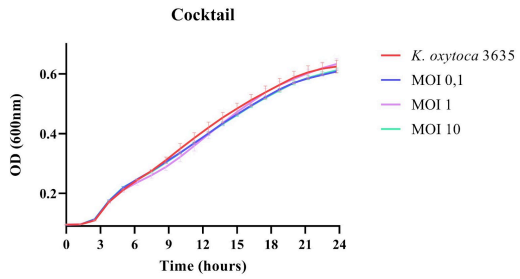
Cocktail
OD (600nm)
Time (hours)
K. oxytoca 3635
MOI 0,1
MOI 1
MOI 10

G.

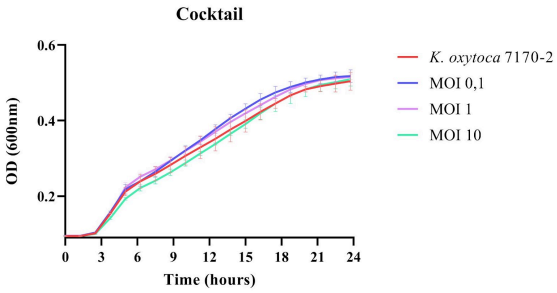
Cocktail
OD (600nm)
Time (hours)
K. oxytoca 7170-2
MOI 0,1
MOI 1
MOI 10

H.

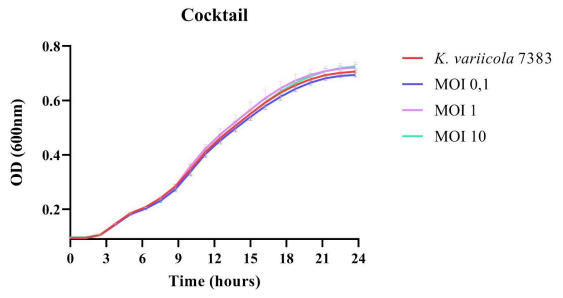
Cocktail
OD (600nm)
Time (hours)
K. variicola 7383
MOI 0,1
MOI 1
MOI 10

I.

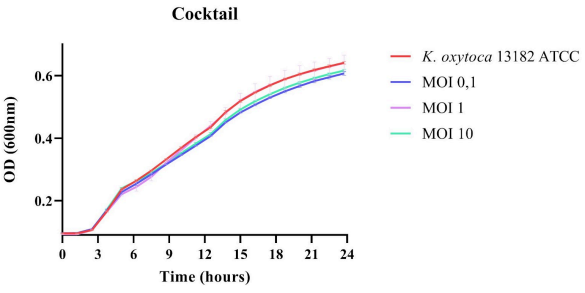
Cocktail
OD (600nm)
Time (hours)
K. oxytoca 13182 ATCC
MOI 0,1
MOI 1
MOI 10

J.

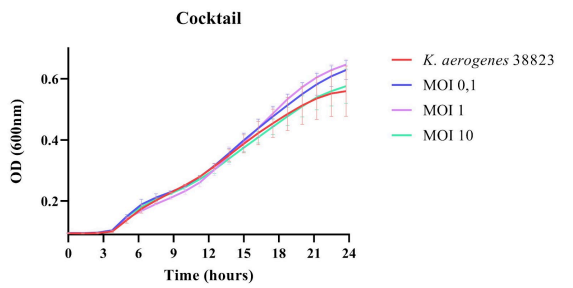

K.

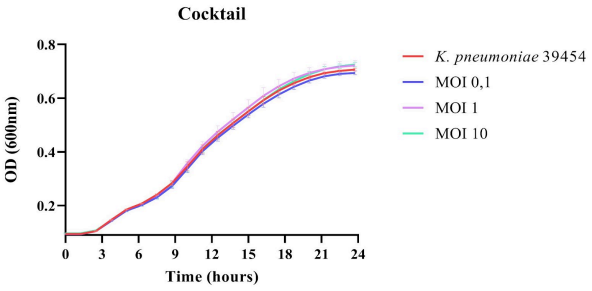

L.

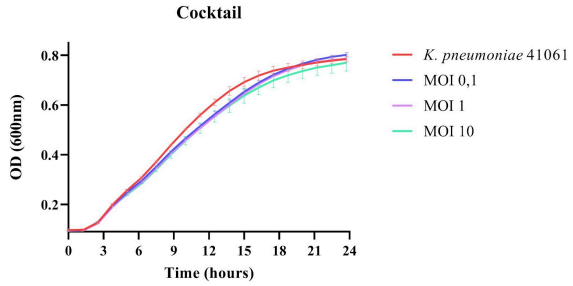

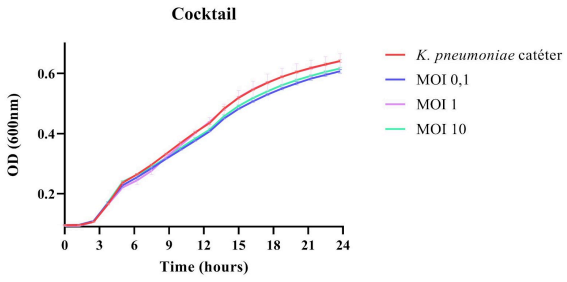

Biofilm prevention assay

1. Phage KO2 - Host bacterium *K. oxytoca* 13182 ATCC

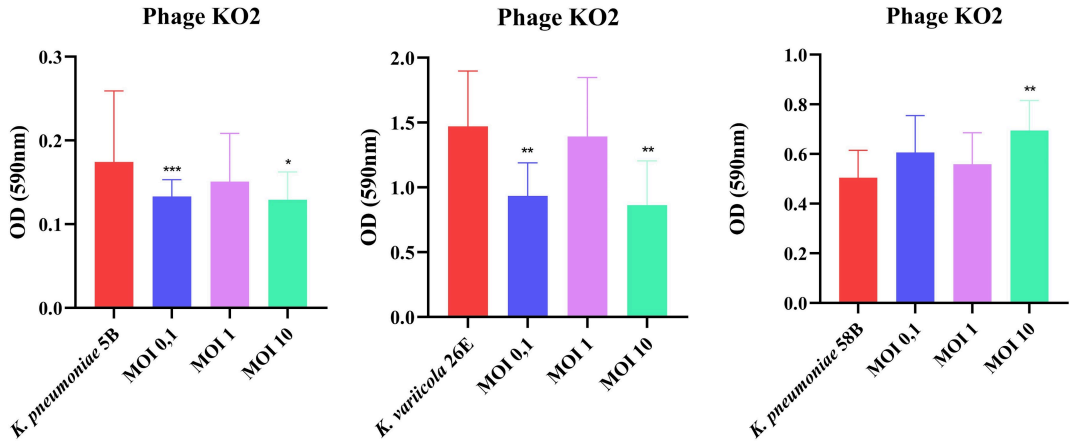

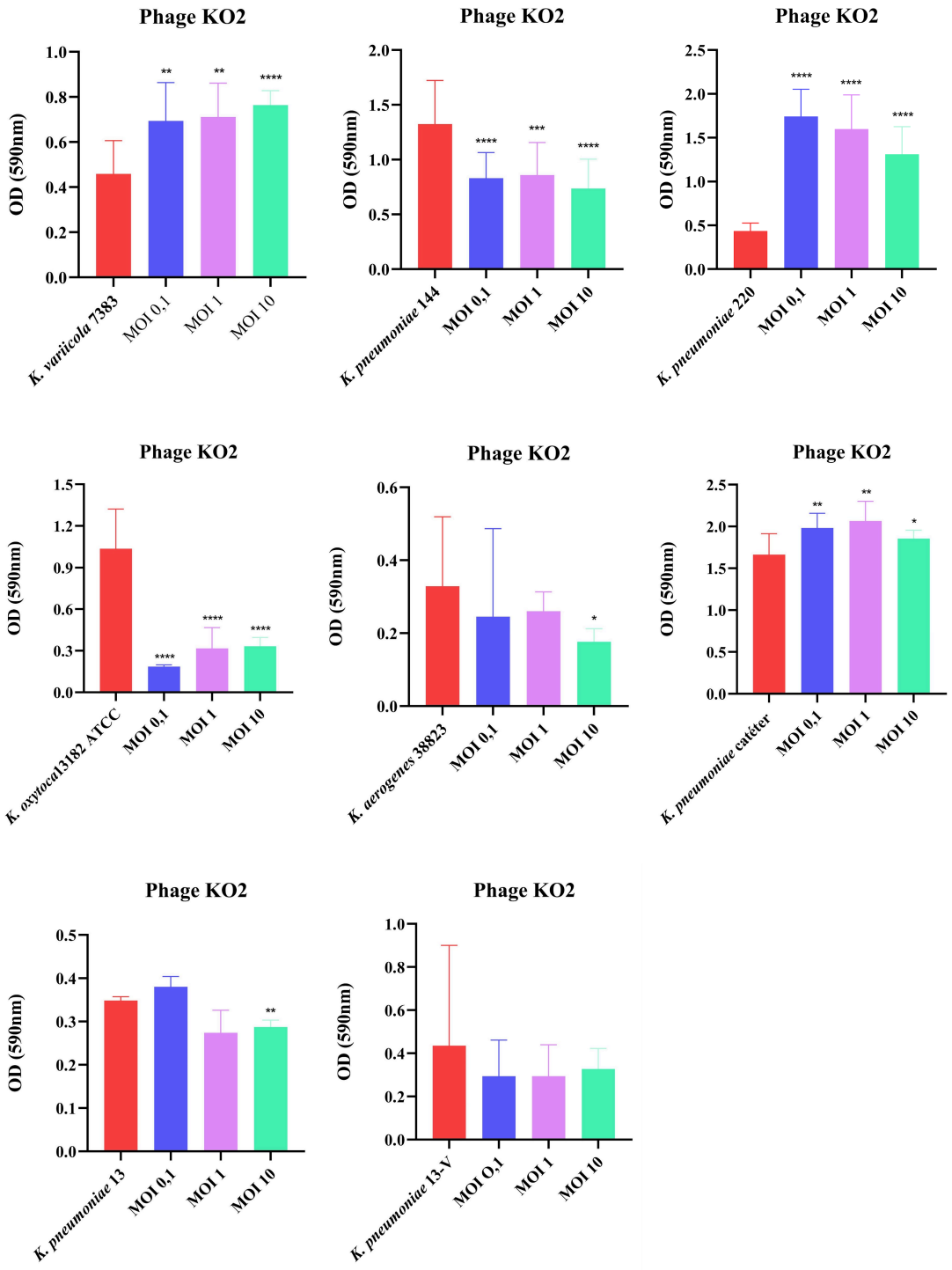

2. Phage KV3 - Host bacterium *K. variicola* 26E

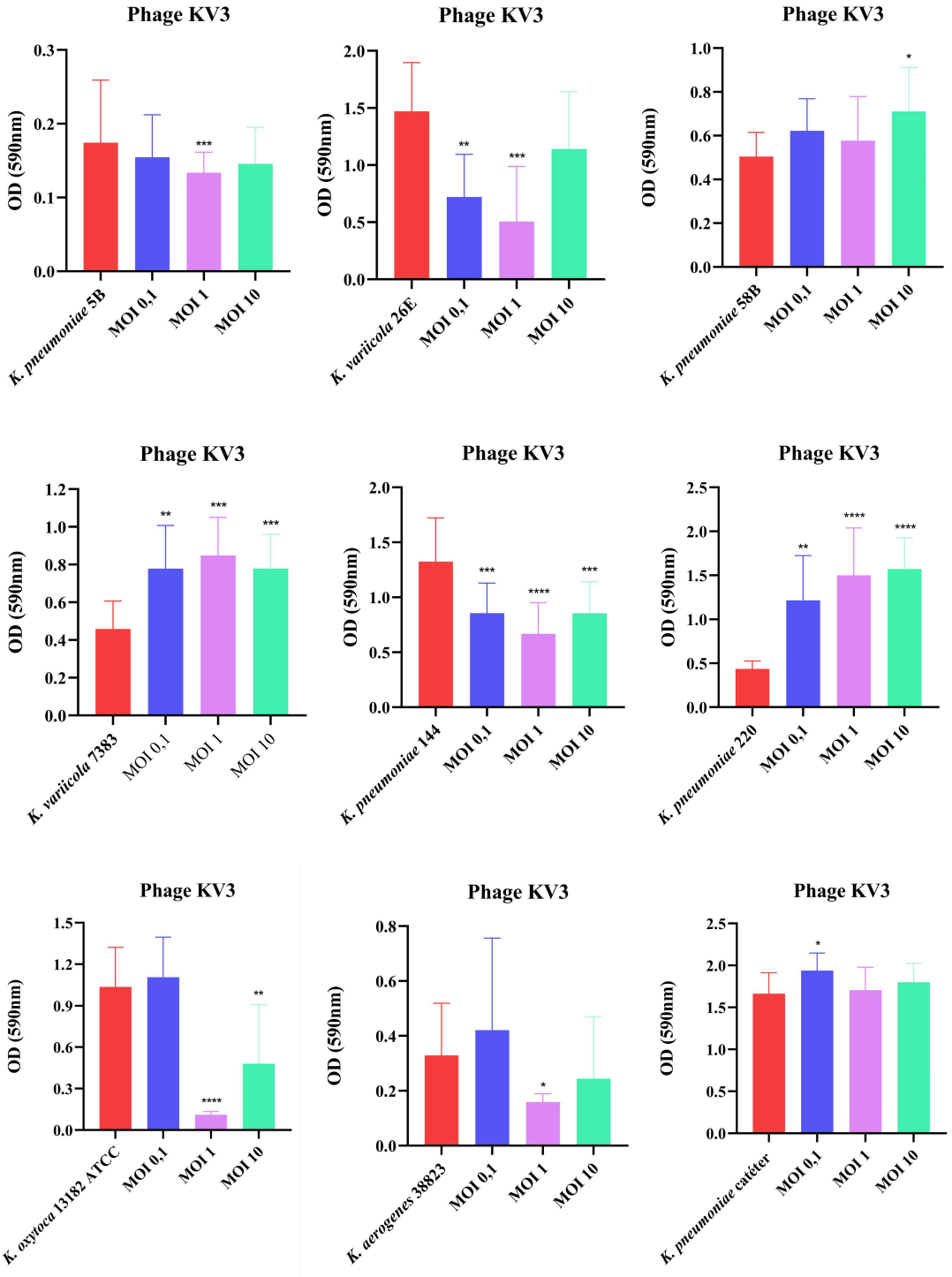
Phage KV3
OD (590nm)
K. pneumoniae 5B
MOI 0,1
MOI 1
MOI 10
Phage KV3
OD (590nm)
K. variicola 26E
MOI 0,1
MOI 1
MOI 10
Phage KV3
OD (590nm)
K. pneumoniae 58B
MOI 0,1
MOI 1
MOI 10
Phage KV3
OD (590nm)
K. variicola 7383
MOI 0,1
MOI 1
MOI 10
Phage KV3
OD (590nm)
K. pneumoniae 144
MOI 0,1
MOI 1
MOI 10
Phage KV3
OD (590nm)
K. pneumoniae 220
MOI 0,1
MOI 1
MOI 10
Phage KV3
OD (590nm)
K. oxytoca 13182 ATCC
MOI 0,1
MOI 1
MOI 10
Phage KV3
OD (590nm)
K. aerogenes 38823
MOI 0,1
MOI 1
MOI 10
Phage KV3
OD (590nm)
K. pneumoniae cathéter
MOI 0,1
MOI 1
MOI 10

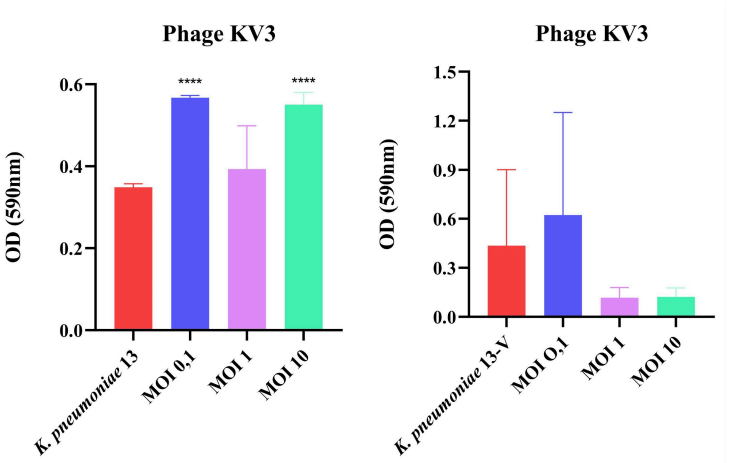

3. Phage KP4 - Host bacterium *K. pneumoniae* 13

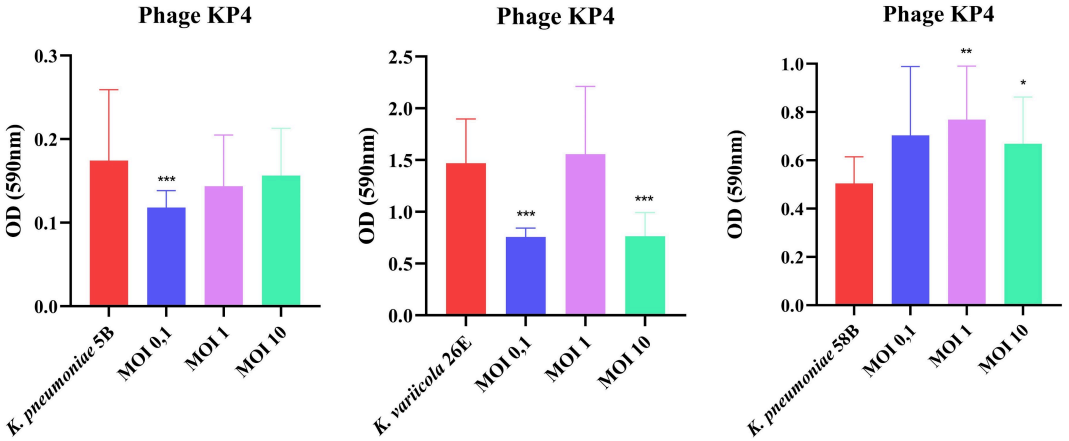

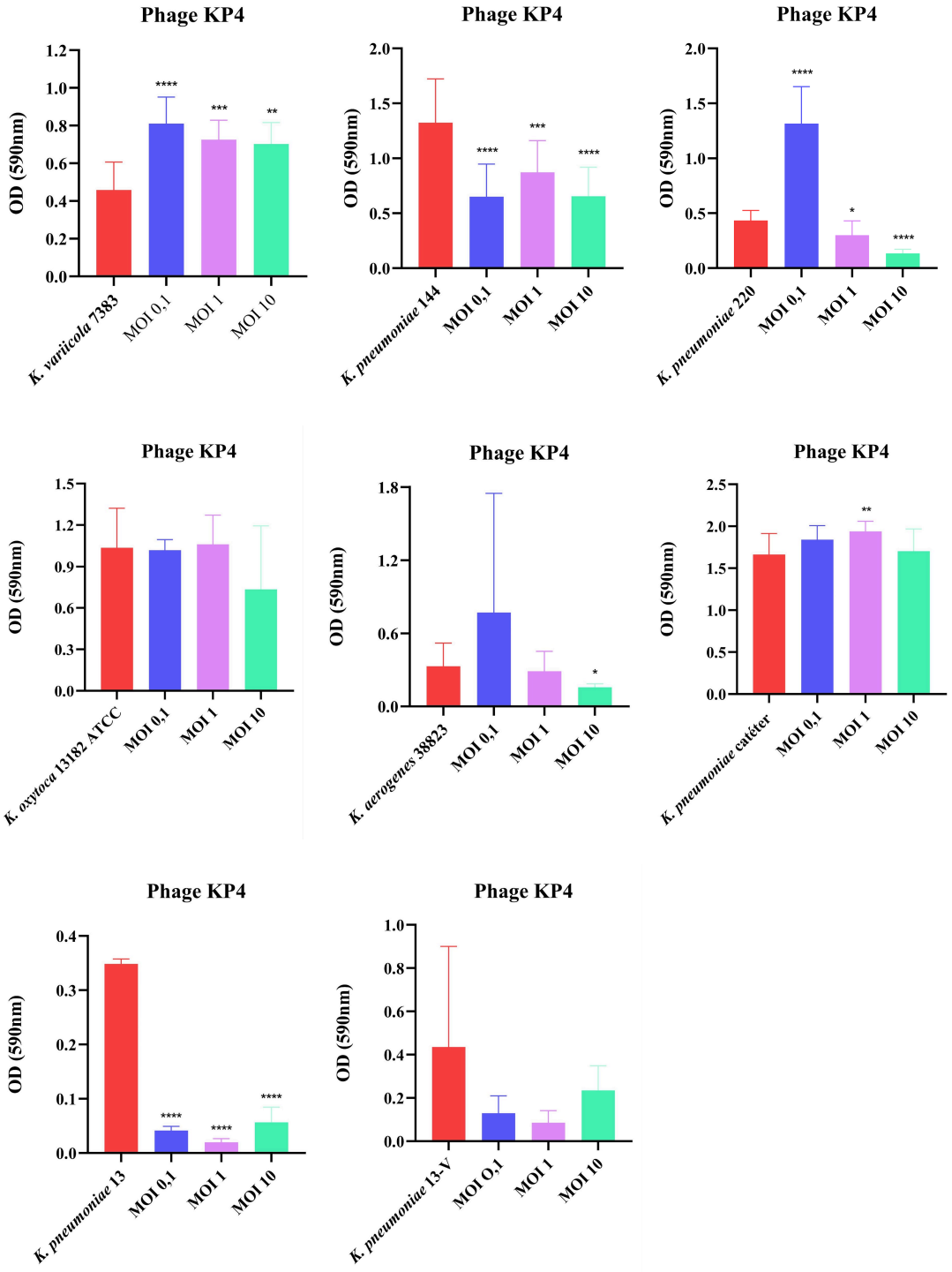

4. Phage KP6 - Host bacterium *K. pneumoniae* 58B

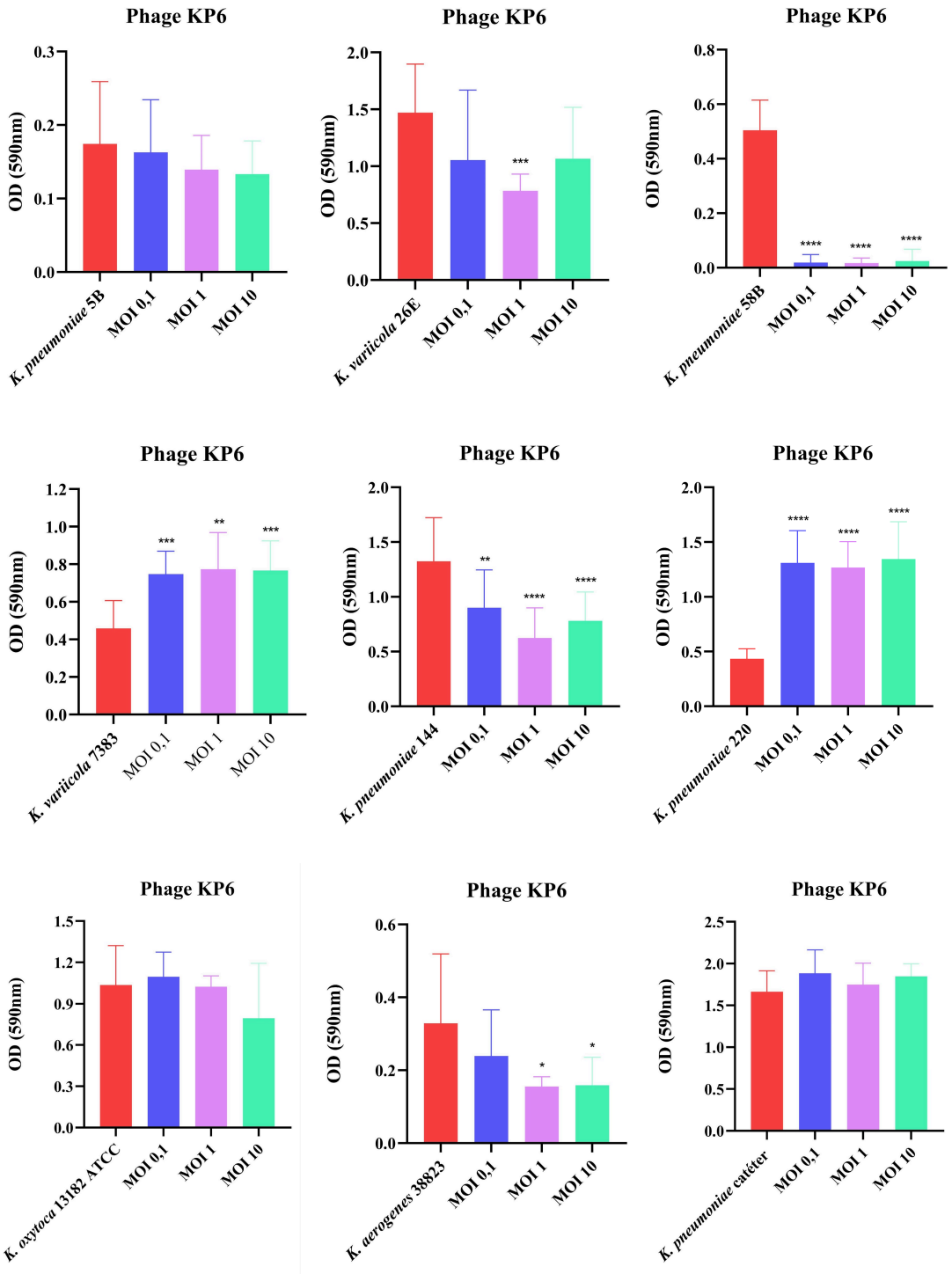
Phage KP6
OD (590nm)
0.0
0.1
0.2
0.3
K. pneumoniae 5B
MOI 0,1
MOI 1
MOI 10
Phage KP6
OD (590nm)
0.0
0.5
1.0
1.5
2.0
***
K. variicola 26E
MOI 0,1
MOI 1
MOI 10
Phage KP6
OD (590nm)
0.0
0.2
0.4
0.6
0.8
****
****
****
K. pneumoniae 58B
MOI 0,1
MOI 1
MOI 10
Phage KP6
OD (590nm)
0.0
0.2
0.4
0.6
0.8
1.0
1.2
***
**
***
K. variicola 7383
MOI 0,1
MOI 1
MOI 10
Phage KP6
OD (590nm)
0.0
0.5
1.0
1.5
2.0
**
****
****
K. pneumoniae 144
MOI 0,1
MOI 1
MOI 10
Phage KP6
OD (590nm)
0.0
0.5
1.0
1.5
2.0
****
****
****
K. pneumoniae 220
MOI 0,1
MOI 1
MOI 10
Phage KP6
OD (590nm)
0.0
0.3
0.6
0.9
1.2
1.5
K. oxytoca 13182 ATCC
MOI 0,1
MOI 1
MOI 10
Phage KP6
OD (590nm)
0.0
0.2
0.4
0.6
*
*
K. aerogenes 38823
MOI 0,1
MOI 1
MOI 10
Phage KP6
OD (590nm)
0.0
0.5
1.0
1.5
2.0
2.5
K. pneumoniae cathéter
MOI 0,1
MOI 1
MOI 10

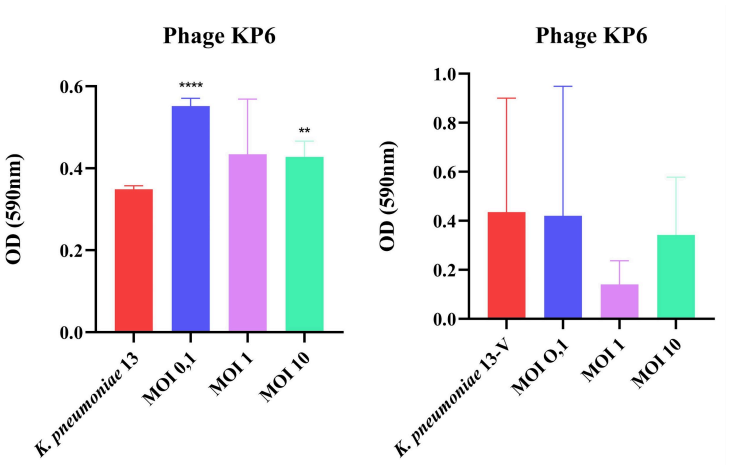

5. Phage KP7 - Host bacterium *K. pneumoniae* 58B

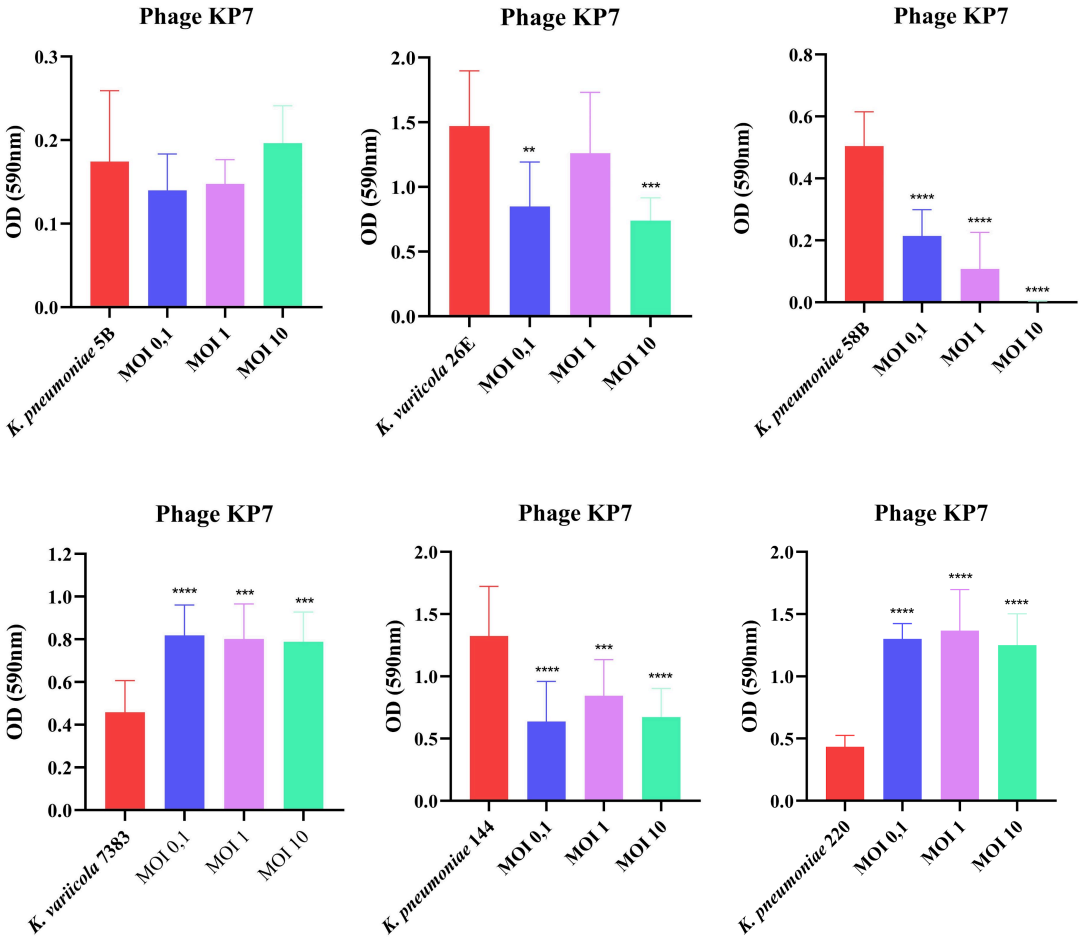

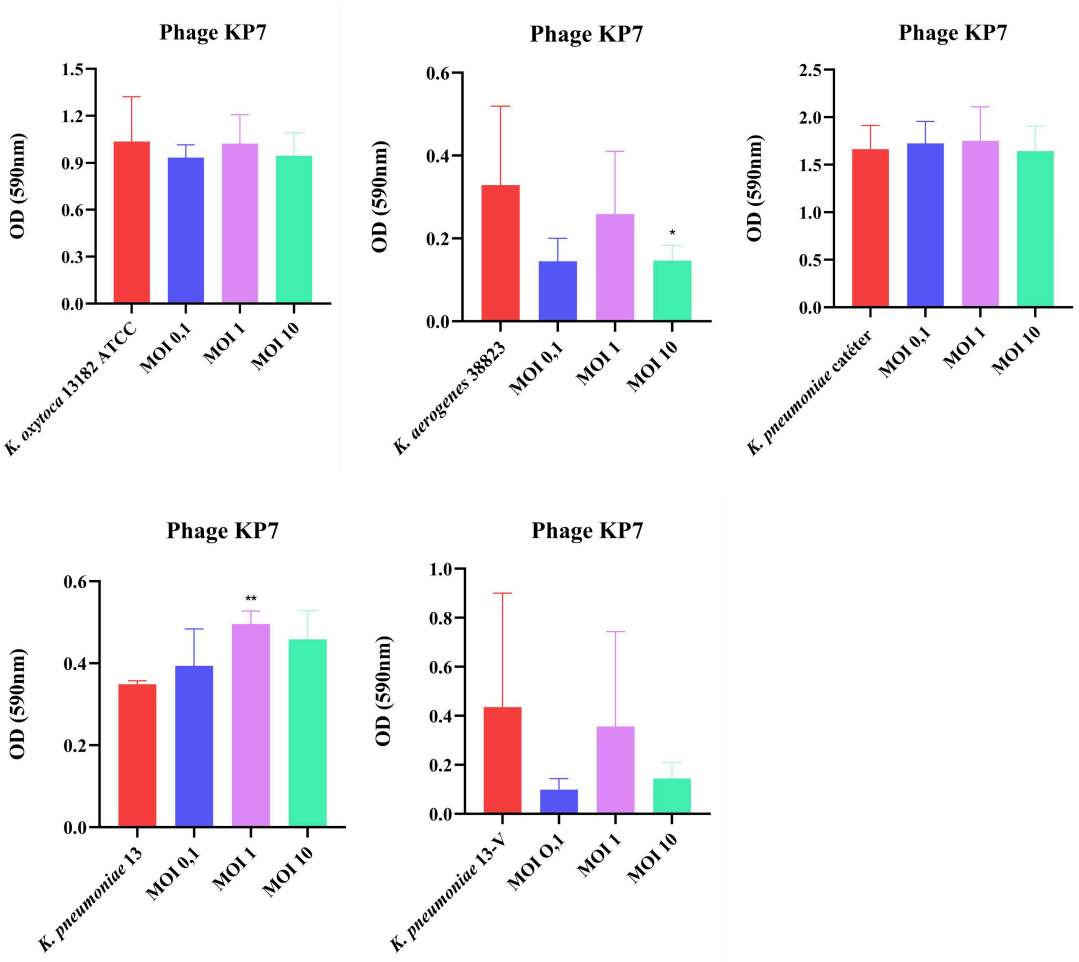

6. Phage KP8 - Host bacterium *K. pneumoniae* 5B

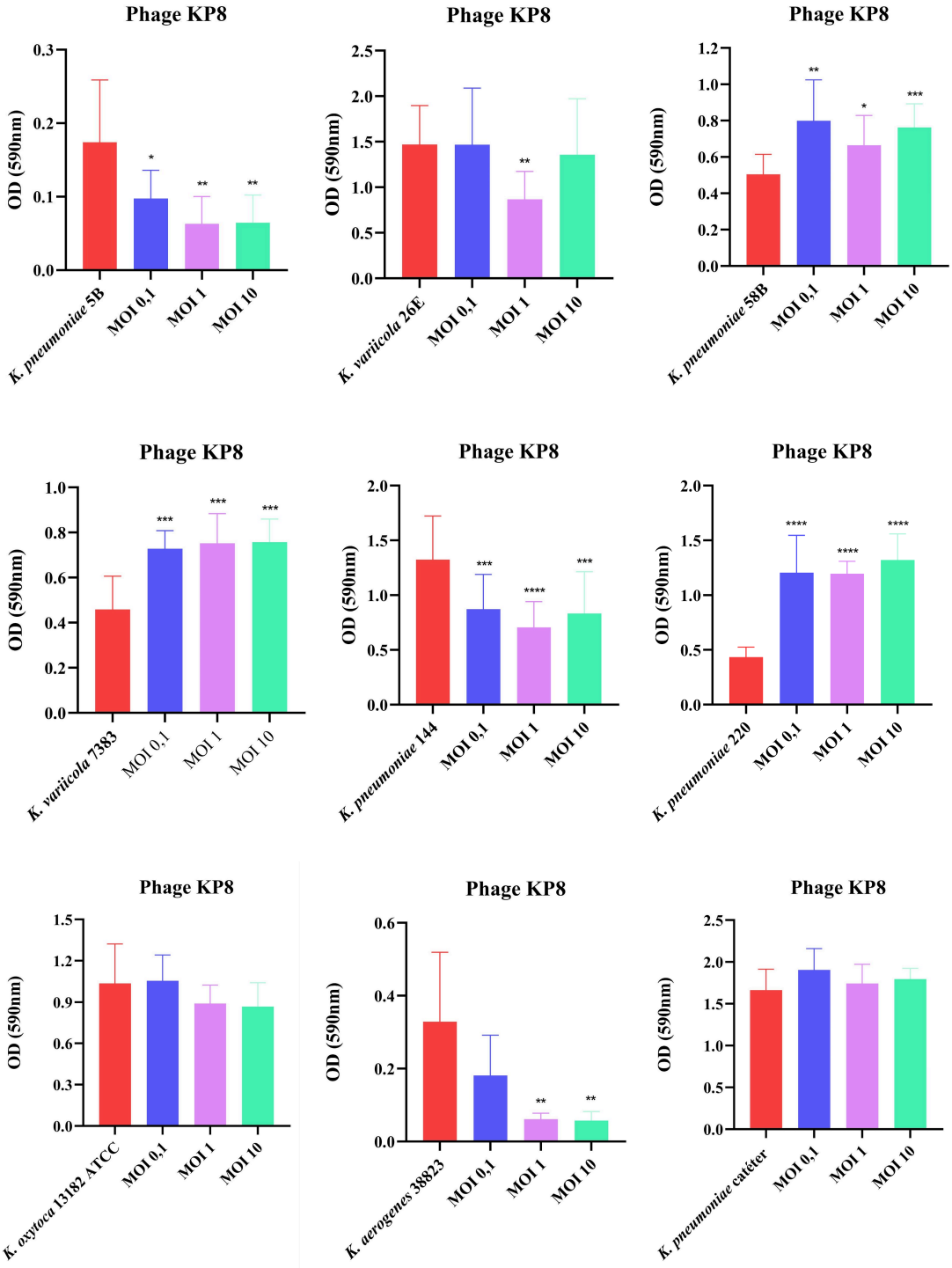
Phage KP8
OD (590nm)
K. pneumoniae 5B
K. varicola 26E
K. pneumoniae 58B
K. varicola 7383
K. pneumoniae 144
K. pneumoniae 220
K. oxytoca 13182 ATCC
K. aerogenes 38823
K. pneumoniae cathéter
MOI 0,1
MOI 1
MOI 10

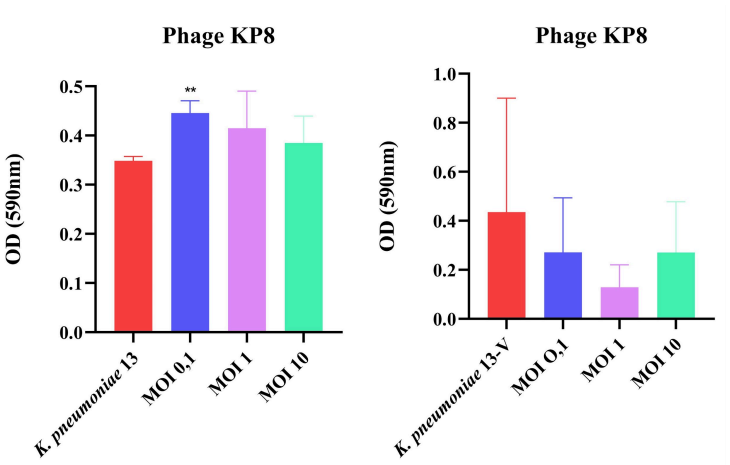

7. Phage KP9 - Host bacterium *K. pneumoniae* 5B

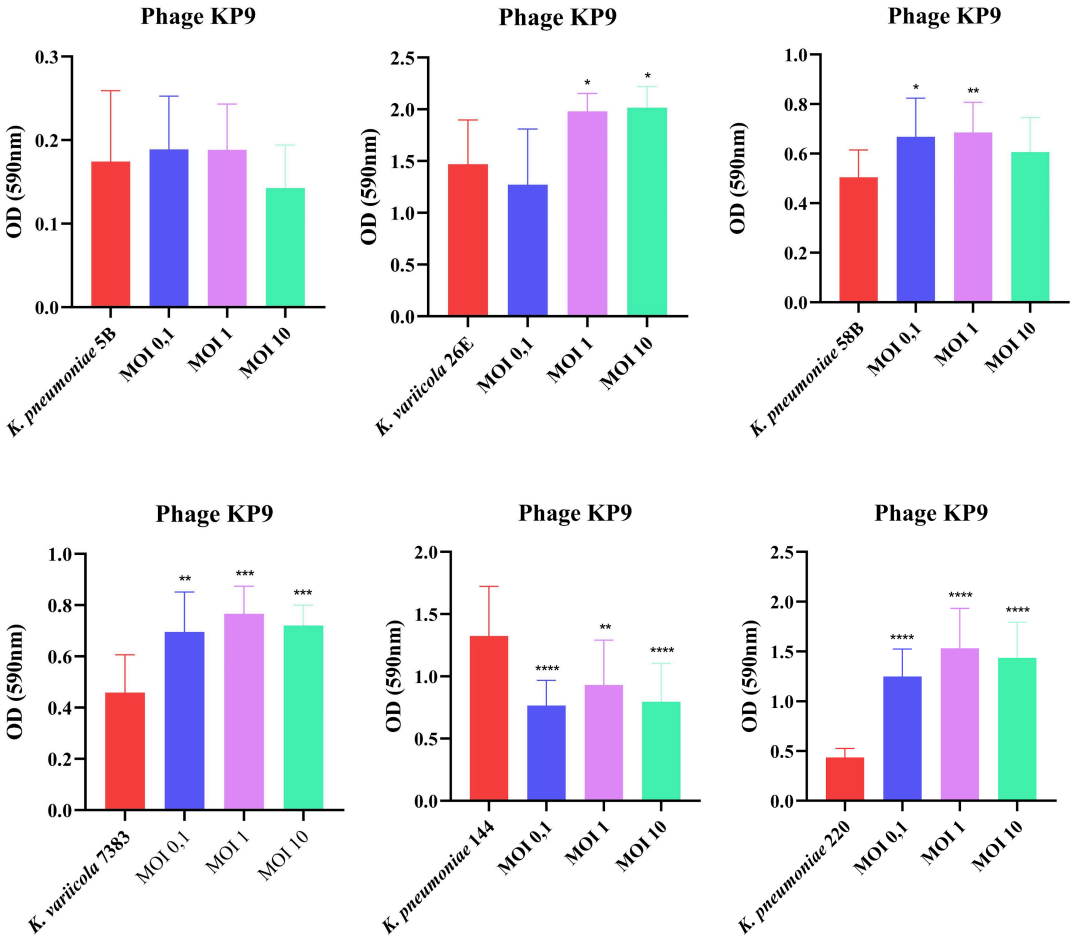

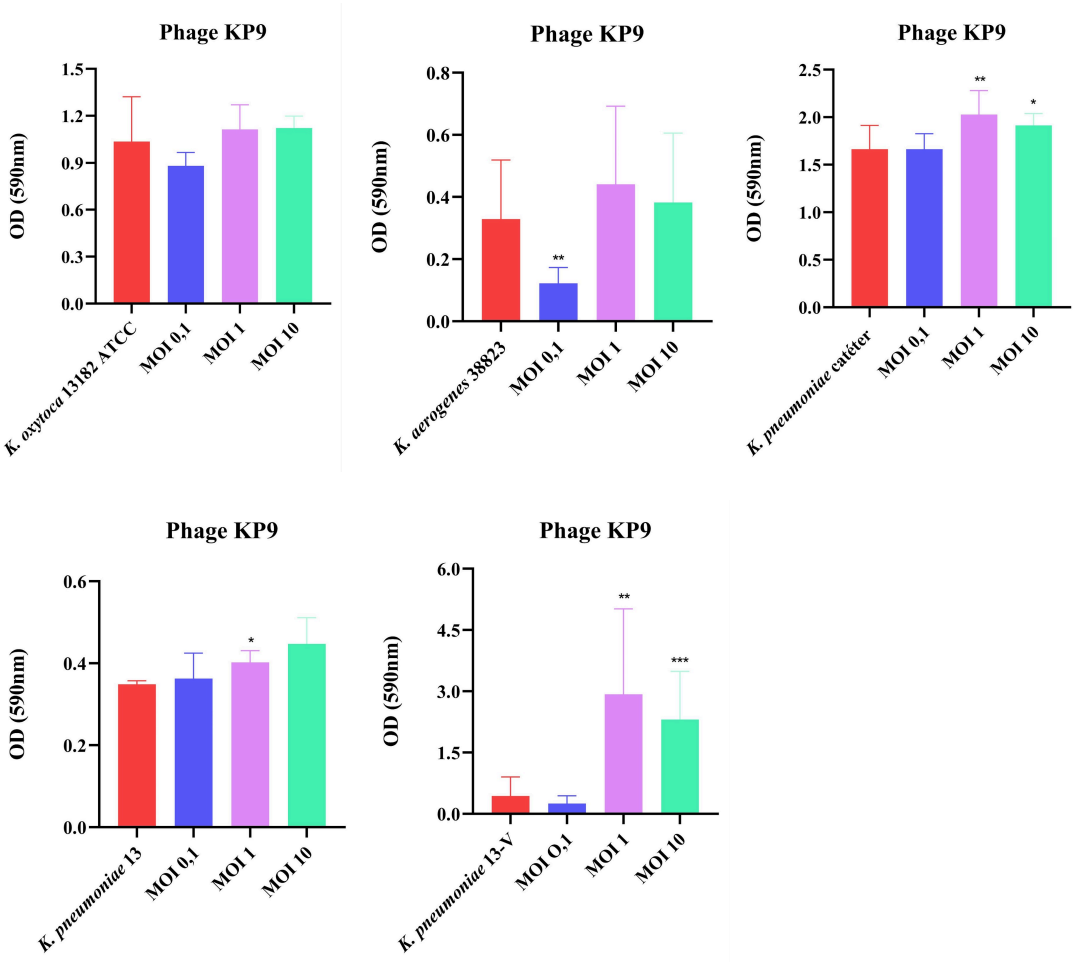

8. Phage cocktail composed of KP4, KP6, KP7 and KP8

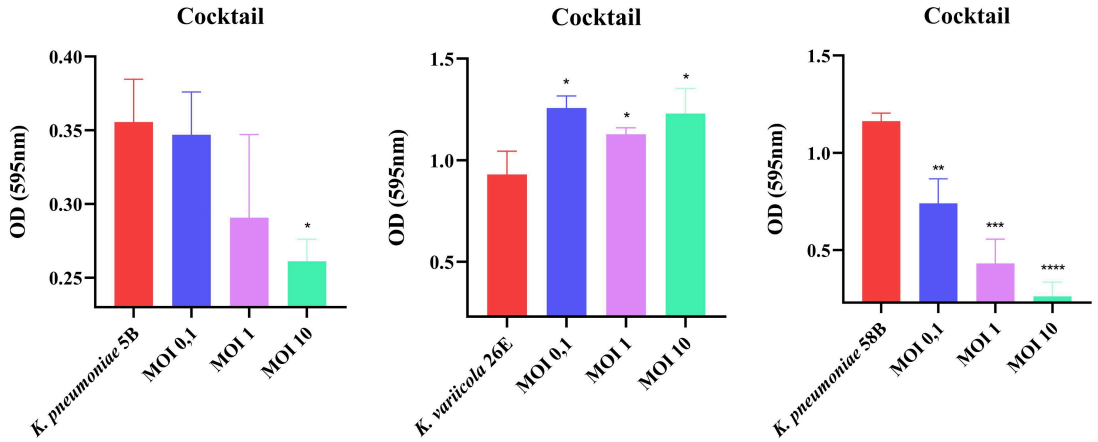

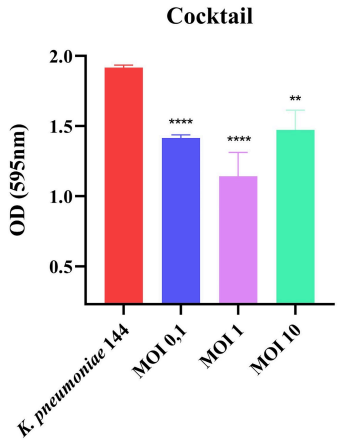
Cocktail
OD (595nm)
2.0
1.5
1.0
0.5
****
****
**
K. pneumoniae 144
MOI 0,1
MOI 1
MOI 10

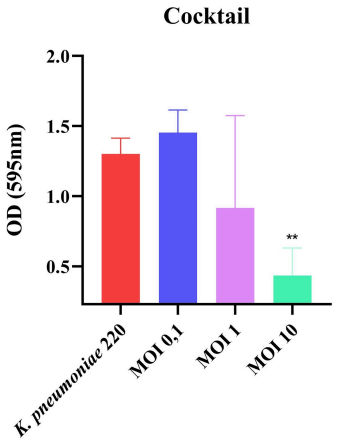
Cocktail
OD (595nm)
2.0
1.5
1.0
0.5
**
K. pneumoniae 220
MOI 0,1
MOI 1
MOI 10

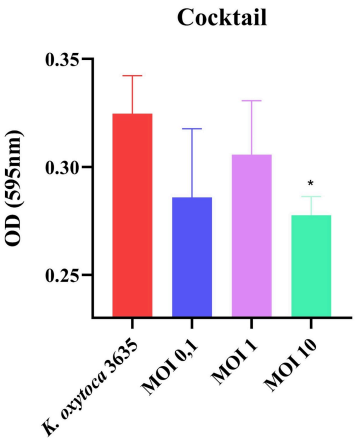
Cocktail
OD (595nm)
0.35
0.30
0.25
*
K. oxytoca 3635
MOI 0,1
MOI 1
MOI 10

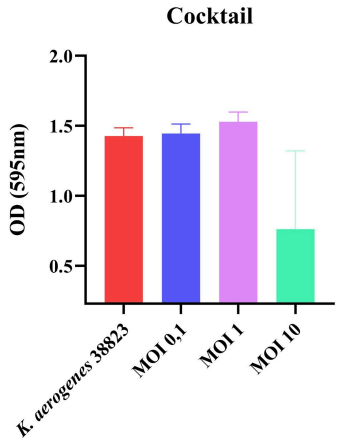
Cocktail
OD (595nm)
2.0
1.5
1.0
0.5
K. aerogenes 38823
MOI 0,1
MOI 1
MOI 10

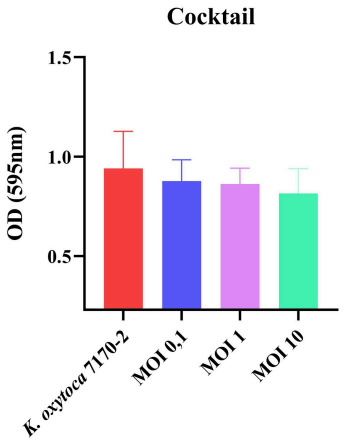
Cocktail
OD (595nm)
1.5
1.0
0.5
K. oxytoca 7170-2
MOI 0,1
MOI 1
MOI 10

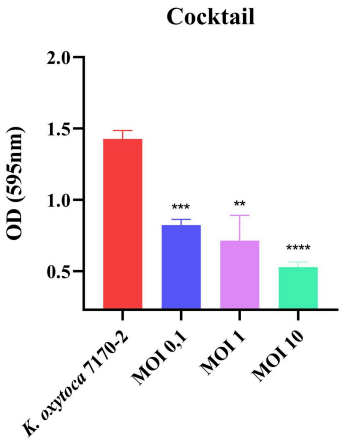
Cocktail
OD (595nm)
2.0
1.5
1.0
0.5
***
**
****
K. oxytoca 7170-2
MOI 0,1
MOI 1
MOI 10

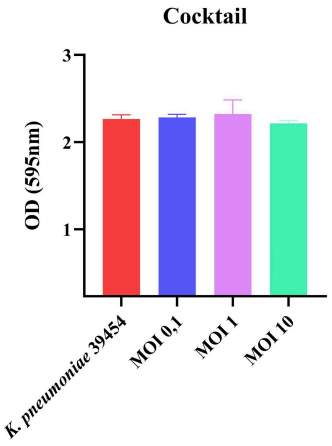
Cocktail
OD (595nm)
3
2
1
K. pneumoniae 39454
MOI 0,1
MOI 1
MOI 10